

STRUCTURAL STUDIES OF THE E.COLI METHIONINE ABC  
TRANSPORTER AND ITS COGNATE BINDING PROTEIN

Thesis By

Neena Sujata Kadaba

In Partial Fulfillment of the Requirements for the

degree of

Doctor of Philosophy

CALIFORNIA INSTITUTE OF TECHNOLOGY

Pasadena, California

2008

(Defended April 1, 2008)

© 2008

Neena Sujata Kadaba

All Rights Reserved.

## Acknowledgements.

I would first like to thank Doug Rees and members of the Rees lab who were extraordinarily helpful throughout the past few years. In particular, Heather Pinkett and Zhenfeng Liu were an amazing resource of information at every step, and I could not have accomplished much without their help. Additionally, Allen Lee, Mika Walton and Jeff Lai were a tremendous source of technical help, and I appreciate their patience in answering questions.

Many friends have also been a source of support over the past few years. In particular, I would like to extend a tremendous amount of thanks to Daniel Feldman for his encouragement and friendship over the past several years—it has made this process so much easier.

Finally, I would like to thank my family for their unconditional love and support. My mother, sister, and grandparents have encouraged every one of my endeavors, often making personal sacrifices for my benefit. They have instilled in me a love of learning, the confidence to pursue my goals relentlessly, and the desire to do something meaningful, and I hope they will be proud of my current and future accomplishments.

## **Abstract.**

ATP binding cassette (ABC) transporters use ATP hydrolysis to facilitate the transfer of diverse substrates across the membrane. Members of the methionine uptake transporter family, thought to be of considerable biological interest, have not been structurally characterized thus far. The crystal structure of the methionine importer MetNI from *Escherichia coli* has been solved to 3.7 Å resolution. The inward-facing conformation of this transporter adopts a more extreme arrangement than seen previously. While the permease domain consists of just five transmembrane helices per monomer, the ATP-binding cassette domain possesses a C-terminal domain in addition to the conserved architecture shared amongst this family. Analysis of the C-terminal extension has revealed a regulatory domain found in other proteins involved in amino acid metabolism, and further classifies this protein as part of the ACT family. Methionine binding in this region suggests a novel mechanism for regulation of transport that possibly stabilizes the inactive conformation of this family of transporters, as this domain is positioned between the nucleotide binding domains. Additionally, crystallization studies of the cognate binding protein to the MetNI system, MetQ were successful. The structure of the MetQ binding protein from *E. coli* was solved to 1.8 Å resolution, revealing a bi-lobed structure consistent with many other substrate binding proteins, yet possessing a few differences when compared with previously characterized methionine binding proteins from other organisms. The substrate binding pocket revealed a bound L-methionine residue, which shares key features with other methionine binding proteins and appears to be appropriately selective for L-methionine binding. These combined studies have provided insight into the methionine uptake system and into the ABC transporter mechanism of transport.

## Table of Contents.

Acknowledgements.....	iii
Abstract.....	iv
Table of Contents.....	v
List of Figures and Tables.....	vi
Abbreviations.....	ix
Chapter One. Introduction.....	1
1.1 Overview.....	1
1.2 ABC Transporter Structures.....	4
1.3 The Catalytic Cycle of ABC Transporters.....	16
1.4 Regulatory Mechanisms: The ACT Domain.....	20
Chapter Two. MetNI.....	24
2.1 Introduction.....	24
2.2 Structure of the MetNI Transporter.....	29
Appendix One. Methods and Data Relevant to Chapter Two.....	49
A1.1. Materials and Methods.....	49
Chapter Three. MetQ.....	62
3.1 Introduction.....	62
3.2 Methionine Binding Proteins.....	67
3.3 Structural Analysis of MetQ.....	70
Appendix Two. Methods and Data Relevant to Chapter Three.....	79
A2.1. Materials and Methods.....	79
Chapter Four. Conclusions.....	85
References.....	87
About the Author.....	106
Index.....	107

## List of Figures and Tables.

### Chapter One.

Figure 1.1—A conceptual diagram of ABC exporters and importers	2
Figure 1.2—The structure of the histidine ATP binding cassette	4
Figure 1.3—The structure of the vitamin B <sub>12</sub> ABC transporter	5
Figure 1.4—The structure of the BtuCD-BtuF transporter complex	7
Figure 1.5—The structure of the metal-chelate type ABC transporter	9
Figure 1.6—The structure of the ModA-ModBC transporter complex	10
Figure 1.7—The structure of the maltose transporter complex	12
Figure 1.8—The structure of the multidrug exporter SAV1866	14
Figure 1.9—A comparison of two MalK structures	17
Figure 1.10—A conceptual diagram of the action of “coupling helices”	18
Figure 1.11—A schematic of the mechanism of ABC transporters	19
Figure 1.12—Two views of the ferredoxin-like fold	21
Figure 1.13—The ACT domain of 3-phosphoglycerate dehydrogenase	22

### Chapter Two.

Figure 2.1—The structure of L-methionine	25
Figure 2.2—The <i>E. coli</i> methionine uptake transporter	31
Figure 2.3—Side view of the methionine ABC transporter	32
Figure 2.4—Xenon binding sites on the MetNI transporter	33
Figure 2.5—The asymmetric unit of the MetNI crystal form	33
Figure 2.6—An overlay of the two distinct transporters	34
Figure 2.7—The five helices that comprise the TMD core	35

Figure 2.8—The differences between TMD domains	36
Figure 2.9—The coupling helix and surrounding regions	37
Figure 2.10—The structural motifs of the ATPase cassette	39
Figure 2.11—View of the MalK and MetN NBDs	40
Figure 2.12—Another view of the MalK and MetN NBDs	41
Figure 2.13—A comparison of the linker regions	44
Figure 2.14—A view of the ACT domain	45
Figure 2.15—Another view of the ACT domain	46
Figure 2.16—A bottom-up view of the ACT domain	47

### **Appendix One.**

Figure A1.1—Sequence alignment of the TMDs	53
Figure A1.2—Sequence alignment of the NBDs	54
Figure A1.3—Purification data for MetNI	55
Figure A1.4—Crystals of MetNI	56
Figure A1.5—Initial density for MetNI	57
Table A1.1—Summary of secondary structure for MetN	58
Table A1.2— Summary of secondary structure for MetI	59
Table A1.3—Data processing statistics: Xe, native, and Se soak	60
Table A1.4—Data processing statistics: Selenomethionine MetNI	61

### **Chapter Three.**

Figure 3.1—The structure of tp32	68
Figure 3.2—The structure of pg110	69
Figure 3.3—The structure of MetQ	71
Figure 3.4—An overlay of MetQ, tp32, and pg110	72

Figure 3.5—The ligand binding site of MetQ	73
Figure 3.6— An overlay of MetQ and LAOBP	74
Figure 3.7— The surface electrostatics of MetQ	75
Figure 3.8— A comparison of the connector regions	76

**Appendix Two.**

Figure A2.1—Sequence alignment of methionine binding proteins	81
Figure A2.2—Crystals of MetQ	82
Table A2.1—Summary of secondary structure for MetQ	83
Table A2.1—Data processing statistics	84

## Abbreviations.

ABC – ATP binding cassette

ATP – Adenosine tri-phosphate

*E. coli* – *Escherichia coli*

MetI – TMD for the methionine uptake transporter

MetN – NBD for the methionine uptake transporter

MetNI – Methionine uptake transporter

MetQ – Methionine binding protein

NBD – Nucleotide binding domain

TMD – Transmembrane domain

## Chapter One. Introduction.

### 1.1 Overview

Cell membranes play a vital role in the survival of a cell in its role as a barrier. Proteins embedded within these membranes, however, are responsible for the more specific functions of a cell membrane, and typically account for 50% of the total membrane by weight (Alberts et al., 2002). Transmembrane, or integral membrane proteins, are proteins that are able to traverse the membrane, possessing regions that are hydrophobic within the membrane and hydrophilic on either side of the membrane. Transport proteins, a class of membrane proteins, are responsible for the transfer of various molecules across the cell membrane.

ATP Binding Cassette (ABC) transporters are integral membrane proteins that utilize ATP hydrolysis to facilitate the unidirectional transfer of diverse substrates across the periplasm (Figure 1.1). Substrates for this family of transporters include amino acids, carbohydrates, metals, ions, lipids, drugs, toxins, peptides, osmolytes, siderophores, and vitamins (Higgins, 1992). ABC importers assist in the uptake of nutrients and lipids after receiving the substrate from a substrate-specific binding protein within the periplasm. These cognate binding proteins ensure substrate specificity and unidirectional transport of the transporter. Exporters, however, are typically responsible for the excretion of drugs and toxins, and play a role in the presentation of antigens to cytotoxic T cells. A rising number of medical conditions are linked to ABC transporter functions; the dysfunction of certain human ABC transporters leads to genetic diseases such as cystic fibrosis, while ABC exporters are responsible for multidrug resistance in tumor cells (Biemans-Oldehinkel, 2006). In addition to multidrug resistance, ABC transporters play a role in a variety of human diseases,

ranging from immune deficiency to hypoglycemia, among others. A study of the *E. coli* genome revealed that the ABC transporters are the largest family of paralogous proteins, comprising almost 5% of the *E. coli* genome (Hung et al., 1998; Higgins, 2001). This corresponds to approximately 70 different ABC transporters encoded by *E. coli*.

Architecturally, an ABC transporter comprises four domains (Figure 1.1): two cytoplasmic nucleotide binding domains (NBDs) responsible for hydrolyzing ATP, and two transmembrane domains (TMDs) that form a translocation pathway (Higgins, 1992). These can be encoded as 4 separate proteins, as a tetramer formed by 2 NBDs and 2 TMDs, by 2 half-transporters consisting of one chain that contains one TMD and

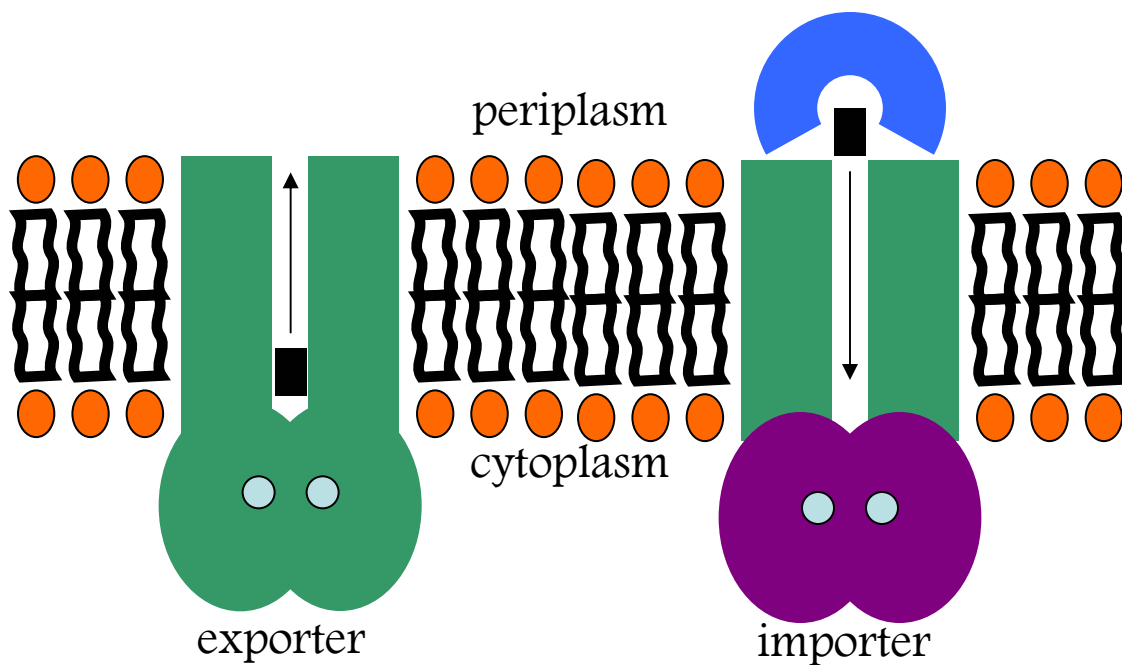


**Figure 1.1.** A conceptual diagram of ABC exporters and importers. ABC importers interact with a substrate binding protein (in blue) that delivers the substrate (in black) to the transmembrane domain that forms the translocation pathway (in green). Two molecules of ATP (in light blue) bind the ATPase domain (in purple) to provide the energy for transport of the substrate from the periplasm to the cytoplasm. ABC exporters transport small molecules in the other direction, and are frequently a single chain or two chains of identical half-transporters, as opposed to the heterotetramer importer. ABC exporter proteins bind ATP and have a similar ATPase domain to the importers, but both ABC exporters and importers have variable translocation domains specific to the substrate(s) being transported.

NBD, or alternatively by one long polypeptide chain encompassing all components (Higgins, 2001). Transmembrane domains are structurally and sequentially diverse, containing between 8 and 20 core helices, thought to reflect the diversity of substrates transported, as these substrates bind within the translocation pathway. The NBDs, however, possess certain sequence motifs. The conservation of a ~215 residue core that comprises the NBD is important in the definition of this family. The most characteristic features in the NBDs are the P- and Q-loops, present in many ATP-binding proteins, and the ABC signature sequence, LSGGQ (Davidson and Chen, 2004). These conserved motifs, essential to ATP-binding and hydrolysis, suggest an archetypal mechanism for alternating between the inward- and outward-facing conformations required for substrate translocation.

The first ATP-binding cassette structure was solved in 1998 (Figure 1.2). This structure, of the *E. coli* histidine transporter (PDB ID: 1b0u), revealed the shared features present in this family of nucleotide binding domains (Hung et al., 1998). The “phosphate binding loop”, or P-loop, common to other ATP binding proteins was identified in this protein as part of the ATP-binding pocket, and was found to correspond to the Walker A motif. The P-loop was identified as wrapping around the  $\beta$ -phosphate of the ATP molecule, and provided hydrogen bonding for the hydrophilic regions of ATP as well as hydrophobic interaction with the adenine base. The “signature sequence” of ABC transporters, a conserved segment containing the LSGGQ sequence, was also located in this structure as being important for transporter activity. Subsequent to this structure being solved, over two dozen other ATP binding cassette structures have been solved in the absence of the permease domain. Perhaps the most well-characterized structure is that of the MalK dimer, which until recently was only characterized as a cassette and not a full transporter. The MalK dimer has been

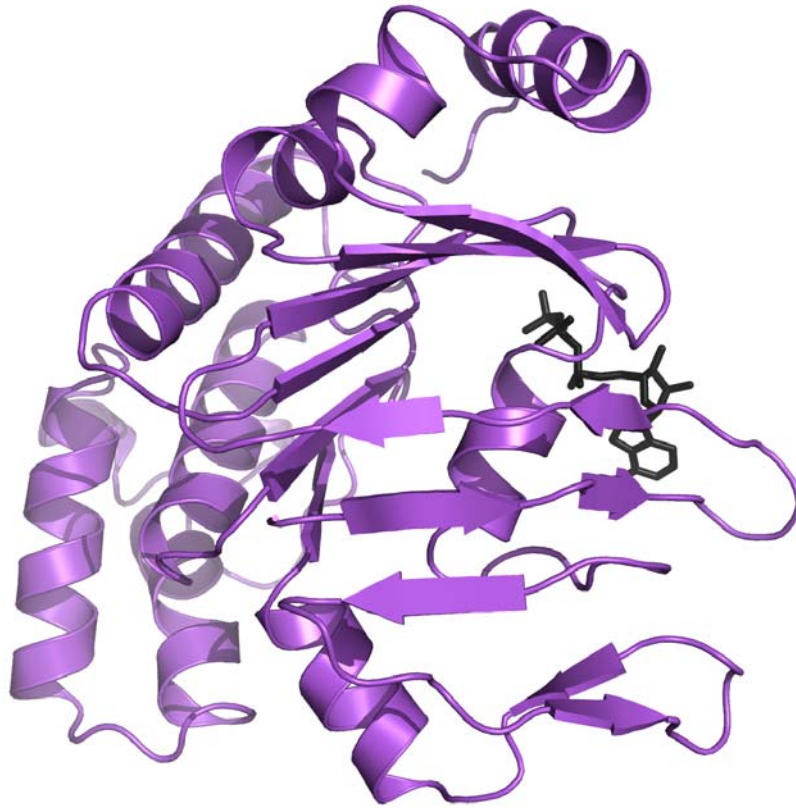


**Figure 1.2.** The structure of the histidine ATP-binding subunit HisP (in purple), solved in 1998. This was the first ATPase domain of an ABC transporter to be solved, and it was solved with a bound ATP molecule (in black). This revealed many basic features of the ATP binding site that were later identified as being common to all ABC transporters.

structurally characterized in multiple nucleotide-bound and nucleotide-free states within the reaction mechanism. However, the transport mechanism is best understood with information from a combination of biochemical and structural studies; in that regard, a discussion of the full ABC transporter structures within the literature (as of March 2008) will be presented first.

## 1.2 ABC Transporter Structures

To date, there have been five distinct structures of ABC importer proteins published. Additionally, there have been structural studies of two ABC exporters in various conformations. The following is an attempt to summarize the findings of each

of these novel structures and place them within a framework that illustrates the various conformations experienced during the transport process.

### The Vitamin B<sub>12</sub> ABC Transporter

The first structure of a complete ABC transporter was solved in 2002 by Locher et al. (2002). This structure (PDB ID: 117v), of the vitamin B<sub>12</sub> ABC transporter from *E. coli*, was solved to 3.2 Å resolution and revealed an interesting conformation of the four subunits (Figure 1.3). In this structure, the two ATPase subunits are in close contact to one another, and many features on the individual BtuD subunit resemble those found in

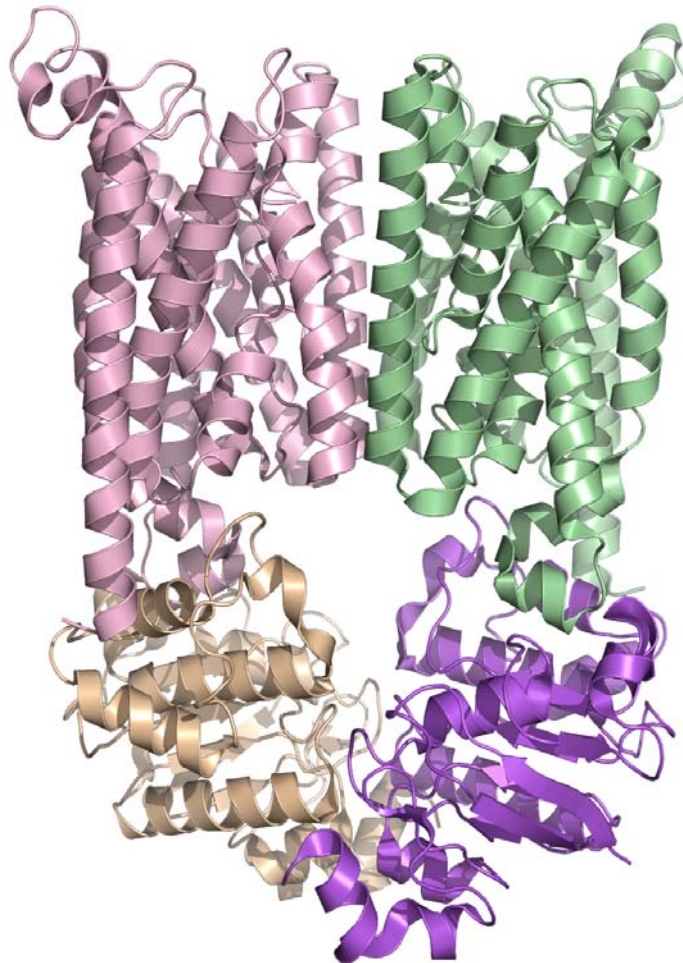


**Figure 1.3.** The structure of the first complete ABC transporter, the vitamin B-12 transporter from *E. coli*. This structure, published in 2002, is representative of an outward-facing conformation, as indicated by the positions of the two transmembrane domains (pink and green) and their relative positions to the two ATPase domains (tan and purple), despite a lack of bound nucleotide.

HisP. Interestingly, there is no nucleotide bound. As with other published ATP binding cassette structures, BtuD consists of a six-stranded  $\beta$ -sheet surrounded by nine  $\alpha$ -helices and a smaller  $\beta$ -sheet made up of 3  $\beta$ -strands. The dimer, as with other ATP binding cassette dimers, shows the cassettes aligned in such a way that they are opposite one another in a head-to-tail fashion. Two ATP binding sites are created in the clefts between the P-loop and signature motifs of different subunits. Most of the interface between these two identical subunits is formed by highly conserved residues, frequently those that are part of the important sequence motifs for this family. Conversely, the novel (at the time) transmembrane region consists of ten helices per monomer; each monomer is also in close contact with its counterpart. The translocation pathway formed by these two transmembrane domains is closed to the cytoplasm, open to the periplasm, and is lined with hydrophobic residues. Another interesting feature revealed by this structure concerns the interface between the transmembrane subunit and the ATPase domain. There is a cytoplasmic loop between TM6 and TM7 within the BtuC transmembrane domain that folds into two short helices that each have significant contacts with the BtuD ATPase domain. Further sequence analysis revealed that this sequence is well conserved amongst ABC transporters, and was further named the “EAA” loop (Saurin et al., 1994). On the ATPase domain, residues from the Q-loop are responsible for contacts with the transmembrane domain. Overall, this structure was a critical turning point in the study of ABC importers, as the techniques used in this structure were useful in the preparation and study of other ABC transporters (Locher, 2004).

The story of BtuCD does not end with this one structure. Attempts to crystallize the complex of BtuCD along with the *E. coli* vitamin B<sub>12</sub> binding protein BtuF proved ultimately successful, as reported by Hvorup et al., in 2007 (Figure 1.4). The 2.6 Å

resolution structure of the BtuCD transporter (PDB ID: 2qi9) in complex with its binding protein possesses features not found in the individual structures, and was able to shed light on the process of how this complex is formed. In this structure, vitamin B<sub>12</sub> is not present, and the vitamin B<sub>12</sub> binding protein BtuF, a bi-lobed structure, has its lobes spread further apart than in the vitamin B<sub>12</sub> structures previously solved (Karpowich et al., 2003). Furthermore, the structure of BtuCD in this complex differs from the previously characterized structure. The transporter is closed to both the cytoplasm and the periplasm, and the two monomers of BtuC, the transmembrane

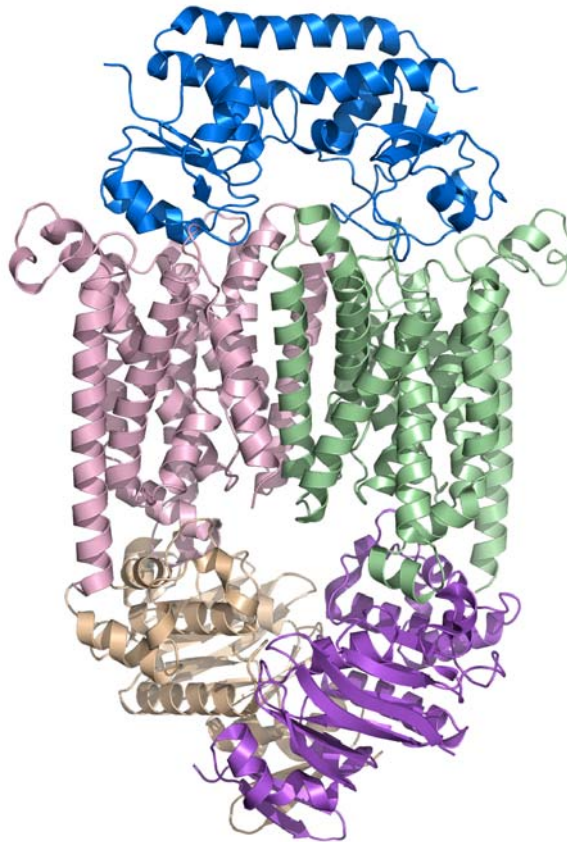


**Figure 1.4.** The structure of the BtuCD-BtuF complex is shown above. This unusual structure revealed another conformation of the BtuCD transporter, despite nucleotide or substrate binding. This structure suggests that it is possible for the translocation pathway to be closed to both the cytoplasm and the periplasm in the absence of nucleotide and substrate.

domain, are in slightly different conformations. The two-fold symmetry present in the first BtuCD structure is not present, and this asymmetry is most striking on the cytoplasmic-facing portion of the membrane spanning subunit. The interface of BtuC and BtuF confirms previous predictions (Borths et al., 2002) that salt bridges between oppositely charged residues play an important role in the attraction between these two proteins. Loops from BtuC insert into the BtuF structure, possibly forcing the substrate into the translocation path. The nucleotide binding domains are in a nucleotide-free open state, but each individual subunit is structurally similar to the previously studied form. The changes between these two structures are a result of a flexible movement of the two BtuD monomers relative to one another, not within each monomer. As a result, the authors believe this structure is reflective of the transporter in a post-translocation stage in the transport mechanism. To further confirm their observations, they pursued a spin-labeling study that allowed them to replace all native cysteines with serine residues, and engineered specific cysteine residues within the TM5 helix in BtuC to use in spin labeling. The spin-labeled cysteines were studied using continuous wave EPR spectra to monitor the environment of the label; studies showed that BtuCD had considerably more flexibility in this region than the BtuCD-BtuF complex. Other spin-labeling studies further supported the structural observations, suggesting that this in fact was a rigid, asymmetric conformation of the BtuCD-BtuF complex.

### **A Metal-Chelate Type Transporter**

The highest resolution ABC transporter structure solved thus far is the putative metal-chelate type transporter HI1470/1 (Pinkett et al., 2007). This 2.4 Å resolution structure (PDB ID: 2nq2) is homologous to the BtuCD structure, as it possesses similar ATPase domains and membrane-spanning subunits that contain ten transmembrane helices per monomer (Figure 1.5). However, this structure revealed an inward-facing

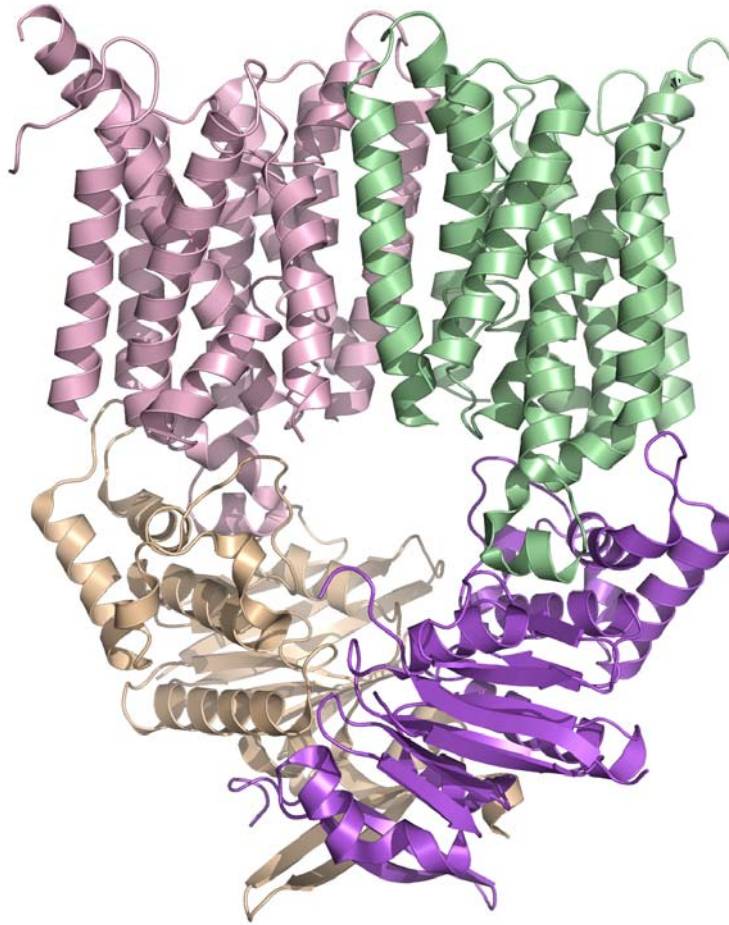


**Figure 1.5.** The structure of the metal-chelate type transporter HI1470/1. This transporter, a homolog of BtuCD, was found to be in the inward-facing conformation, with key differences in the placement of helices in the transmembrane domain (pink and green) and in the relative orientation of the two ATPase units (tan and purple).

conformation as compared to the outward-facing conformation of BtuCD, despite the fact that both structures are nucleotide-free. The relatively small movements illustrated between these two structures are interesting, as the difference between the inward- and outward-facing conformations of these homologs appears to be accomplished with slight shifts in the transmembrane domains. More specifically, the transmembrane domains must undergo a translational movement in the plane of the membrane to shift between these two states. This difference causes the HI1470/1 structure to be closed to the periplasm, while the BtuCD structure is more open to the periplasm. Similarly, the nucleotide binding domains of these two structures exhibit a slight difference; the

HI1470 dimer has a slightly more open conformation than the BtuD dimer. A comparison of these two structures has highlighted certain structural elements that may be important in substrate translocation, ATP binding and hydrolysis, as well as the movement that occurs in both of these domains during the substrate translocation process.

### **The Molybdate Transporter**

The first structure of an ABC transporter in complex with its binding protein was the structure of the molybdate transporter ModBC (Hollenstein et al., 2007). This

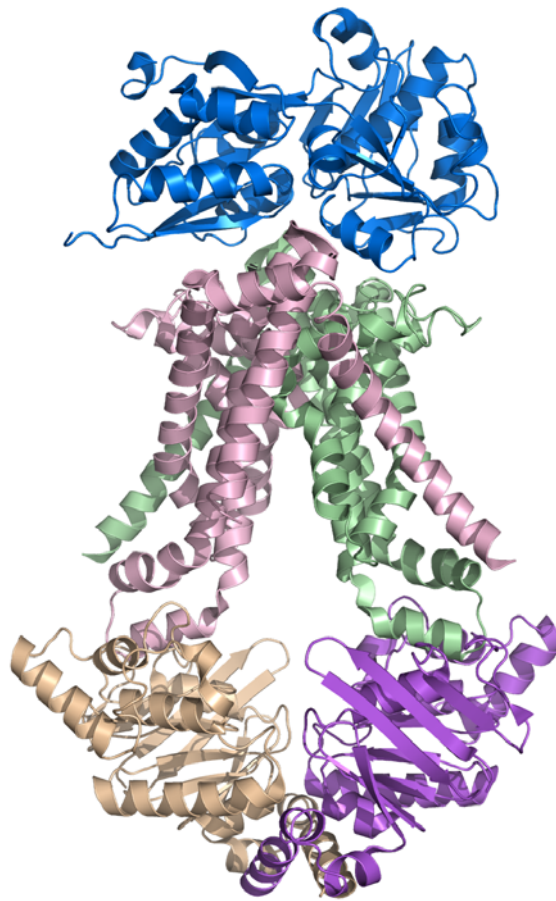


**Figure 1.6.** The structure of the ModA-ModBC complex. This interesting structure revealed a novel transmembrane domain consisting of only six transmembrane helices (pink and green) as well as a new relative orientation of the ATPase subunits that were further apart than other structures. Additionally, the interface of this transporter with its cognate binding protein provides insight on the complex formation needed for transport.

3.1 Å resolution structure (PDB ID: 2onk) reveals a nucleotide-free, open conformation within the nucleotide binding domains ModC (Figure 1.6). The membrane-spanning domain, ModB, revealed a novel, considerably smaller set of six helices per monomer that shape the inward-facing conformation. Interestingly, one helix in each monomer crosses over to interact with the helices of the opposing monomer. In contrast to other structures of the transporter-binding protein complex, the binding protein in this structure contains a bound substrate, and is in a closed form; the overall structure of this complex indicates it is in a conformation that precedes transport. The substrate binding pocket of the binding protein is aligned with the translocation pathway, suggesting that ATP binding is necessary to promote active transport. Small helical regions (“coupling helices”) on a loop from the transmembrane domain mitigate movement between the nucleotide binding domain and the transmembrane domain, as seen in other structures. This region contains the conserved “EAA” motif and is thought to play an important role in communicating movement between the nucleotide binding domain and the transmembrane subunit. This structure fortifies the hypothesis that each cycle of transport translocates one substrate molecule across the membrane, yet requires two ATP molecules, suggesting a stoichiometrical relationship of 1 substrate to two ATP molecules. Mechanistic analysis suggests that transporters share a common “alternating access and release” mechanism as they move between the inward-and outward-facing conformations as a result of binding protein docking, substrate binding, ATP binding, and subsequent ATP hydrolysis.

### **The Maltose Transporter**

Most recently, the structure of the full maltose transporter in complex with the maltose binding protein and the maltose substrate was solved to 2.8 Å resolution (Oldham et al., 2007). This fascinating structure (PDB ID: 2r6g) is perhaps the most

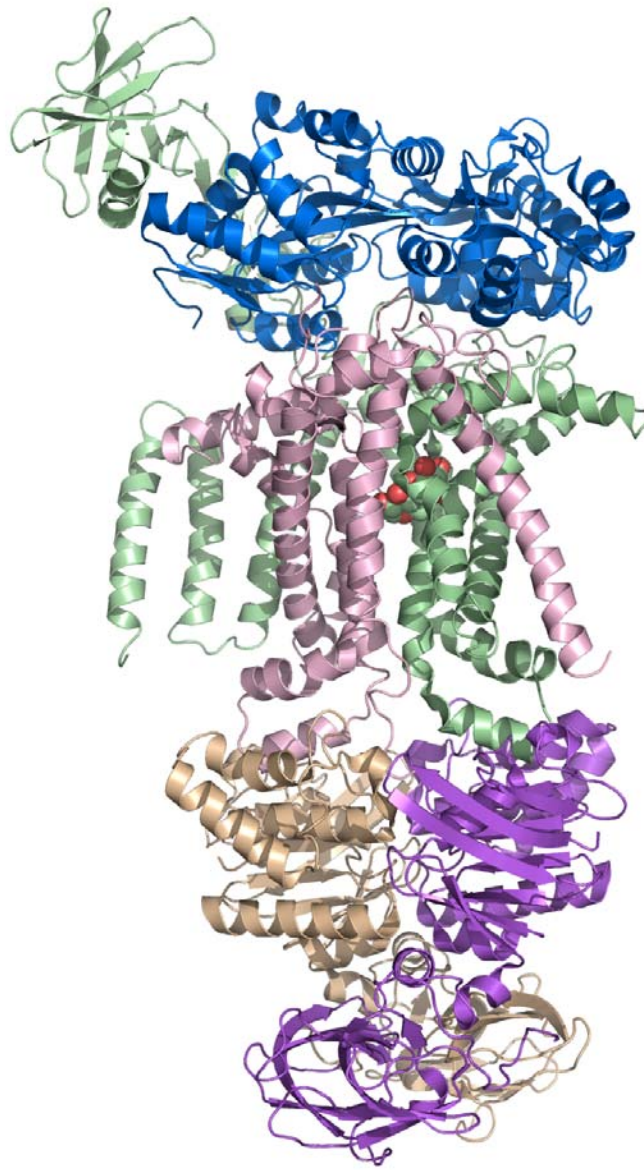


**Figure 1.7.** The structure of the complete maltose transporter, MalFGK, in complex with the maltose binding protein. This fascinating structure revealed the first substrate binding site within a translocation pathway, and provided considerable insight into the ability of the transmembrane domain (pink and green) to interact with the binding protein (blue) and encourage substrate release into the translocation pathway. Additionally, the ATPase subunits are closely intertwined in this ATP-bound state, while this structure reveals the first structure with structurally and sequentially unique transmembrane units (MalF in green, MalG in pink). These two subunits, while quite different in length, share a common core of 6 helices that forms the translocation pathway.

unusual of all ABC transporter structures, as it shows the maltose ligand within the translocation pathway, an observation heretofore unseen (Figure 1.7). The ATP-bound

structure was obtained using a mutation in the Walker B region that prevents ATP hydrolysis, thereby trapping the transporter in a “closed” state. The MalFGK<sub>2</sub> structure revealed the first ABC transporter with two different transmembrane domains comprising the translocation pathway. MalF and MalG share a common core of six helices, in an arrangement very similar to that of the ModBC structure; in this arrangement, one helix from each subunit crosses over and interacts with the opposite subunit. However, MalG and MalF share only 13% sequence identity, and the much longer MalF possesses a C-terminal segment that packs against the MalK subunit and is not present in MalG. The interface between the two transmembrane domains and MalK also shares similarities to the other published structures. The “EAA”, “EAAXXXG”, or “coupling helix” loop, as it has been named, is responsible for the majority of the interaction between the transmembrane domains and the ATPase units. Furthermore, it was established that the glutamate residue present in this loop forms a salt bridge with a highly conserved arginine residue. In the translocation pathway, maltose binding was stabilized by nearby residues. The sugar rings were packed against Tyr383 and Phe436 from MalF, while hydrogen bonding interactions with the maltose ligand are made by Tyr325, Ser329, Asn376, Gly380, Ser433, Asn437, and Asn440, all from MalF. MalG, interestingly, did not contact the maltose ligand. As the maltose ligand was found bound to the MalF maltose binding site, the maltose binding protein was in an open form. Similar to the BtuCD-F structure, the two lobes of the maltose binding protein were pried open, and a loop from the MalG protein named the “scoop” entered the maltose binding site, enabling its movement from the maltose binding site on the maltose binding protein into the MalF binding site within the transporter translocation pathway. This structure has many interesting features, and



**Figure 1.8.** The structure of the multidrug exporter SAV1866 from *S. aureus*. The complete structure is composed of two half-transporters (pink and green) that each possess a transmembrane domain and an ATPase domain. The two half-transporters are considerably intertwined in this conformation, though no nucleotide was bound.

represents the transition state of ligand transport much better than any previously published structure, providing a look at the ability of the translocation pathway to bind and transport this carbohydrate ligand.

### **ABC Exporters**

Structural studies of certain ABC exporters have also been pursued; while these exporters have significant differences from ABC importers, there are common features between these two groups. Perhaps the most striking similarity is between exporter and

importer ATP binding cassette domains, which possess conserved structural characteristics. The crystal structure of SAV1866, a multidrug exporter from *Staphylococcus aureus*, was solved by Dawson and Locher (2006) to 3.0 Å resolution, and shortly afterwards, a structure with bound AMP-PNP was solved to 3.4 Å resolution (Dawson and Locher, 2007). The structure of SAV1866 (PDB ID: 2hyd and 2onj) reveals two half-transporters that are intertwined to make up the active transporter. Each half-transporter consists of a transmembrane (N-terminal) domain and a nucleotide binding (C-terminal) domain, and are twisted around each other in the structure (Figure 1.8). Each transmembrane domain crosses the membrane lipid bilayer six times, resulting in a total of 12 TM helices for the full transporter. The NBD contains the typical ATP-binding cassette motifs and closely resembles the previously published structure of MJ0796 (Smith et al., 2002). While ADP is bound in the ATP binding cassette of SAV1866, Dawson and Locher have hypothesized that the transporter is actually in the ATP bound state, based on the tight binding of the nucleotide and a comparison to the previously published structure of BtuCD. In this structure, it is apparent that there are a few loops in the TMD that allow communication between the NBD and TMD. These loops (which actually have helical regions) are named “coupling helices”, to refer to the fact that they couple the movement of these two domains, depending on the presence of ATP and a substrate. Interestingly, the structure shows that there is a crossing-over that occurs within these helices, as one helix interfaces with the adjacent NBD, while the other interfaces with the opposite NBD. This arrangement also suggests that the nucleotide binding domains are not able to move far apart from one another, as is seen in MsbA (see below) and certain importers. The mechanism of transport suggested by Dawson and Locher involves two states of the transporter: an inward-facing conformation with interior

access to the substrate binding domain, and an outward-facing conformation with external access to release the unwanted substrate. SAV1866 is hypothesized to be in the ATP-bound, outward-facing state, where the substrates would be released into the lipid bilayer or the surrounding medium. The hydrolysis of ATP would convert the transporter back to its inward-facing conformation, in what Dawson and Locher have described as an “alternating access and release” mechanism. In addition to the SAV1866 multidrug exporter, structures in various conformations of the lipid flippase MsbA from three different organisms (*E. coli*, *V. cholerae*, and *S. typhimurium*) have been published (Ward et al., 2007). These structures (PDB ID: 3b60, 3b5w, 3b5x, 3b5y, 3b5z) also possess the characteristic ATPase domain and show different states of homologous transporters, despite the controversy associated with the original crystal structure analyses of these structures.

### 1.3 The Catalytic Cycle of ABC Transporters

Attempts to understand the catalytic cycle of ABC transporters have been underway for many years. It has been shown that both NBDs are required for transport and that one ATP binds to both domains of the dimer, suggesting that these two sites are coupled (al-Shawi et al., 1994; Loo and Charles, 1995). As the NBDs can dimerize and hydrolyze ATP in solution, crystallization studies of native ATP-bound NBDs has proved difficult. However, certain mutations abrogating ATP hydrolysis have enabled the study of ATP bound structures, such as the MJ0796 cassette (Smith et al., 2002). The ATP molecule is substantially bound by the NBD core: the Walker A and B motifs, as well as residues providing a  $\pi$ -stacking interaction with the adenine ring play an important role in this binding. Additionally, a histidine that is part of the His-loop contacts the nucleotide, the Q-loop interacts with the  $\gamma$ -phosphate of ATP through a water molecule,

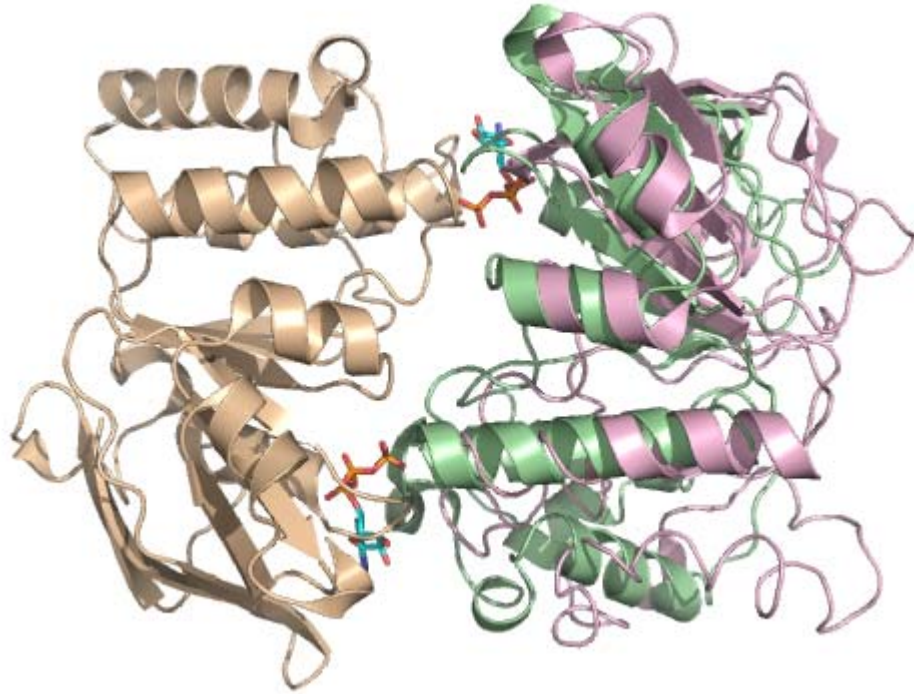


**Figure 1.9.** A comparison of two conformations of the MalK dimer. The overlay of one subunit (shown in tan) allows the differences in the relative placement of the opposing subunit (ATP-bound state in green, non-nucleotide form in pink) to be highlighted. The ATP-bound conformation clearly has the two ATPase subunits much closer together compared with the apo dimer.

and the ABC signature loop stabilizes the ATP molecule bound to the P-loop of the opposing NBD. Similarly, many NBDs do not form dimers in the absence of nucleotide. MalK is the exception to this, as it does form a dimer without nucleotide present, presumably due to the C-terminal extension beyond the homologous NBD region that is thought to be a regulatory domain. Intact transporters appear to be more stable in the absence of nucleotide, perhaps due to the TMDs, as evidenced by the number of nucleotide-free transporter structures. The study of the MalK dimers in various conformations (PDB ID: 1q12, 1q1b, 2awo) revealed a tweezer-like motion between the two dimers upon ATP binding (Davidson and Chen, 2004). The C-terminal “regulatory domain” remains in contact regardless of the nucleotide present, but the homologous nucleotide binding domain experiences considerable changes (Figure 1.9).

A common mechanism has been proposed for both ABC importers and exporters. It has recently been suggested that the binding of ATP promotes the outward-facing conformation, while the production and release of ADP and phosphate stabilizes the inward-facing conformation (Dawson and Locher, 2007). In most descriptions of the catalytic cycle, the P-loop and ABC signature motif are deemed important for interactions with ATP, while the Q-loops are important for the NBD-TMD interface. The “head-to-tail” arrangement of its NBD dimer is a critical element of ABC transporters, as this organization forces the opposing dimers to form two nucleotide binding sites using the conserved sequence motifs. The P-loop of one NBD forms a nucleotide binding site with the ABC signature motif from the opposite NBD, a concept first identified with the structure of the Rad50 protein (Hopfner et al., 2000). Nucleotide-free structures impose fewer constraints on the structure, as evidenced by the variations observed between nucleotide-free structures; the various conformations of these transporters have been classified in “open” or “closed” states. The “coupling

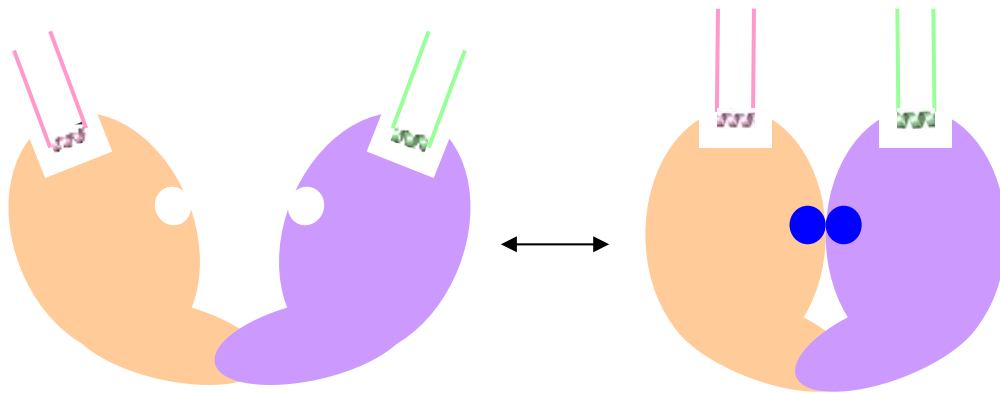


**Figure 1.10.** A conceptual diagram of the “closing” motion of nucleotide binding domains that occurs with ATP binding (ATP is represented in dark blue). This “closing” results in a shift towards the translocation pathway of the coupling helices of the transmembrane domain (in pink and green); this narrowing prepares the translocation pathway for substrate transport, pushing the transporter from an inward-facing to an outward-facing conformation.

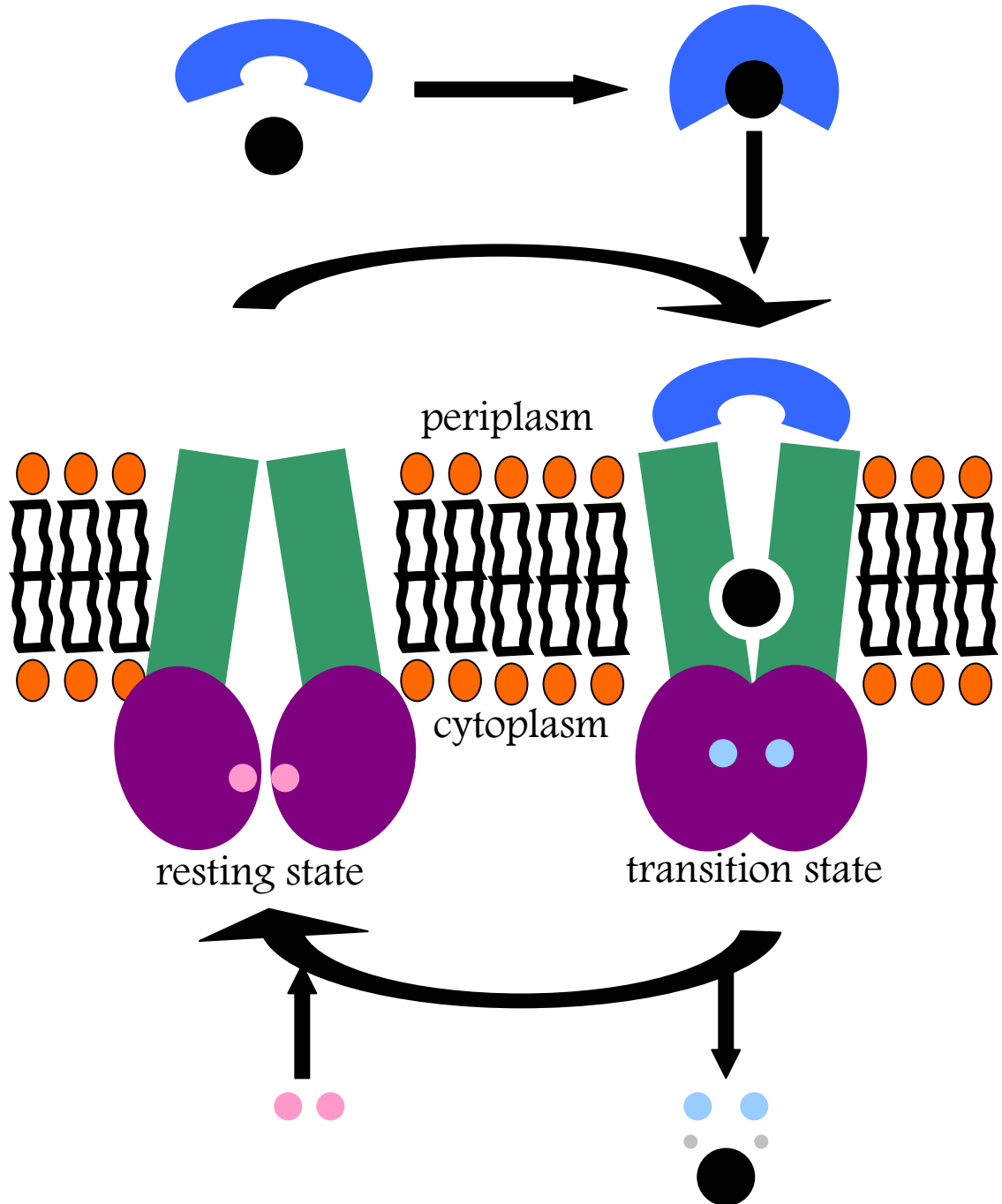


**Figure 1.11.** A schematic of the suggested mechanism of an ABC importer. In the resting state, the inward-facing transporter can bind ATP (pink spheres). ATP binding leads to complex formation with a substrate binding protein (blue) that has substrate bound (black sphere). As the substrate binding protein delivers the substrate to the transporter, the transporter shifts to the outward-facing conformation (in the transition state) and the substrate travels through the transmembrane domain, leading to release of the substrate and ADP (blue spheres) and P<sub>i</sub> (gray spheres) into the cytoplasm. The transporter then returns to the resting state awaiting the next cycle of ATP binding.

helices”, described as the important part of the TMD and its interface with the NBD, comprise the key shared feature amongst transmembrane regions. Movement of these helices towards or away from the translocation pathway appears to be important for the transmission of information between these two domains (Figure 1.10). Mutations in this area result in a decrease in transport or no transport at all (Hollenstein et al., 2007).

The full catalytic cycle may be summarized through a few different states (Figure 1.11). In the “open” state, NBDs are apart. Examples of this state include the ModBC-ModA or HI1470/1 structures. Once ATP binding occurs, the transporter can shift into a “closed” conformation, where the ATP is bound tightly between the NBD motifs previously mentioned, such as the P-loop and the ABC signature loop. Examples of an ATP-bound structure would include the MalFGK<sub>2</sub> structure, as well as the SAV1866 exporter structure. In addition to the movement of NBDs, a key difference between these two conformations is the movement of the “coupling helices” and the subsequent shift of transmembrane helices. In moving from the “open” to “closed” states, the transmembrane helices shift towards each other. Once hydrolysis of ATP occurs, the transporter shifts back to the “open” conformation, its resting state. The stoichiometry of transport has been established; studies of glycine transporter OpuA (Patzlaff et al., 2003) as well as studies of the maltose transporter MalK have revealed that there appear to be two ATP molecules required per one molecule of substrate transported (Dawson and Locher, 2007). Overall, this mechanism corresponds to the “alternating access and release” mechanism first postulated by Jardetzky in 1966.

#### **1.4 Regulatory Mechanisms: The ACT Domain**

The regulation of many ABC transporters can occur at the gene level. However, ABC transporters often possess C-terminal domains connected to the nucleotide binding

domains that are proposed to function as regulatory domains (Biemans-Oldehinkel, 2006). These “autoregulatory” domains are present in a variety of ABC transporters: MalK, OpuA, CFTR, and others. Each of these domains, however, is hypothesized to act in different ways. One such mechanism predicted to be important for some amino acid ABC transporters is the ACT domain.

The ACT domain, initially identified by Aravind and Koonin (1999), is a novel ligand-binding domain based upon a similarity in three different structures: aspartokinase, chorismate mutase, and TyrA (ACT). This shared domain of unknown function was identified in aspartokinases, chorismate mutases, prephenate dehydrogenases, prephenate dehydratases, homoserine dehydrogenases, malate dehydrogenases, phosphoglycerate dehydrogenases, phenylalanine and tryptophan-4-monooxygenases, phosphoribosylformylglycinamide synthase, uridylyl transferase and removing enzyme, GTP pyrophosphokinase/phosphohydrolase, tyrosine and phenol metabolism operon regulators, as well as several uncharacterized proteins from archaea, bacteria, and plants that contain from one to four copies of this domain (Aravind and Koonin, 1999). Luckily, some of these proteins had been structurally

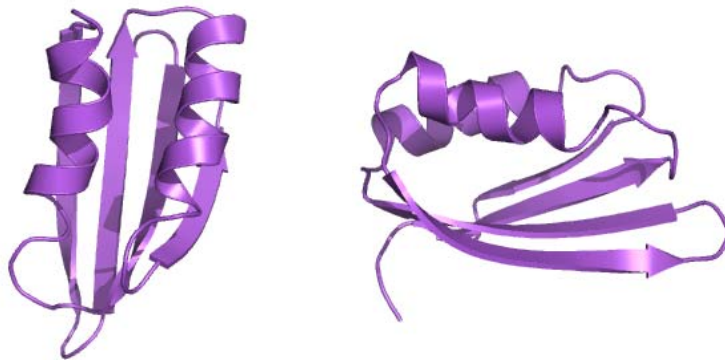


**Figure 1.12.** Two views of the ferredoxin-like domain that make up each monomer of the ACT domain. Four  $\beta$ -strands make up an antiparallel  $\beta$ -sheet, with two  $\alpha$ -helices covering one face of the strand. This domain dimerizes to form the complete ACT domain.



**Figure 1.13.** The ACT domain of 3-phosphoglycerate dehydrogenase. The two ferredoxin-like domains form an 8-stranded  $\beta$ -sheet capped by 4  $\alpha$ -helices. The two serine molecules (in blue) bind at the interface of these two domains; this binding site is shared amongst other ligands utilizing this domain.

characterized, allowing a further analysis of this domain. The structure of 3-phosphoglycerate dehydrogenase (PDBID: 1psd) revealed this domain to be the C-terminal regulatory domain of 70-80 amino acids that formed a  $\beta$ -sheet with strand order 4-1-3-2 surrounded by helices (Figure 1.12). Upon further analysis, this domain was identified as having the ferredoxin-like fold, according to SCOP. A ferredoxin-like fold is defined as having the  $\beta\alpha\beta\beta\alpha\beta$  topology (Chipman and Shaanan, 2001). In the structure of 3-phosphoglycerate dehydrogenase, this domain binds L-serine, the final product of this biosynthetic pathway, and an allosteric regulator of this enzyme. The ACT domain is thought to possess a common ligand-binding area, critical to the function of this fold in regulation; many of the enzymes possessing this domain are known as “classic” allosteric regulators. Further analysis of this domain revealed that this domain forms a dimer, resulting in an 8-stranded  $\beta$ -sheet, with 2 ligand molecules

bound at the interface, suggesting that this is a conserved regulatory fold. While certain ACT family members show sequence homology, others have more divergent sequences while maintaining the same topology and ligand binding site (Chipman and Shaanan, 2001). A study of the types of proteins possessing ACT domains revealed that the majority of these are involved in amino acid and purine biosynthesis, and were previously known to be allosterically regulated proteins (Liberles et al., 2005). While the mechanism of action of this domain is not fully understood, it has been suggested that ligand binding leads to low flexibility within this domain and the rest of the structure, as rotations to allow for normal activity are blocked (Grant, 2006). As ACT domains have been identified in Archea, Bacteria, and Eukarya, they have been described as a “conserved, evolutionarily mobile module that, when fused to other proteins, makes them susceptible to regulation by small molecules” that probably appeared early on in the evolutionary process (Grant, 2006).

## Chapter Two. MetNI.

### 2.1 Introduction

The high-affinity methionine transport system MetD of *E. coli* consists of MetN, the ATPase domain, MetI, the transmembrane domain, and MetQ, the cognate binding protein located in the periplasm. The progression of study that resulted in the identification and characterization of MetD dates back to the mid-1950s, when amino acid transport in bacteria became a significant topic of research. While the methionine transporter was first partially described by Piperno and Oxender in 1968, numerous studies in the 1970s by Robert Kadner characterized the methionine uptake system in *E. coli*. A study by Kaback et al. (1970) suggested that methionine uptake (among other amino acids) was enhanced by the presence of D-(-)-lactate, although membrane vesicles were unable to accumulate methionine, forging questions in the minds of these researchers about what type of transport systems brought methionine into the cell, and whether these transport systems utilized a binding protein and/or ATP, or were able to directly derive energy from some portion of the electron transport chain (Kadner, 1974). Other amino acids were thought to be transported into the cell via multiple mechanisms, some of which employed a binding protein and ATP, while others directly utilized energy from the electron transport chain, as described by Lombardi and Kaback (1972). Kadner, however, set out to provide a more complete characterization of the methionine uptake system. Interestingly, Kadner also was responsible for initial characterization of the BtuCD Vitamin B<sub>12</sub> ABC transporter system (Kadner and Watson, 1974), a connection that was derived from the biosynthesis-related ties between these two nutrients established by Davis and Solowey (1950).

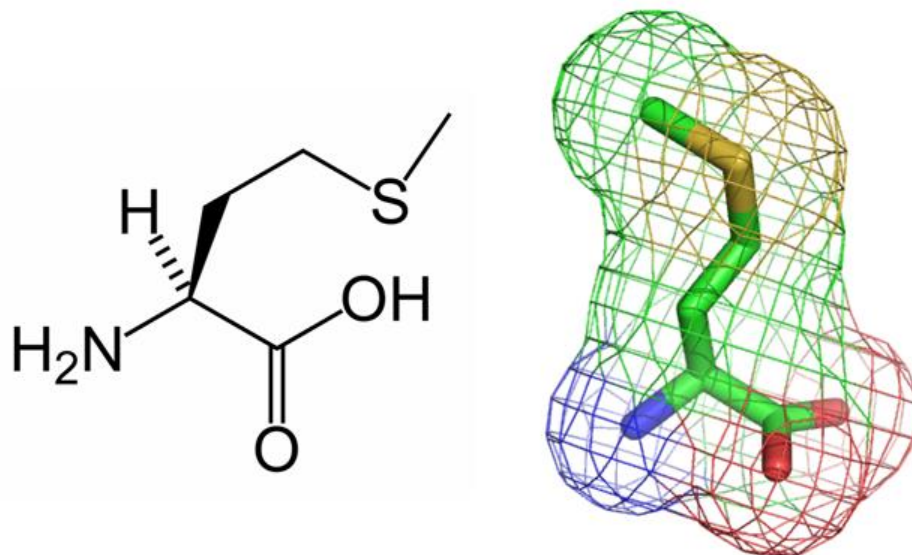


**Figure 2.1.** Above is the structure of the amino acid L-methionine, in both chemical (left) and 3-dimensional (right) forms. It is this amino acid that is being transported by the MetNI transport system.

The first studies by Kadner on this system described a temperature-dependent methionine uptake system that allowed for the accumulation of methionine (Figure 2.1) against a gradient. Kadner (1974) reported that the internal pool of methionine is estimated to be 0.1-0.3 mM, as the vast majority of intracellular methionine is converted to other metabolites such as spermine and spermidine within five minutes after uptake. Kadner suggested that this uptake was somehow dependent on energy, but was unsure whether this energy source came from glycolysis or oxidative phosphorylation. He was further able to identify two separate methionine transport systems: a high-affinity system (with a  $K_t$  of approximately  $7.5 \times 10^{-8}$  M) and a low-affinity system (with a  $K_t$  of approximately  $40 \times 10^{-6}$  M) that differed over 400-fold in their ability to transport L-methionine. In his initial characterization, he was also able to identify certain methionine derivatives or dipeptides that acted as inhibitors to the methionine uptake system, and to determine that D-methionine, ethionine, and other

amino acids had low inhibitory activity. However, further studies began to slightly contradict his initial paper. Later the same year, he published a paper (Kadner and Watson, 1974) further describing the two uptake systems for methionine, named MetD and MetP. These studies suggested that the higher-affinity system, MetD, was in fact able to transport D-methionine as well as L-selenomethionine. Kadner went on to study and better understand the MetD and MetP mutants and the effects of these mutants on methionine activity; mutants of MetD lack high-affinity transport for L-methionine and low-affinity uptake for D-methionine (Kadner, 1977).

As Kadner progressed in his study of the methionine uptake system, he encountered a mechanism of regulation in *E. coli*. In 1975, Kadner described that the activity of the methionine uptake transporter is regulated by the concentration of the internal methionine pool. He found that the activity of the transporter is depressed when cells are grown in the presence of methionine, but not methionine mimetics such as  $\alpha$ -keto- $\gamma$ -methiol-butyrates, D-methionine, or methionine sulfoxide. His research additionally suggested that this transport system was regulated by gene repression. Studies of the MetD system by Kadner revealed that D-methionine was a useful methionine source for *E. coli* and was transported by the MetD system (Kadner, 1977). He further hypothesized that there were two substrate binding domains within the MetD system for both stereoisomers. Energetics studies suggested that transport was driven by phosphate bond energy (Kadner, 1975), but the use of ATP was not confirmed conclusively until another study. Another paper published in 1975 provided further evidence that the source of metabolic energy that allowed the transport of methionine was in fact ATP. The transport of methionine was found to be sensitive to arsenate but mostly insensitive to azide or dinitrophenol. Furthermore, adenosine

triphosphatase mutants were created that affected transport and supported the idea that methionine transport utilizes ATP (Kadner and Winkler, 1975).

It was not until 2002 that the genes for the MetD system were identified and described as possibly comprising an ABC transporter (Merlin et al., 2002). Within the gene locus initially identified by Kadner, Merlin et al. were able to find six genes, of which four were unidentified and two (Abc and YaeE) were thought to be an ABC transporter ATPase and an ABC transporter permease, respectively. These two genes, Abc and YaeE, were labeled as an ABC transporter due to sequence homology, particularly the Abc protein that contained many ABC transporter sequence motifs. The permease, YaeE, was hypothesized to possess five transmembrane helices. Further analysis using the BLAST tool identified YaeC as a possible methionine binding protein; the three genes were subsequently renamed to MetN, MetI, and MetQ to represent the ATPase, transmembrane domain, and binding protein, respectively. Merlin et al. also studied the genetic organization of the MetD locus within a variety of other sequenced bacteria. A similar organization was found in *S. typhimurium*, *S. typhi*, *Y. pestis*, *V. cholerae*, *P. multocida*, *H. influenzae*, *A. tumefaciens*, *S. meliloti*, *B. melitensis*, and *M. loti*, suggesting that each of these organisms has a similar methionine uptake system. Their studies described MetD deletants that were able to grow on a media supplemented with L-methionine (due to uptake from the MetP system) but were unable to grow on a media supplemented with D-methionine as its sole methionine source. Furthermore, the MetJ repressor acts as a regulator of the three metD genes at the genetic level, as shown by both Merlin et al. (2002) and Gál et al. (2002). Efforts to identify genes encoding other methionine uptake system, MetP, have thus far not been successful.

Building further on the concept that a similar organization for this gene is present in multiple organisms, Zhang et al. (2003) redefined this system as a methionine uptake transporter (MUT). Their phylogenetic analysis revealed that this methionine uptake system was present in multiple organisms in the form of sequence-divergent primordial paralogs. These proteins make up the methionine uptake transporter family, one of the first functionally characterized novel families of bacterial ABC permeases. An analysis of MetD mutations in *S. typhimurium* led to the mapping of the MetD gene near 4.8 minutes on the *E. coli* genome, which coincides with an ABC transporter mapping (Zhang et al., 2003). Regulation by these genes and other methionine biosynthetic genes by the MetJ repressor has been established (Weissbach and Brot, 1991; Greene and Spiegelman, 1996; Sekowsha et al., 2000), along with a MetJ DNA binding site consensus sequence (Saint-Girons et al., 1984) and the identification of a MetJ binding site in the promoter region of the MetD ABC transporter locus (Liu et al., 2001). Homologues of each of the three proteins within the MUT family share a similar size, and the transmembrane regions for all of them are hypothesized to have five transmembrane segments. The relationships revealed in the phylogenetic analysis suggest that these genetic duplications occurred early during evolutionary history, as the topology of the phylogenetic trees does not follow the phylogenies of these organisms. It has been hypothesized that there were several sequence-divergent primordial paralogs, which would account for the topology seen.

Zhang et al. (2003) went on to reveal that both L-methionine and D-methionine were transported by the MetD transporter system. Studies using radiolabeled (<sup>14</sup>C) L- and D-methionine showed that both L- and D-methionine were substrates of the same MetD transporter system. Inhibition studies confirmed previous studies on this subject; while other amino acids were not inhibitors, N-formyl L-methionine was.

Furthermore, the use of energy poisons such as sodium arsenate abolished uptake of methionine, while others were less effective, suggesting that ATP is in fact the energy source for transport, as believed.

Studies have also elucidated possible pharmaceutical interest in this family of transporters, as several members of the MUT family are required for bacterial pathogenicity. It has been found that the MUT family member of *S. typhimurium* is essential for infection in mouse models (Pattery et al., 1999). A mutation in the MUT in the organism *H. influenzae* leads to reduced infection in rats (Chanyangam et al., 1991). The *H. pylori* MUT plays a role in the production of urease, which is essential for colonization of this organism (Hendricks and Mobley, 1997). Strains of *Y. pestis* frequently depend upon exogenous methionine for survival, and may also make MUTs important in this organism (Brubaker, 1972). The importance of this family of transporters is not fully understood, but the implications within the pharmaceutical field are clearly growing, necessitating further study of this system.

To further investigate this system, we have determined the structure of the *E. coli* methionine ABC transporter MetNI following overexpression and affinity purification with dodecyl maltoside.

## **2.2 Structure of the MetNI Transporter**

Crystallographic analysis revealed a nucleotide-free state (Figure 2.2 and Figure 2.3) that was refined to 3.7 Å after phasing with single isomorphous replacement and anomalous scattering from a xenon derivative (Figure 2.4). The sequence register was verified with a difference Fourier density map from data collected on selenomethionine-substituted crystals, which identified 34 selenomethionine sites, as well as improved maps generated from solvent flattening and non-crystallographic symmetry averaging.

The overall architecture of MetNI reveals two copies of the ATPase MetN in complex with two copies of the transmembrane domain MetI. The methionine transporter has a smaller transmembrane domain than other published ABC transporter structures, consisting of only five transmembrane helices per monomer. The cytoplasmic ATPase contains the expected conserved ABC region, but possesses a C-terminal extension of approximately 100 amino acids that comprises an ACT regulatory domain that has not been seen previously as part of an ABC transporter. The relative positions of the two ATPase subunits and their corresponding transmembrane domains illustrate a distinct inward-facing orientation. Additionally, each of the two copies of MetN in the transporter adopts slightly different conformations, resulting in an asymmetrical organization of the MetN dimer due to a proposed hinge between the conserved ABC region and the C-terminal domain.

Analysis of this crystal form established the presence of two transporters in the asymmetric unit (Figure 2.5). Interestingly, these two transporters are in slightly different conformations, with one heterotetramer in a slightly more inward-facing orientation than the other. This difference is subtle, however, as the two different heterotetramers have an overall r.m.s.d. of 1.2 Å between each other. Individual subunits resemble one another closely through non-crystallographic symmetry relationships. However, when overlaid, the differences between the two transporters are visible; one heterotetramer has the ATPase units pushed slightly together, with accompanying changes within the transmembrane domain (Figure 2.6). The movement between these two states may be minor, but it extends across the whole transporter. The cytoplasmic-facing portion of the transmembrane domains of the less inward-facing transporter is tilted closer to the translocation pathway. The ATPase domains of the less inward-facing transporter are rotated slightly as well, and there is a

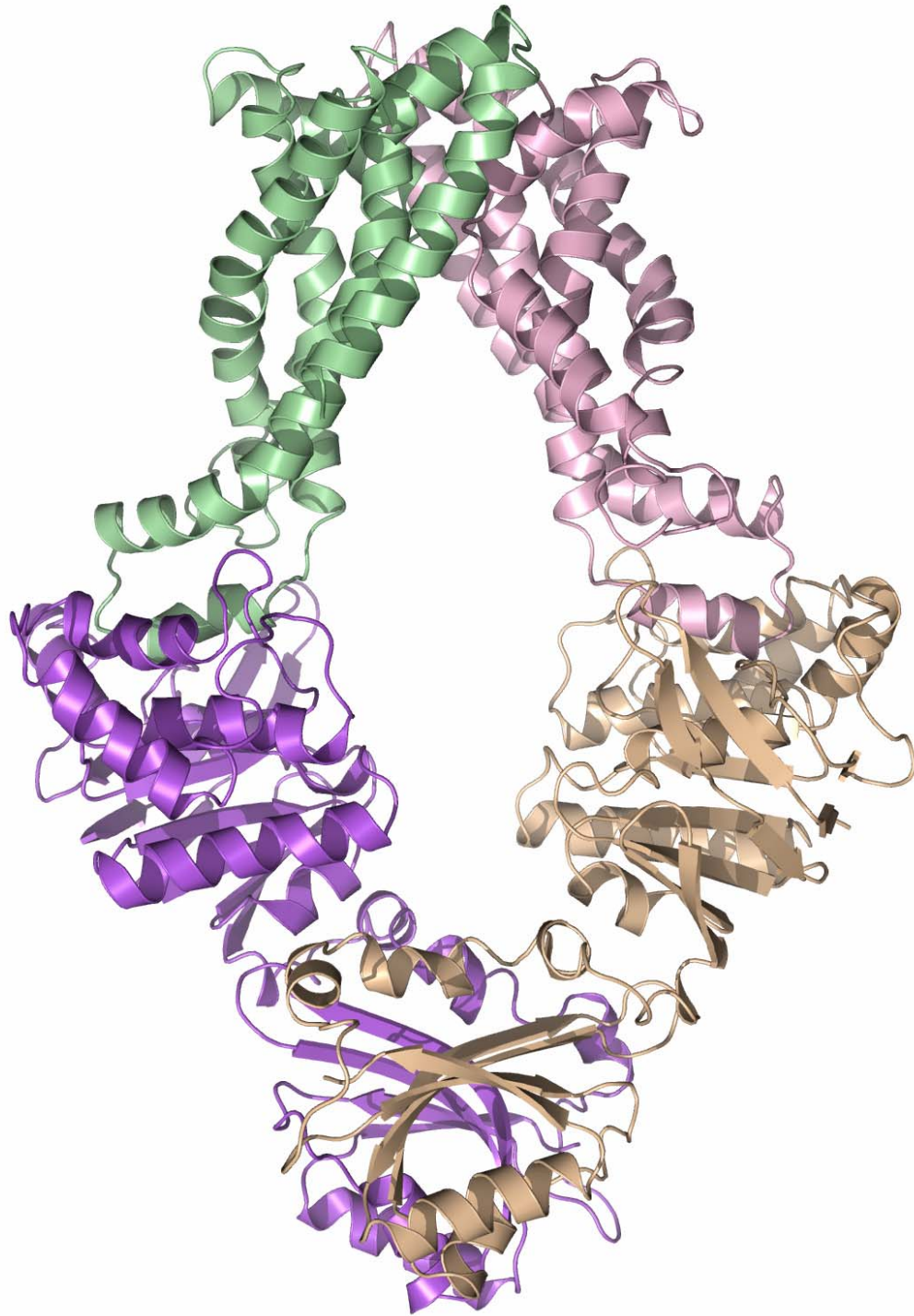


**Figure 2.2.** The *E.coli* methionine transporter MetN<sub>2</sub>I<sub>2</sub> is a tetramer consisting of two copies of the transmembrane (MetI) permease protein (pink and green) in complex with two copies of an ATP binding cassette (MetN) protein (tan and purple). The transmembrane protein consists of five transmembrane helices, with the N-terminus into the periplasm and C-terminus facing the cytoplasm. Each ATP binding cassette protein consists of a domain homologous with other ABC transporters and a C-terminal regulatory domain. In this conformation, the two regulatory domains are in close contact, while the ATP binding cassette regions are held apart from one another.

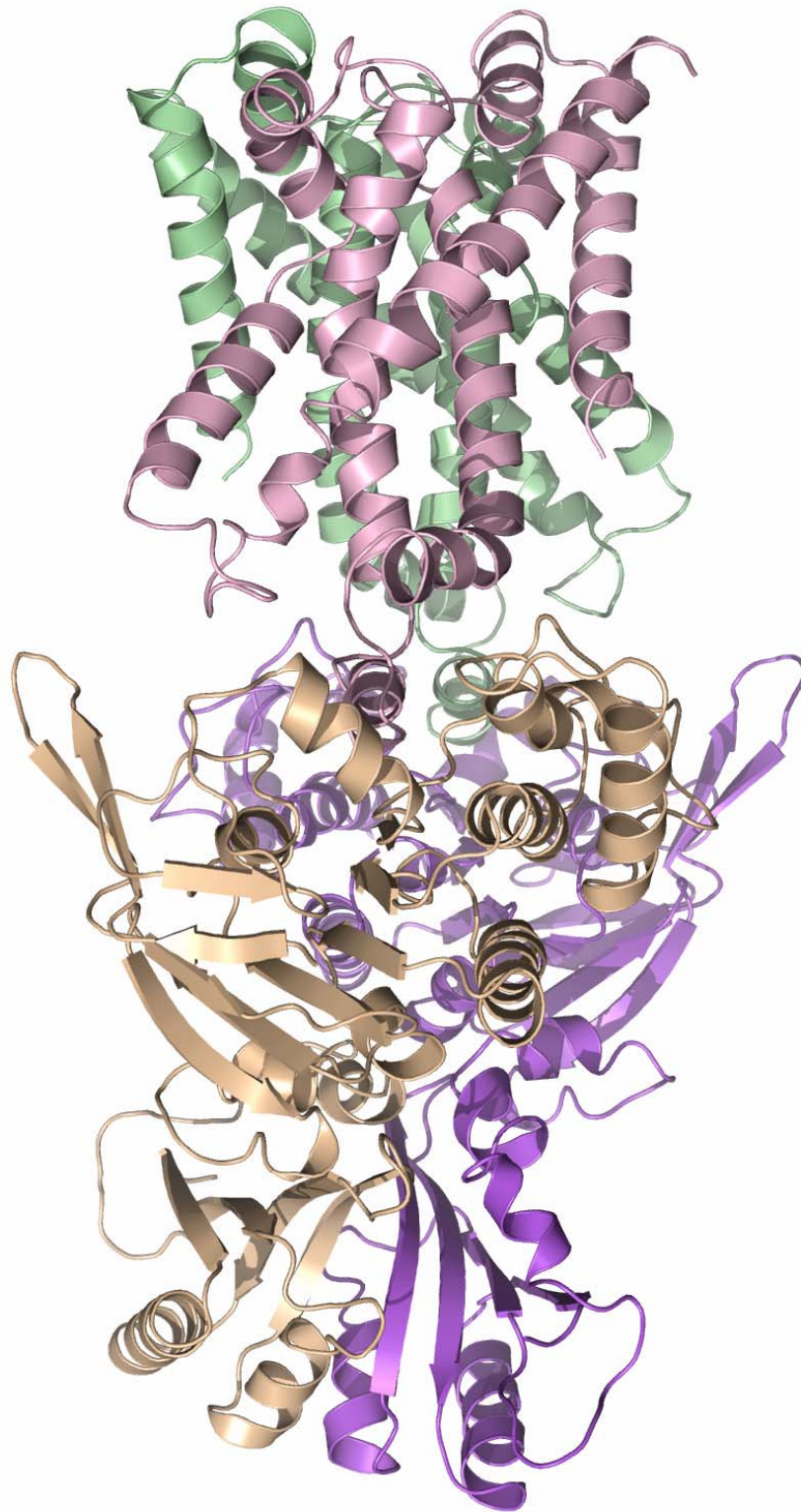


**Figure 2.3.** A side view of the transporter clearly illustrates the asymmetry between the two chains of MetN. There is a two-fold axis of symmetry between each chain of MetI, but the relationship between the two copies of MetN is considerably more complicated. The two copies of MetN are in different conformations, despite axes of symmetry between each domain when viewed separately.

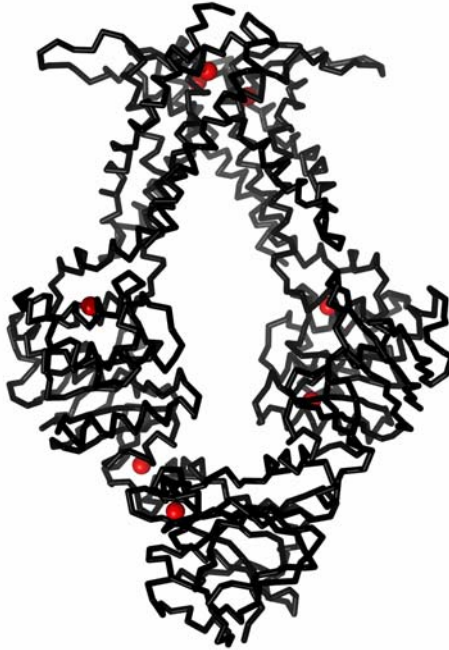


**Figure 2.4.** The initial chain trace of the MetNI transporter (black) with the Xenon binding sites (red spheres) is shown above. There were 17 total Xe atoms bound to the two transporters within the asymmetric unit.

**Figure 2.5.** The asymmetric unit of the MetNI crystal form is shown below. The two intact transporters are packed end to end. There are other crystal contacts within the ATPase domain, but none within the transmembrane domain.

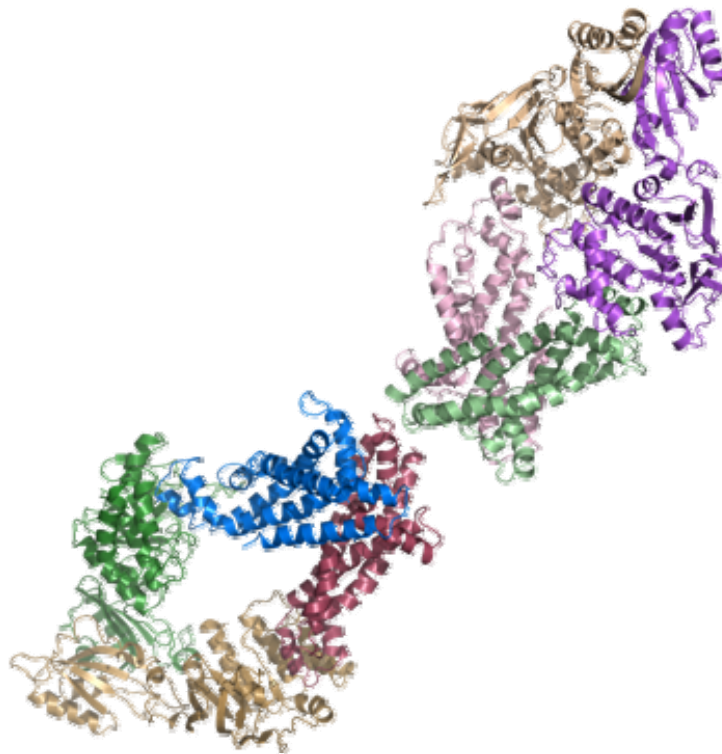




**Figure 2.6.** Above is an overlay of the two full transporters within the asymmetric unit. While the transmembrane domains and homologous ATPase regions possess small differences, there is a much larger range in the position the C-terminal extension, shown with the brown, purple, green, and tan regions representing this extra ACT-like domain

noticeable twist in the position of the ACT domain that makes up the C-terminal extension. This movement may be indicative of the types of changes accompanying the large scale transition between the inward- and outward-facing conformations.

### **Transmembrane Domain**

Each set of the membrane-spanning subunits of MetI are related by an approximate two-fold rotation axis ( $\sim 180^\circ$ ) and are otherwise essentially identical. A subunit of the transmembrane domain MetI consists of 5 transmembrane helices organized similarly to the core of the membrane-spanning subunits of ModB, MalF, and MalG, as ModB, MalF, and MalG contain an N-terminal helix not seen in MetI (Figure 2.7). As a result, the N-terminus of MetI lies in the periplasm, while the C-terminus

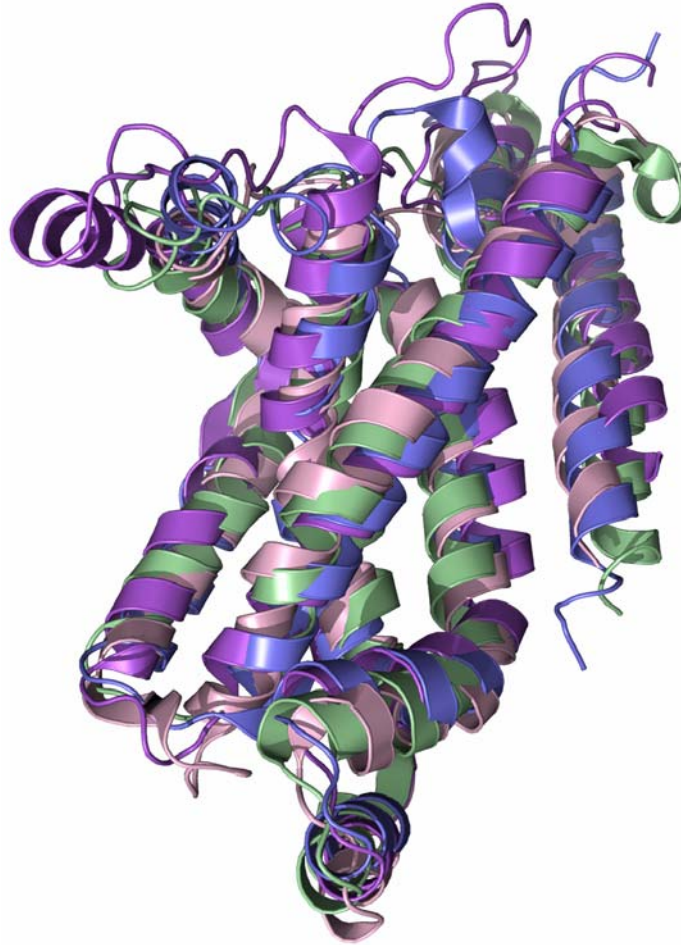


**Figure 2.7.** The five transmembrane helices that make up the core of the transmembrane domains of MetI (pink), ModB (green), MalF (blue) and MalG (purple) are closely related in structure. Above is a picture of the core of these four transmembrane domains superimposed.

protrudes into the cytoplasm, a difference from other observed structures that all possess an even number of transmembrane helices per monomer and consequently have both termini in the cytoplasm. Helix TM 1 begins in the periplasm and forms a diagonal across the outside face of the other four helices, while TM 2 is a kinked helix that traverses from the cytoplasmic edge of the membrane back towards the periplasm. A loop helps to transition into TM 3, which leads to the short “coupling helix” that interfaces with the ATPase domain and, along with TM 4 makes up the central core of the translocation pathway. The C-terminal TM 5 helix traverses the membrane once

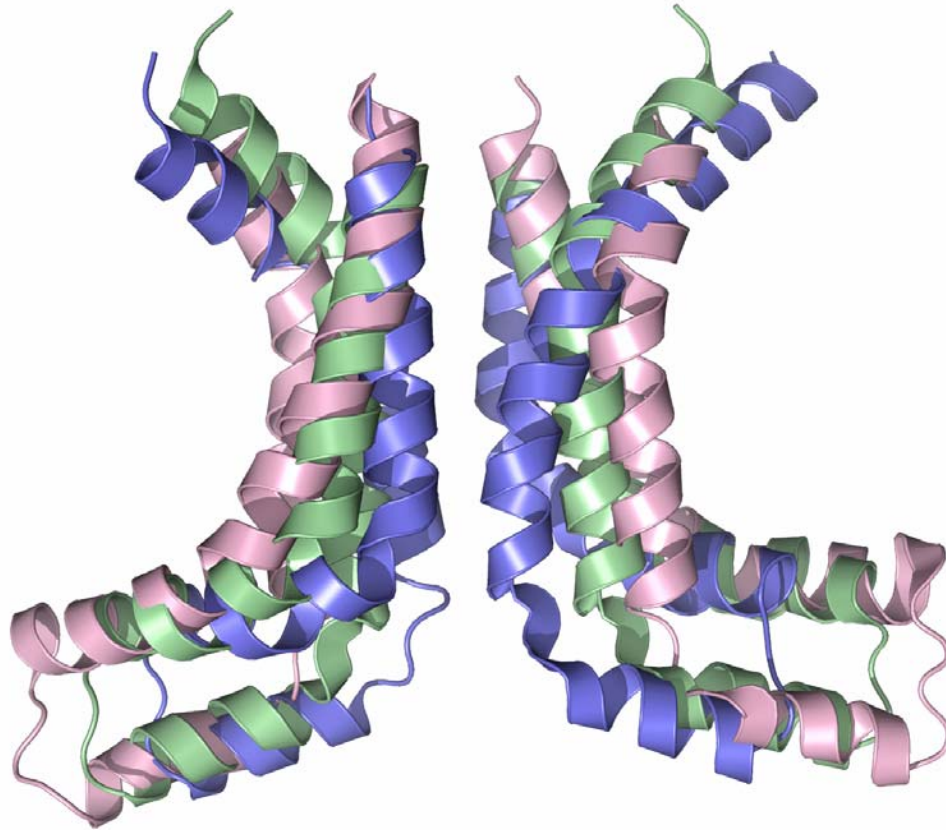


**Figure 2.8.** The diagram above illustrates the difference in translocation pathways (showing the coupling helix and the two helices on either side) between MetI (pink), ModB (green), and MalFG (blue). The MetI model clearly shows a much larger pathway with the coupling helices tilted much further away from the translocation pathway than the ModB or MalFG transmembrane helices.

more, ending in the cytoplasm, on the opposite side from TM2, as these two helices form the outer core of the helices close their counterparts on the other monomer.

Comparisons to other ABC transporters such as BtuCD and HI1470/1 are difficult, as the helical structure of these 10-helix domains differs significantly from the MetI structure, resulting in distinct organizations. When comparing individual subunits, the root mean square deviation (r.m.s.d.) of structurally equivalent C $\alpha$  atoms of ModB and MetI is  $\sim 3.4$  Å, that of MalG and MetI is  $\sim 2.7$  Å, and that of MalF and MetI is  $\sim 2.6$  Å (Figure 2.7). The relative positions of the two copies of MetI demonstrate a wider, more inward-facing conformation than either the ModB or the MalFG dimers. Interestingly, the region of highest sequence similarity between these

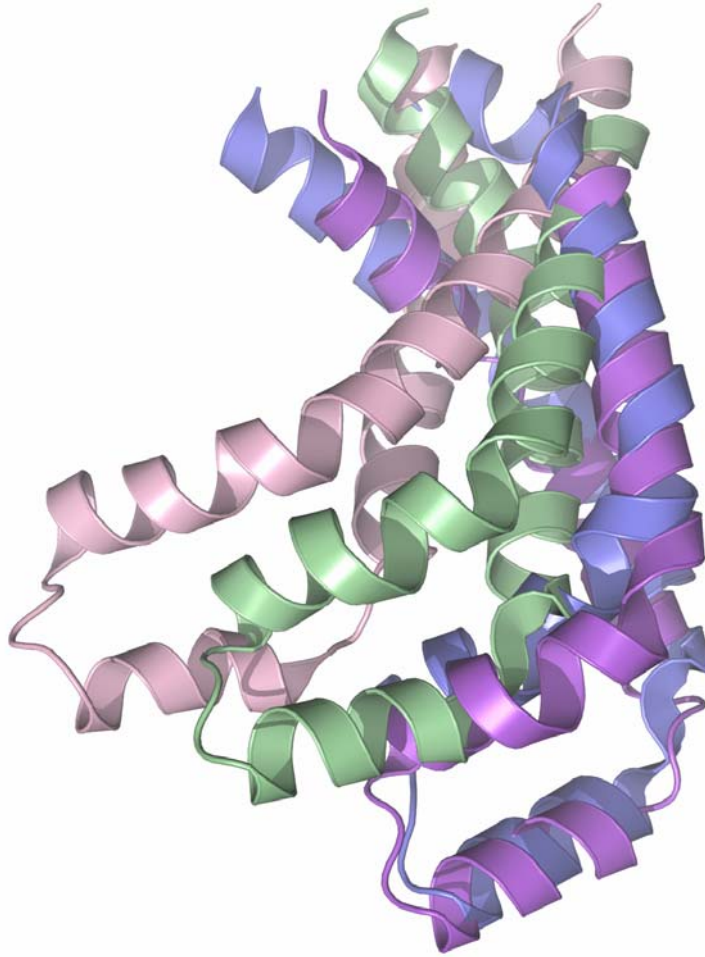


**Figure 2.9.** The coupling helix and the segments of helices in close proximity to this helix display a large change between the nucleotide-free, inward-facing MetI conformation (pink) and the ATP-bound, substrate-occluded MalFG conformation (purple), with the ModB conformation (green) appearing as an intermediate between the two. Rotational motion towards the translocation pathway accounts for the major differences between the MetI and MalFG conformations; the opposing transmembrane domains were superimposed to highlight this movement.

structures consists of the previously named “coupling helix” and the two transmembrane helices on either side, the region which forms the central core of the translocation pathway (Table A1.1).

The coupling helix and the neighboring transmembrane helices display the most significant change between the nucleotide-free, inward-facing MetI conformation and the ATP-bound, substrate-occluded MalFG conformation. For MetI, these elements correspond to TM3-coupling helix-TM4, while on MalF this region corresponds to TM6-coupling helix-TM7, and for MalG and ModB it is TM4-coupling helix-TM5, due

to their N-terminal extensions beyond the 5-TM core shared by all four proteins. As a whole, this region in MalFG exhibits the greatest shift toward the translocation pathway, as the two transmembrane helices are pushed closer to the central axis of the translocation pathway than those of MetI or ModB (Figure 2.8 and Figure 2.9). This movement is presumably crucial to activating the permease pathway for transport; the communication between the ATPase domain and this transmembrane region is accomplished through a translation of the coupling helix toward the translocation pathway to allow for ATP hydrolysis and transport. Superposition of this region of the MalFG dimer with the corresponding portion of the MetI dimer illustrates this tilt of the cytoplasmic-proximate region of the MalFG transmembrane domain towards the center of the translocation pathway as compared with MetI<sub>2</sub>, with ModB<sub>2</sub> appearing as an intermediate between these two states. The TM3 helix on MetI exhibits a rotation of approximately 22° away from the translocation pathway as compared with TM6 (TM 6) of MalG (MalF), while the TM4 helix of MetI is similarly rotated approximately 24° away from MalFG, with the greatest distance on the cytoplasmic-facing region of these helices being roughly 10 Å. The difference in positions of the coupling helices themselves appear based on a translational shift towards the translocation pathway rather than a tilting movement. These short helices, part of the EAAXXXG motif previously described by Saurin et al. (1994), exhibit considerable sequence similarity, and each possess an important glutamate residue. This residue, Glu121 in MetI, is thought to modulate the relationship between the TMD and NBD through a salt bridge with an arginine, present in MetN as Arg47. The coupling helices in MetI appear to be shifted away from the translocation path by approximately 8 Å from the corresponding residues on MalFG, with a minimal change in the slope. Conversely, the periplasmic-adjacent regions of MetI<sub>2</sub>, MalFG, and ModB<sub>2</sub> show considerable overlap, supporting

the hypothesis that movement of these transmembrane domains is tweezer-like depending on the state of nucleotide binding. Additionally, the similarities extend to TM2 of MetI (and its equivalents in ModB, MalF, and MalG), particularly with respect to the shared helix length (a short 15 residues) and a kink in the helix caused by a proline residue (Pro67 in MetI).

### ATPase Domain

The MetN ATP binding cassette protein consists of two domains, the approximately 225 amino-acid ATPase domain that is homologous with many other ABC transporters, and a C-terminal domain, comprised of the last 118 residues. The

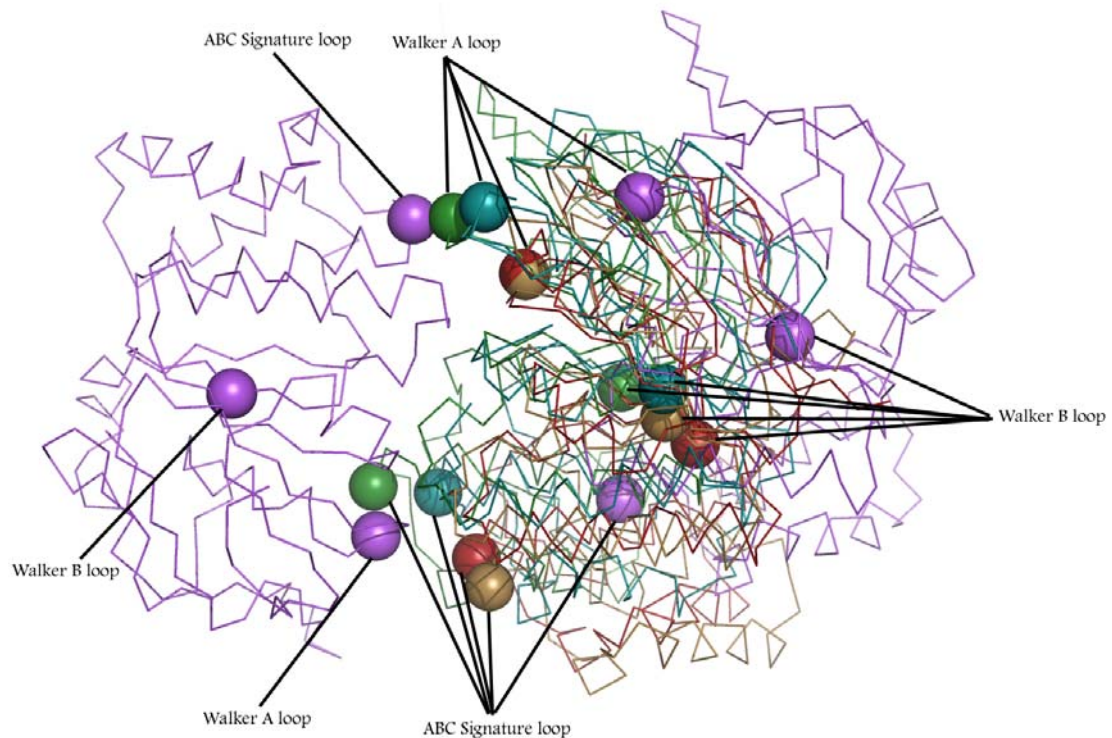


**Figure 2.10.** A comparison of the structural motifs (labeled above) present in each of the previously studied ATP binding cassettes is shown here. In each case, one ATPase subunit was superimposed with the MetN subunit shown in purple. The right side of the diagram shows the placement of the maltose transporter (green), the molybdate transporter (gold), the metal-chelate transporter (red) and the vitamin B-12 transporter (blue). The MetN subunits are clearly further apart than any others, and are separated by both a translation and rotation.

ATPase domain of the methionine transporter possesses the characteristic features shared by many ABC transporters that were first identified in the structure of HisP (Hung et al., 1998). Similar to other characterized ATPase domains, the MetN monomer possesses a six-stranded  $\beta$ -sheet with strand order 2-3-4-1-5-6, with strand 6 being antiparallel to the five other strands. This domain possesses another  $\beta$ -sheet, comprised of four  $\beta$ -strands in an antiparallel structure with strand order 2-1-3-4. The two sheets surround one of the  $\alpha$ -helices, and are bordered by another 8 helices that make up this domain. The features found in this structure are similar to those described in the structure of HisP, which further divided the ATPase structure into two separate domains consisting of an  $\alpha$ - plus  $\beta$ - type structure in one domain and a primarily helical second domain. Interestingly, when this overall fold was first identified, it was

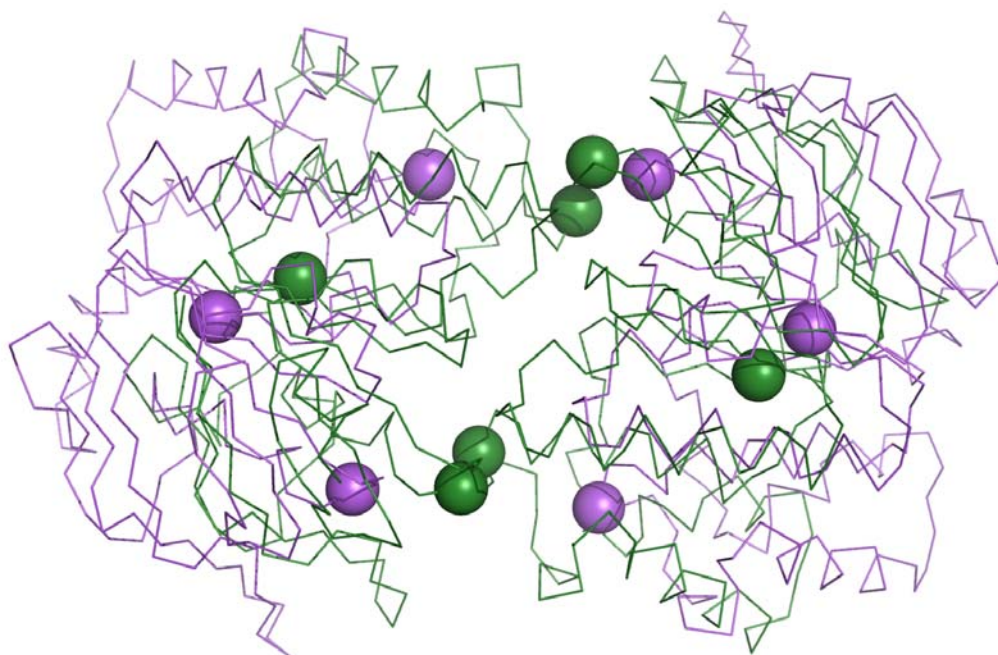


**Figure 2.11.** A top-down view of the ATP-binding cassettes of MetN (purple) and MalK (green) reveals differences in the relative positions of conserved motifs in a simpler view. The Walker A, Walker B, and Signature motifs are highlighted (see Figure 2.10 for labels). In this cartoon, the alignment is based on both subunits in the dimer.

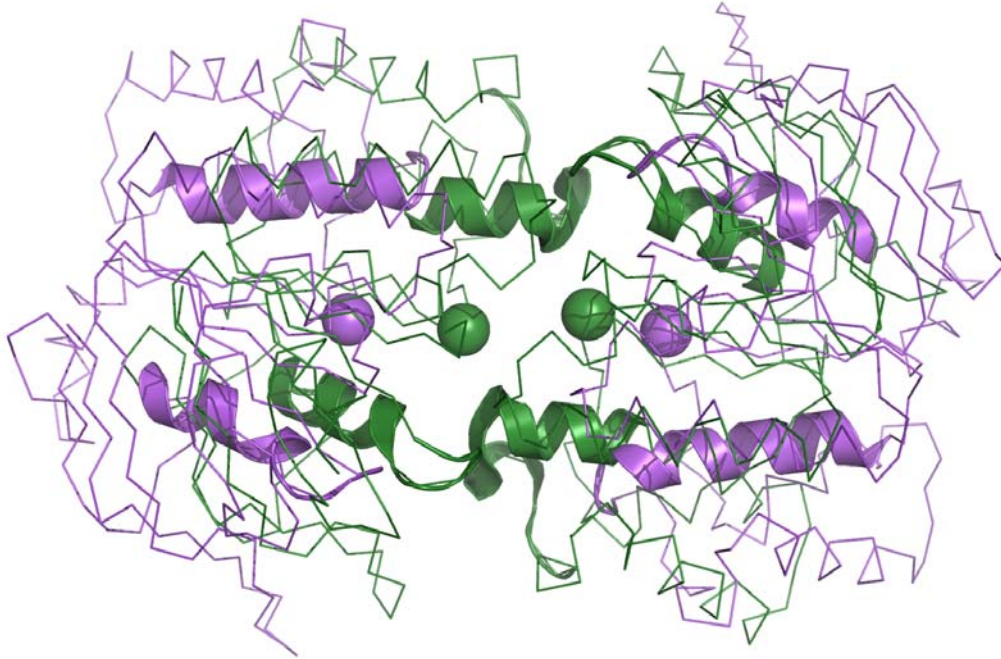


**Figure 2.12.** Another top-down view of the ATP-binding cassettes of MetN and MalK displays the P loop and associated helix, the Walker A loop and associated helix, and the Q loop (Q). This view more clearly depicts the rotation or swinging motion that must occur to move between these two conformations, as the helices especially are at different angles

shared by no other structures within the PDB (Hung et al., 1998). Since that time, however, it has been established as a common, homologous fold amongst the ABC transporter family, as both importers and exporters share these features. The HisP and subsequent ABC transporter ATPase structures also elucidated certain motifs present within this family, which have been identified within the MetN structure. The Walker A/B motif includes residues 38-45 and 161-165, while the signature sequence extends from 141-145 (Figure 2.10, Figure 2.11, and Figure 2.12).

When comparing the homologous regions of various transporter structures to MetN, r.m.s.d. values of structurally equivalent C $\alpha$  atoms for the individual subunits were 1.7 Å with HI1470, 1.8 Å with ModC, 2.3 Å with BtuC, and 2.6 Å with MalK. Interestingly, the monomer with the highest level of sequence homology to MetN is HisP, which has not been solved as a full transporter. HisP and MetN have an r.m.s.d.

of 1.8 Å. While each of the 5 ATP binding cassettes from the structures of full transporters are relatively closely related in structure, the positions of the components within the respective dimers varies significantly depending on the overall transporter conformation. The MetNI dimer reveals a more pronounced inward-facing transporter, with a much greater distance between the ATPase subunits than any other transporter structure solved at present. While the recently published MalK structure depicts the conformation of the ATP-bound state (Oldham et al., 2007), the organization of MetN portrays an inward-facing conformation with widely separated NBDs. The contrasting relationship between the MalK dimer and the MetN dimer suggests that a tweezer-like swinging motion brings the two subunits together (Figure 2.12). The rotational and translational shift between the MetN closed state and the substrate-bound conformation of MalK is more significant than the differences observed between other inward- and outward-facing conformations, such as the changes between the conformations of HI1470/1 and BtuCD. The regions closest to the membrane appear to experience the most significant movement between the two states; this corresponds with the cytoplasmic-facing rearrangement between the transmembrane helices, suggesting that the central portion of the transporter undergoes the greatest shift through the transport process. More simply, the ATP binding cassette dimer moves between open and closed states in a tweezer-like swinging motion that is similar to the motion of the transmembrane domain yet in the opposite direction. The differences in distance between the motifs of the catalytic core on each subunit of the MetN dimer versus the MalK dimer are considerable, as the distances between corresponding residues on MalK are 10 Å closer together than those on MetN, on average. Using residues of the P-loop and the signature motif, the intersubunit differences between opposing residues on the MetN dimer are

approximately 28 Å. In contrast, these differences shrink to 11 Å and 16 Å for the maltose and molybdate structures and to 14 Å and 16 Å for BtuCD and HI1470/1 (Pinkett et al., 2007). The swinging motion is more apparent when residues on the periplasmic-proximate and the membrane-proximate regions of these two dimers are considered: distances between residues on the periplasmic face are considerably shorter than distances on the membrane facing region. The MetN conformation is clearly only open to the cytoplasm, and this arrangement may be modulated by the C-terminal domain of the ATP binding cassette.

### **Regulatory Domain**

The C-terminal domain of the MetN subunit consists of two elements: a regulatory domain, and a linker region connecting the regulatory and ATPase domains. Co-crystallization of MetNI with high concentrations (1mM) of L-selenomethionine revealed two clear selenomethionine binding sites in the C-terminal region of MetN. This domain, separated from the ATP binding cassette domain by a series of short helices and loops, exhibits a ferredoxin-like fold that consists of an  $\alpha/\beta$  sandwich with an anti-parallel  $\beta$ -sheet. The two copies of MetN interact in this region to form a dimer; each copy shares the  $\beta\alpha\beta\beta\alpha\beta$  topology and together an 8-stranded  $\beta$ -sheet is formed. Previously named an ACT domain by Aravind and Koonin (1999), this dimer is a structurally conserved, regulatory ligand-binding domain thought to be fused onto a variety of proteins important in amino acid metabolism through the course of protein evolution (Chipman and Shaanan, 2001). Structural studies of 3-phosphoglycerate dehydrogenase, a previously identified member of this family, revealed that the ACT domain binds serine as an allosteric regulator in the same position as that seen in MetN, supporting the hypothesis that the ACT domain shares a common ligand-binding mode, despite differing substrates (Schuller et al., 1995). In addition, the regulatory and

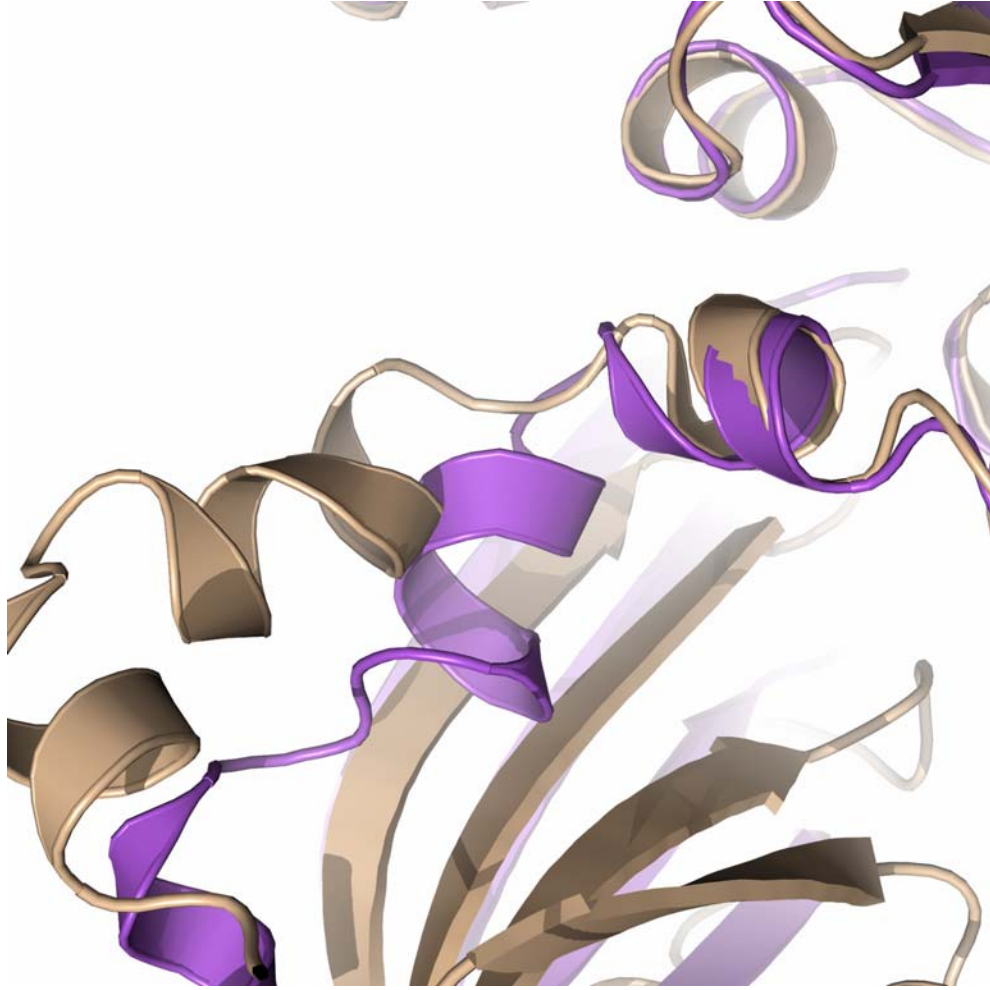


**Figure 2.13.** A view of the two different conformations of the linker region is shown above. The two chains of MetN (in purple and tan) align well over most of the structure, yet they diverge into two different conformations within this linker region (above, center).

catalytic domains of 3-phosphoglycerate dehydrogenase are separate, just as the ATP binding cassette and ACT domain of MetN are clearly divided by a linker region.

In MetN, movement of these two domains relative to one another is accomplished through a hinge mechanism within the linker region. The linker itself comprises the 40 residues in between the regulatory and ATPase domains, and possesses four short  $\alpha$ -helices and five loop regions. The transporter structure has revealed two different conformations of this linker region, resulting in an asymmetrical

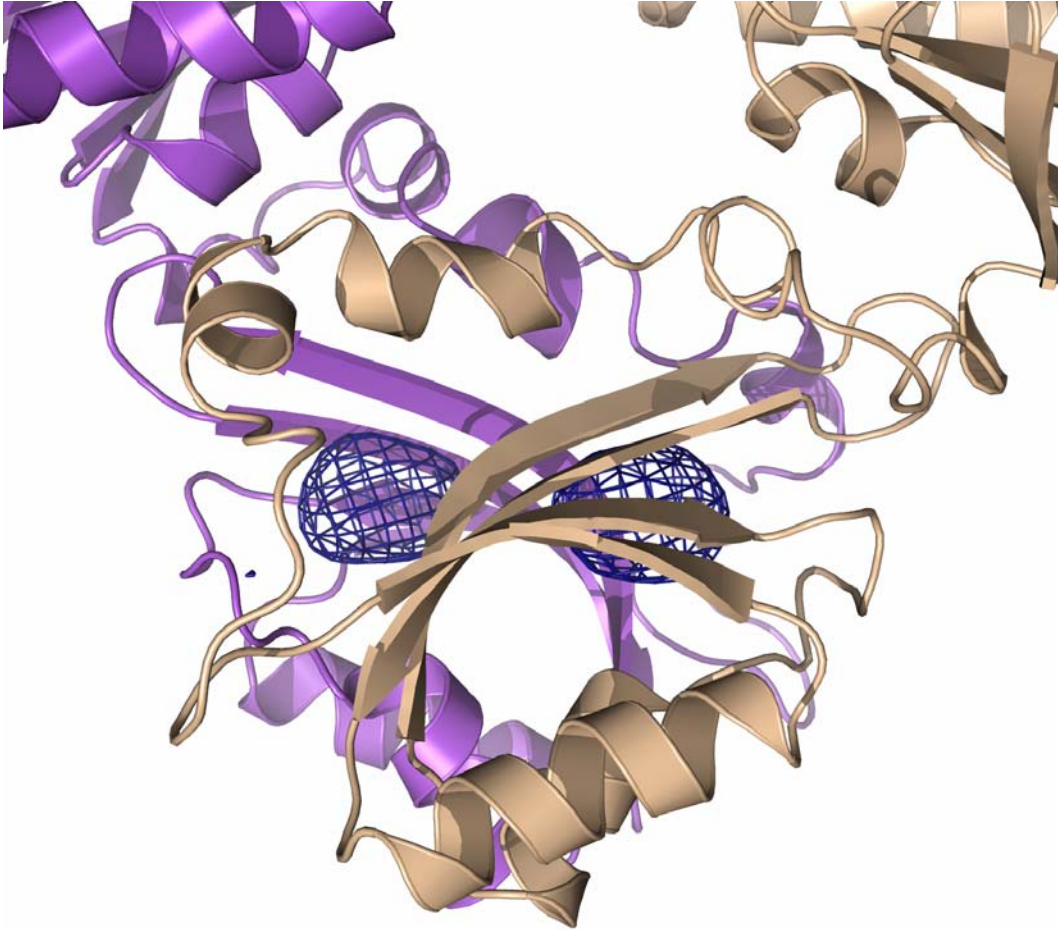


**Figure 2.14.** A close-up side view of the ACT domain shows an 8-stranded  $\beta$ -sheet formed by the interface of the two monomers. The selenomethionine binding sites, depicted with blue density at a  $\sim 6\sigma$  contour level, are at the dimer interface, and are bordered by the four helices also part of this dimer.

relationship of the two MetN chains (Figure 2.13). The ATP binding cassette region as well as the ferredoxin-like fold of the C-terminal extension exhibit approximate two-fold rotational symmetry between the two chains, but the rotation axes for the C-terminal extension and the ATP binding cassette differ in orientation by approximately  $20^\circ$ . These two orientations account for the asymmetry seen in the structure, and are the result of two different conformations of the linker region. This hinge mechanism, observed in MetN through differing conformations of the linker region between the two domains, is most likely responsible for the movement between varying states of the ACT

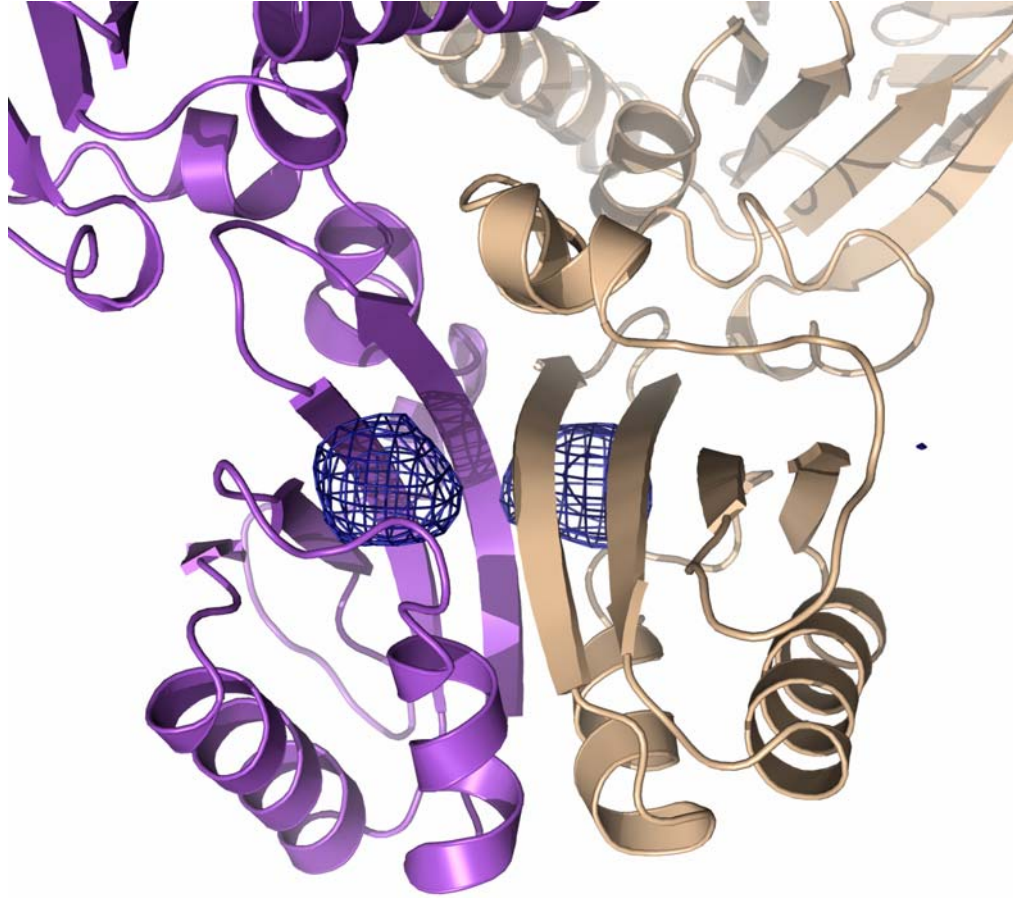


**Figure 2.15.** Another view of the ACT domain depicts the two methionines side-by-side within this dimer interface. Allosteric ligand binding at this same location is found throughout other members of the ACT family.

domain. The two ACT domains are in closer proximity to one another than the remainder of MetN, suggesting that this conformation is keeping the ATP binding cassettes from interacting, thereby blocking ATP binding and methionine transport (Figure 2.14, Figure 2.15, and Figure 2.16). While the methionine binding site was not well characterized at this resolution, the binding sites are located in close proximity to Met301 and Met312. This unusual feature could be an indication that there is competition between intercellular and intracellular methionine binding at this site. Biochemical studies corroborate that high methionine levels inhibit transport (Zhang, 2003). Interestingly, no selenomethionine was bound in any region of the

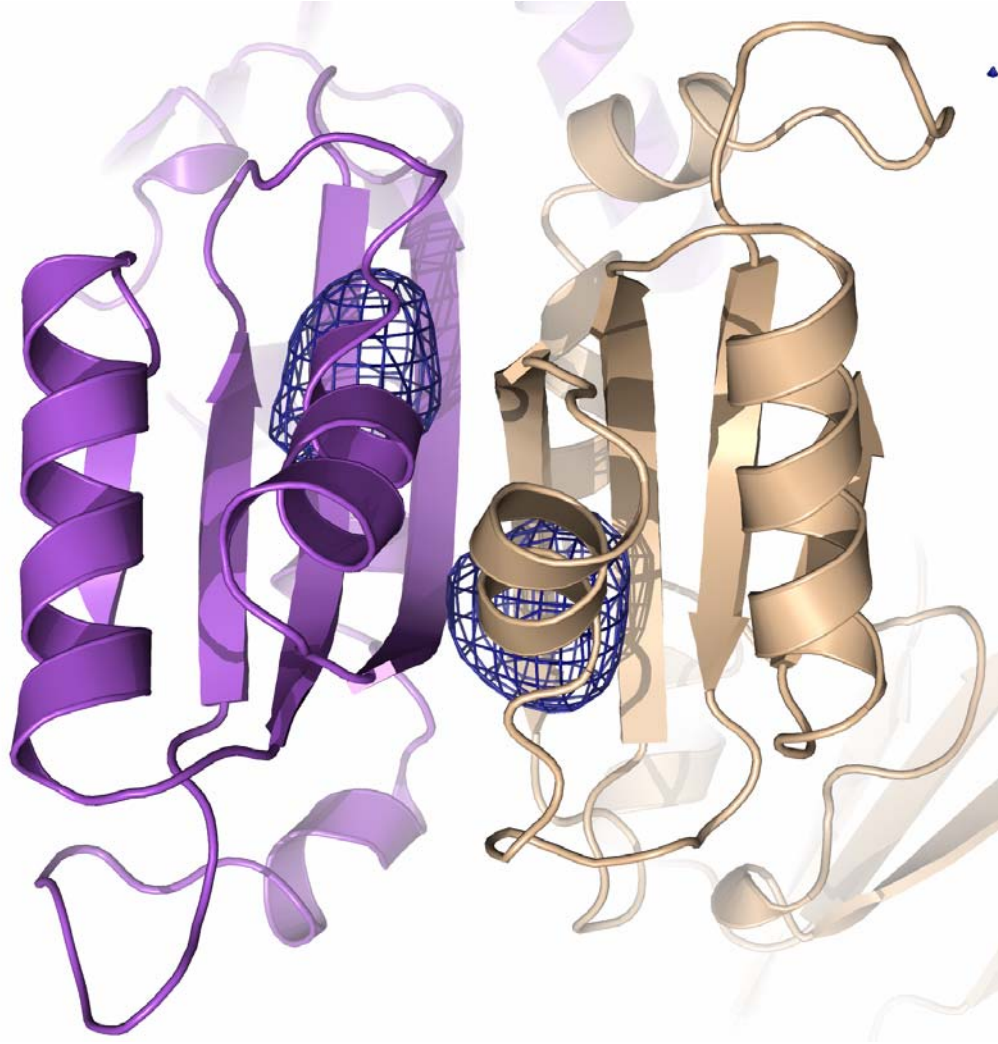


**Figure 2.16.** Above is a bottom-up view of the C-terminal ACT-like domain, showing the L-selenomethionine binding sites at the interface of this dimer.

transmembrane domain, suggesting that the ACT domain has a higher affinity for selenomethionine than the translocation pathway. The presence of a regulatory domain may indicate that transport in these regulated ABC transporters is substrate need-dependent, as MetNI is inactivated with high levels of intracellular methionine. This regulatory activity adds a further dimension to the current models of ABC transporter mechanisms, suggesting that transport is primarily dependent upon the need for

substrate rather than simply the presence of ATP and substrate delivered by a cognate binding protein.

In conclusion, this structure has provided insights onto the structural organization of ABC importers. First, this structure has identified the smallest transmembrane domain characterized thus far, suggesting that these 5 helices form a minimal core for an adequate translocation pathway. Second, the ATPase domains are stabilized in a conformation with a much greater distance between the two subunits than seen before. Third, the regulation of transport is modulated by a previously identified regulatory domain, and in cases of ligand binding in this area, the transporter is stabilized in an inward-facing conformation that precludes ATP binding. This mechanism supports earlier findings by Kadner and allows for insight into the molecular mechanism of this regulatory mechanism, providing a better understanding of how transporters can be regulated at the level of protein function.

## Appendix One. Methods and Data Relevant to Chapter Two.

### A1.1. Materials and Methods

#### Cloning and Expression

The *E.coli* methionine ABC transporter operon was identified from the NCBI website. Following a similar strategy used in the BtuCD and HI1470/71 structure determinations (Locher et al. 2002, Pinkett et al. 2007), *metN* and *MetI* were cloned from *E. coli* K-12 genomic DNA (American Type Culture Collection) into a modified fusion pET21b(+)/pET19b vector that can co-express the *metI* and *metN* genes simultaneously using separate T7 promoters. The entire *MetNIQ* operon was isolated from the genomic DNA by PCR and inserted into a pCR-Blunt II-TOPO vector (Invitrogen). The *metN* (ATPase subunit) gene was subsequently isolated by PCR using two oligonucleotides which inserted NdeI and XhoI sites. The PCR fragment was ligated into a pET19b vector (Novagen/EMD) using the NdeI and XhoI sites to introduce an N-terminal 10xhistidine tag. Similarly, the *metI* (transmembrane subunit) gene was isolated by PCR using two oligonucleotides which inserted NdeI and XhoI sites and removed the STOP codon from the end of the gene. The PCR fragment was ligated into a pET21b (+) vector (Novagen/EMD) using the NdeI and XhoI sites to introduce a C-terminal 6xhistidine tag.

The *metI* gene was isolated by PCR using the *metI*-pET21b (+) plasmid as the template with two oligonucleotides designed to anneal upstream and downstream of the entire promoter/expression region of the pET21b (+) plasmid, and introduce SphI and BglII sites at the ends of the PCR product. This PCR fragment was digested with SphI and BglII and ligated into the *metN*-pET19b vector. The SphI and BglII sites in the *metN*-pET19b vector are located in a non-coding region of the pET19b plasmid. The

modified pET19b vector can express the *metI* and *metN* genes simultaneously using separate T7 promoters. A mutagenesis reaction was then performed on the *metNI*-pET19b plasmid to insert a STOP codon immediately after the *metI* gene so that the C-terminal 6xhistidine tag will not be expressed. The reaction was performed using the Quickchange Mutagenesis Kit (Stratagene). As a result, the final plasmid contains an ATPase subunit with an N-terminal MGHHHHHHHHHSSGHIDDDDKH sequence, while the transmembrane subunit has no additional residues. The cloning was performed by Allen Lee.

The cloned plasmid was transformed into BL21 (gold) cells (Novagen) and protein expression was carried out at 37°C in Terrific Broth with 0.2 mg/mL ampicillin and 1% glucose instead of glycerol in an 80 L New Brunswick fermentor containing 60 liters of medium. The cells were induced at OD 600=4.0 with 2 mM IPTG for 2 hours before harvesting and storing at -80°C.

#### Purification and Crystallization

In the purification of MetNI, 10 g of cell paste is re-suspended in 50 mL of a 50 mM Tris pH 7.5, 20 mM imidazole, and 1 M sodium chloride solution with 40 mL dH<sub>2</sub>O added. The solution is clarified using a homogenizer, after which 10 mL of a 10% n-dodecyl-β-D-maltopyranoside (Anatrace) solution and a protease inhibitor tablet (Roche) is added, bringing the final concentration to 1% n-dodecyl-β-D-maltopyranoside.

The 100 mL solution was split into two solutions of 50 mL each and placed on ice. Each of these solutions was sonicated using a program that allowed for 0.5 seconds on, followed by 1.5 seconds off, in one-minute increments. The two solutions were alternatively sonicated for one minute each, until each solution was sonicated for a total of 4 minutes. After sonication, the solutions were re-combined and stirred for 1 hour

at 4 °C before centrifugation at 39,700 x g for 30 minutes. The supernatant was loaded and equilibrated onto a 5 g Ni-sepharose affinity chromatography column (Amersham), washed with 92 mM imidazole, and eluted with 250 mM imidazole, 25 mM Tris pH 7.5, 500 mM NaCl, and 0.1% DDM. The eluate was dialyzed overnight into a solution containing 0.1% DDM, 25 mM Tris pH 7.5, 500 mM NaCl, 5 mM dithiothreitol, 2.5 mM MgCl<sub>2</sub>, and 2.5 mM ATP before it was concentrated to 20 mg/ml using an Amicon Ultra MWCO100 concentrator (Millipore). Protein purity was estimated to be greater than 90% using SDS gel electrophoresis.

Selenomethionine substituted protein was made using *E. coli* B834 (DE3) cells (EMD Biosciences). Cells were grown in M9 medium supplemented with seleno-D,L-methionine. Procedures for purification and crystallization of the selenomethionine-substituted protein were identical to that of the native protein.

Crystallization experiments were carried out with the hanging drop method at 20 °C, using 2 µL protein plus 2 µL precipitant solution. Chunky, diamond-shaped crystals were obtained using solutions in the range of 28-32% PEG 400, 0.05 M Li<sub>2</sub>SO<sub>4</sub>, 0.2 M (NH<sub>4</sub>)<sub>2</sub>HPO<sub>4</sub>, 0.05-0.15 M (NH<sub>2</sub>)<sub>2</sub>SO<sub>4</sub>, and 0.1 M Sodium Citrate pH 4.2-4.5. Crystals grew to 0.3 x 0.3 x 0.4 mm<sup>3</sup> in two to three weeks, and were frozen in liquid nitrogen prior to data collection.

Xenon-derivatized crystals were formed by exposing the native crystal to 100psi Xe gas for 10 minutes in a pressure chamber. Selenomethionine-soaked crystals were obtained by soaking native crystals in 1-20 mM L-selenomethionine for 30 minutes to 3 hours.

#### Data Collection and Structure Determination.

A 3.7 Å resolution native dataset was collected at the Stanford Synchrotron Radiation Laboratory beam line 11-1 and processed using MOSFLM and SCALA (Leslie,

1992). A 3.8 Å resolution Xenon-derivatized dataset (1.5 Å wavelength) was collected at the Stanford Synchrotron Radiation Laboratory beam line 9-2 and processed using MOSFLM and SCALA. A 3-wavelength 5.5 Å resolution dataset using selenomethionine-substituted crystals was collected at the Advanced Light Source beam line 8.2.1 and processed using MOSFLM and SCALA (Leslie, 1992). A peak wavelength 4.5 Å resolution dataset of an L-selenomethionine-soaked crystal was collected at Stanford Synchrotron Radiation Laboratory beam line 9-2 and processed using MOSFLM and SCALA.

Initial protein phases and heavy atom binding sites were found from the Xe-derivatized data using single isomorphous replacement in the program SHELX (Schneider and Sheldrick, 2002), and were further refined through solvent flattening and histogram matching using SHARP (Bricogne et al., 2003). SIRAS was carried out in SHARP using the Xe-derivatized data with the native data and solvent flattening and averaging were performed using the programs MAIN and DM (Cowtan, 1994). Jens Kaiser obtained the initial protein phases and heavy atom binding sites and established non-crystallographic symmetry. Manual building was done in COOT (Emsley and Cowtan, 2004), and refinement was carried out using REFMAC and CNS (v 1.2) (Brunger, 2007). The sequence register of the C-terminal extension of MetN was confirmed using a structure of this short, soluble domain solved by Eric Johnson. The sequence register of MetI was additionally confirmed using the structures of the molybdate and maltose transporters (Hollenstein et al., 2007; Oldham et al., 2007).

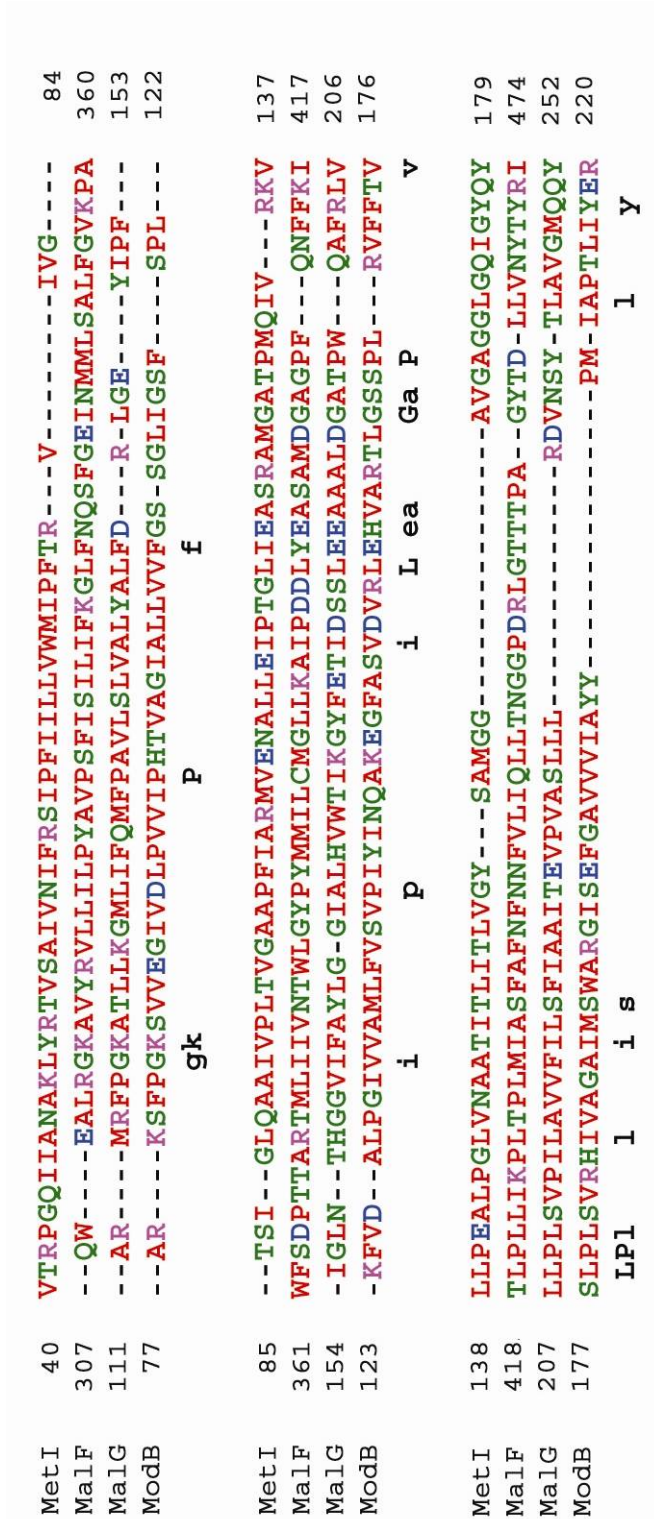


**Figure A1.1.** The sequence alignment of MetI, the transmembrane domain, with the transmembrane domains of MalF, MalG, and ModB, is shown above. The highest level of sequence similarity is within the segment containing the coupling helix and extending to the helices on either side of this important helix. This alignment was performed using MUSTANG (Konagurthu et al, 2006).

```

MetN      1  --MIKLSNITKVFHQGTRTIQALNNVSLHVPAGQIYGVIGASGAGKSTLIRCVNLLERPT 58
MalK      2  -ASVQLQNVTKAWG-----EVVVSKDINLDIHEGEFVVFVGPSCGKSTLLRMIAGLETIT 56
ModC      1  MFLKV--RAEKRLG----NFR--LNVDFFEMGR-DYCVLLGPTGAGKSVFLELIAGIVKPD 51
          n tK  g          nv l          v          GpsGaGKStllr iagle pt

MetN      59  EGSVLVDGQELTTLSESELTKARRQIGMIFQHFNLLSSRTVFGNVALPLELDNTPKDEVK 118
MalK      57  SGDLFIGEKRMNDTPPAER-----GVGMVFQSYALYPHLSVAENMSFGLKLAGAKKEVIN 111
ModC      52  RGEVRLNGADITPLPPERR-----GIGFVPQDYALFPHLSVYRNIAAYGLR--NVERVERD 104
          G v  g  t lpp er          giGmvfQ yaL phlsv N a gL  n k e

MetN      119  RRVTELLSLVGLGDKHDSY-PSNLSGGQKQRVAIARALASNPKVLLCDEATSALDPATIR 177
MalK      112  QRVNQVAEVLQLAHLL-DRKPKALSGGQRQVAIGRTLVAEPSVFLLDQPLSNLDAALRV 170
ModC      105  RRVREMAEKLGI AHL L-DRKPARLSGGERQVALARALVIQPRLLLLDEPLSAVDLKTG 163
          rRV e ae lglahl l dr P  LSGGqrQrVAiaRaIv P vlllDepI SaLD at

MetN      178  SILELLKDIRRRRLGLTILLITHEMDVVKRICDCVAVISNGELIEQDTVSEVFSHP----K 233
MalK      171  QMRIEISRLHKRLGR TMIYVTHDQVEAMTLADKI VVLDAGRVAQV GKPLELY---HYPAD 227
ModC      164  VLMEELRFVQREFDVPILHVTHDLIEAAMLADDEVAVMLNGRIVEKGLKELF---SAKN- 219
          eel  rrlg til vTHd ea laD vaV nGr e gk EIf

```

**Figure A1.2.** The sequence alignment of the ATP-binding cassette subunits is shown above. Included are the maltose transporter and the molybdate transporter. This alignment was performed using MUSTANG (Konagurthu et al, 2006).

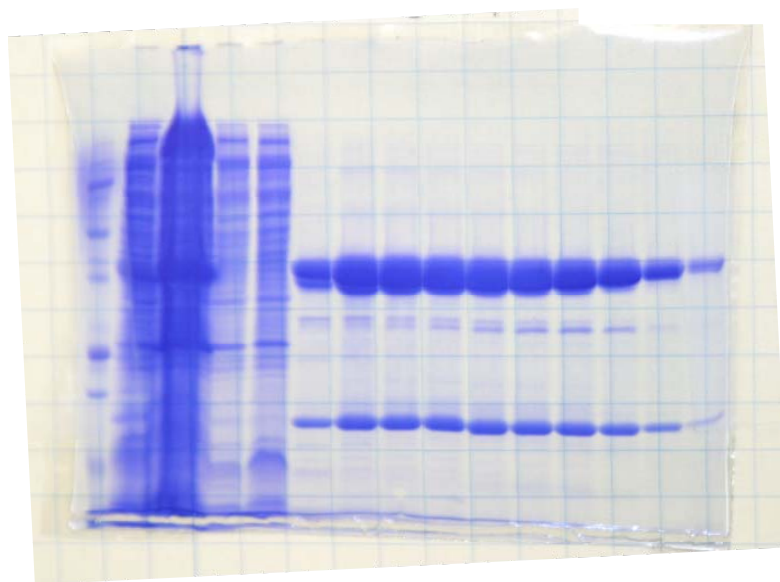
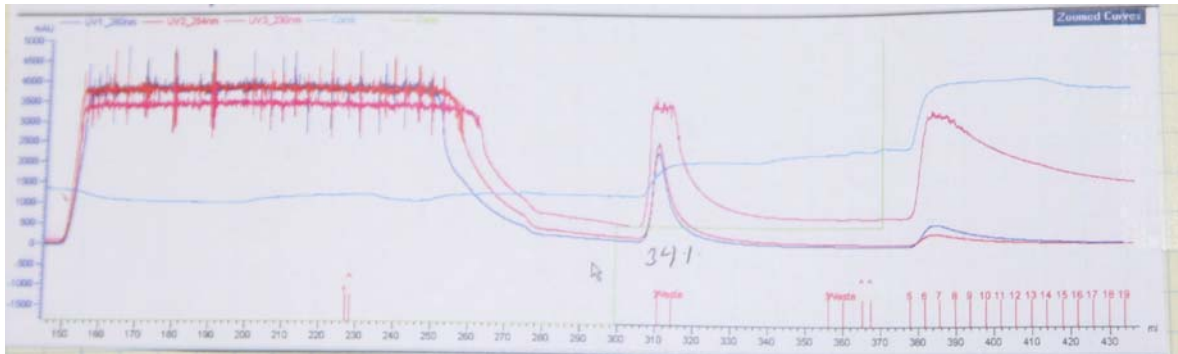


**Figure A1.3.** Above are the experimental data regarding the purification of MetNI. The top figure represents the chromatograph recorded during a typical purification. The loading of the sample (onto a Ni-sepharose column) is followed by a washing step (2<sup>nd</sup> peak), followed by the elution of the purified protein with a solution containing 250 mM imidazole. Below is a typical gel obtained in purification. The first lane is a molecular marker. The second, third, fourth and fifth lanes are the loaded sample, the resuspended pellet after centrifugation, a sample from the flow through and a sample from the wash step, respectively. The remaining lanes represent the purified sample; at 23kD the lower band represents the transmembrane domain, while at 47kD the upper band represents the ATPase domain.

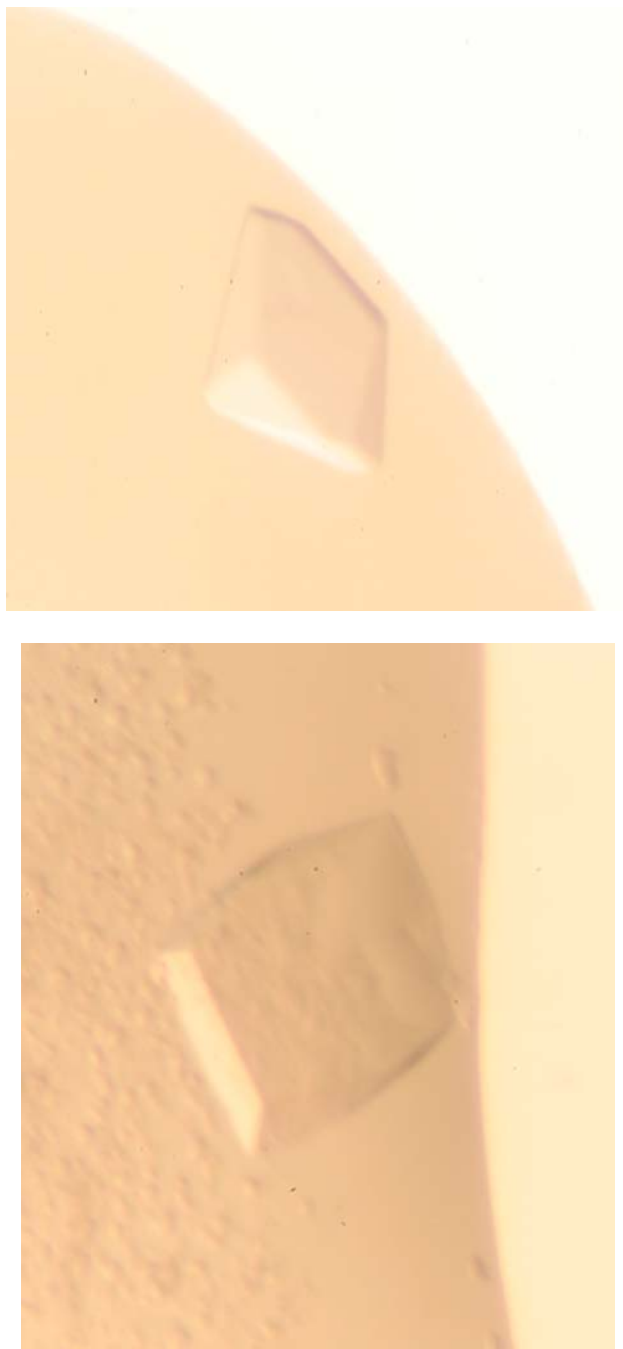


**Figure A1.4.** Above are pictures of crystals of the transporter. These orthorhombic crystals formed in beautiful, large shapes. The total crystal size was approximately  $0.3 \times 0.3 \times 0.4 \text{ mm}^3$ .



**Figure A1.5.** Above is the initial density seen for the transporter, after phasing using Xenon and the initial solvent flattening using DM.

**Table A1.1:** Summary of Secondary Structure for MetN

Secondary Structure	Residue Range
$\beta$ 1	1-11
$\beta$ 2	17-28
$\beta$ 3	32-39
$\beta$ 4	59-65
$\beta$ 5	67-70
$\beta$ 6	84-89
$\beta$ 7	160-170
$\beta$ 8	193-199
$\beta$ 9	209-215
$\beta$ 10	218-223
$\beta$ 11	266-273
$\beta$ 12	295-303
$\beta$ 13	309-318
$\beta$ 14	334-343
$\alpha$ 1	42-62
$\alpha$ 2	75-82
$\alpha$ 3	99-108
$\alpha$ 4	114-127
$\alpha$ 5	130-135
$\alpha$ 6	144-156
$\alpha$ 7	174-190
$\alpha$ 8	201-206
$\alpha$ 9	234-239
$\alpha$ 10	242-249
$\alpha$ 11	252-258
$\alpha$ 12	281-290
$\alpha$ 13	322-331

**Table A1.2:** Summary of Secondary Structure for MetI

<b>Secondary Structure</b>	<b>Residue Range</b>
$\alpha$ 1 (TM 1)	8-41
$\alpha$ 2 (TM 2)	52-65
$\alpha$ 3 (TM 2)	68-82
$\alpha$ 4 (TM 3)	89-114
$\alpha$ 5 (coupling helix)	118-126
$\alpha$ 4 (TM 4)	131-166
$\alpha$ 5 (loop)	172-183
$\alpha$ 6 (TM 5)	186-207

**Table A1.3:** Processing, Phasing, and Refinement Statistics for Xe, Native and SeMet soak

<b>Data processing</b>			
Dataset	<b>Xenon</b>	<b>Native</b>	<b>SeMet soak</b>
Spacegroup	P 2 <sub>1</sub> 2 <sub>1</sub> 2 <sub>1</sub>	P 2 <sub>1</sub> 2 <sub>1</sub> 2 <sub>1</sub>	P 2 <sub>1</sub> 2 <sub>1</sub> 2 <sub>1</sub>
Unit Cell dimensions (Å)	a= 97.74 b= 169.20 c= 290.60	a= 97.77 b= 165.81 c= 288.92	a= 97.74 b= 169.20 c= 290.60
Wavelength (Å)	1.5	1	.979
Resolution (Å)	40-3.8	40-3.7	40-4.7
Unique reflections	61583	68389	28494
redundancy	8.0 (7.8)	11.3 (12.2)	7.4 (6.8)
<sup>a</sup> Completeness	99.9 (99.9)	94.3 (100.0)	97.5 (95.8)
<sup>b</sup> R <sub>merge</sub>	.11 (.81)	.11 (.92)	.07 (.59)
<b>Phasing power from Xe dataset</b>			
Isomorphous phasing power from (centric/acentric)	.674/.771		
Anomalous phasing power	.744		
Figure of Merit (centric/acentric)	.186/.257		
Figure of Merit after DM	.74		
<b>Refinement<sup>c</sup></b>			
Resolution (Å)	40-3.7		
Reflections used	49914		
Test reflections	5048		
<sup>d</sup> R <sub>work</sub> (%)	31.0		
<sup>d</sup> R <sub>free</sub> (%)	35.4		
Average B factor (Å <sup>2</sup> )	169.67		
Rmsd bond length (Å)	0.02		
Rmsd bond angle (°)	2.78		
<b>Ramachandran (%)</b>			
Most favored	91.0		
Allowed	4.2		
Disallowed	4.8		

<sup>a</sup>Numbers in parentheses refer to the highest resolution shell only.

<sup>b</sup>R<sub>merge</sub> =  $\sum |I_h - \langle I \rangle_h| / \sum I_h$ , where  $\langle I \rangle_h$  is average intensity over symmetry equivalents.

<sup>c</sup>The data processing statistics describe the data sets used for the initial structure determination. The datasets were re-processed by Jens Kaiser for the final refinement and data deposition.

<sup>d</sup>R-factor =  $\sum |F_{obs} - F_{calc}| / \sum F_{obs}$ .

**Table A1.4:** Processing, Phasing, and Refinement Statistics from Semet protein

<b>Data processing</b>			
<b>Dataset</b>	<b>Peak</b>	<b>Inflection</b>	<b>Remote</b>
Spacegroup	P 2 <sub>1</sub> 2 <sub>1</sub> 2 <sub>1</sub>	P 2 <sub>1</sub> 2 <sub>1</sub> 2 <sub>1</sub>	P 2 <sub>1</sub> 2 <sub>1</sub> 2 <sub>1</sub>
Unit Cell dimensions (Å)	a= 93.79	b= 159.59	c= 294.33
Wavelength (Å)	.9796	.9795	.972
Resolution (Å)	30-6.0	30-6.0	30-6.0
Unique reflections	22391	22386	22387
redundancy	12.1 (12.6)	12.1 (12.6)	11.9 (12.2)
<sup>a</sup> Completeness	99.9 (100.0)	99.9 (100.0)	99.9 (100.0)
<sup>b</sup> R <sub>merge</sub>	.153 (.47)	.148 (.51)	.149 (.50)

<sup>a</sup>Numbers in parentheses refer to the highest resolution shell only.

<sup>b</sup>R<sub>merge</sub> =  $\sum |I_h - \langle I \rangle_h| / \sum I_h$ , where  $\langle I \rangle_h$  is average intensity over symmetry equivalents.

## Chapter Three. MetQ.

### 3.1 Introduction

An integral component of the complete ABC importer system is the substrate binding protein; the substrate binding protein is responsible for the delivery of the substrate to the ABC importer. In Gram-negative bacteria, this substrate binding protein is secreted and contained within the periplasm by the outer membrane. In Gram-positive organisms, the substrate binding proteins are typically tethered to the plasma membrane in some manner, through a lipid anchor or through fusion to the membrane-spanning region of the transporter (Williams et al., 2004). These substrate binding proteins (whether soluble proteins or lipoproteins) are responsible for binding a specific ligand and associating with the transmembrane domain of the ABC transporter to facilitate the transport of the substrate across the periplasm. This mechanism of delivery helps to confer substrate specificity and affinity upon the ABC transporter (Tam and Saier, 1993). Without its substrate binding protein, an ABC transporter is typically unable to retain its full activity and becomes a low-efficiency transporter. Further supporting this idea is the evidence that  $K_a$  values for most substrate binding proteins are within an order of magnitude of the  $K_m$  of the corresponding ABC transporter, suggesting that the binding protein delivery system is responsible for much of the transporter's substrate affinity (Tam and Saier, 1993).

The identification of these binding proteins and their relationship to transport was not fully elucidated until the early 1970s. The first evidence that these proteins were located within the periplasm came from experiments that demonstrated their sensitivity to osmotic shock, leading to the ability to isolate these periplasmic proteins (Neu and Heppel, 1965). This description of osmotic shock set off a plethora of further

studies concerning these unidentified proteins, leading to a hypothesis that they were important for bacterial transport (Barash and Halpern, 1971). However, more definite genetic and biochemical proof of a link between these binding proteins and their involvement in transport was provided via a study of the galactose transport system. This study established that the galactose binding protein was a vital part of the galactose transport system by identifying a mutation that selectively disabled the galactose binding protein but did not affect the entire gene locus (Boos, 1972). In the following years, X-ray structures of various periplasmic binding proteins were solved, although a further biochemical understanding of these systems was not yet achieved. A study comparing the biochemical activities of a variety of periplasmic carbohydrate binding proteins suggested that the high affinity these proteins have for their respective substrates is responsible for a rapid response in binding. Furthermore, it was proposed that these binding proteins confer the high specificity and sensitivity to their corresponding transport systems (Miller et al., 1983). This concept, combined with the hypothesis that these proteins interact with their membrane-bound counterparts (Higgins, 1992), suggested a system that had multiple components working together to bind a substrate with high specificity and transport it across the membrane.

Interestingly, many of these substrate binding proteins share structural similarity, as the structures have been revealed to be bi-lobed structures with two nonequivalent domains surrounding the ligand. This is thought to be tied to evolutionary relationships between many of these substrate binding proteins, despite low sequence similarity between these proteins. Numerous ABC importer substrate binding protein structures have been published over the past 30 years (Quicho et al., 1996). Among the published structures are those with ligands that are carbohydrates like the maltose or glucose/galactose binding proteins, amino acids like the

leucine/isoleucine/valine, histidine, or lysine/ornithine/arginine binding proteins, and other ligands such as the phosphate, vitamin B<sub>12</sub>, or sulfate binding proteins (Quioco and Ledvina, 1996). These structures demonstrate low sequence similarity, a lack of conserved sequences, and size deviations from one another, as the size of these proteins can vary from 23 kD to 60 kD. However, the common feature shared among these structures is the presence of two distinct domains bisected by a hinged crevice that forms the ligand binding pocket and allows for movement between the ligand-bound and ligand-unbound states. The two domains of the substrate binding protein are typically comprised of a  $\beta$ -sheet surrounded by  $\alpha$ -helices. Certain substrate binding proteins enclose the ligand completely, while in other cases, the ligand is in a somewhat solvent-accessible region (Quioco and Ledvina, 1996). Three groups of substrate binding proteins have been described based upon the connectivity between the two domains. Group I binding proteins possess three short connecting segments between the two domains, resulting in the domains being comprised of separate segments from the first and second half of the entire polypeptide chain. Group II binding proteins possess two crossovers between the domains, to form one domain from the N- and C-terminal ends of the polypeptide chain, and the second domain from the middle segment (Quioco and Ledvina, 1996). Group III binding proteins possess a single  $\alpha$ -helical connection between the two domains (Karpowich et al., 2003). Examples of group I binding proteins include the maltose binding protein, the L-arabinose binding protein, and the leucine/isoleucine/valine binding protein. The oligopeptide binding protein, the lysine/arginine/ornithine binding protein and the histidine binding protein are part of Group II of these binding proteins, while the vitamin B<sub>12</sub> binding protein and a periplasmic metal binding protein are members of Group III (Lee et al., 2002).

Mechanistically, these proteins are thought to be similar as well, utilizing a conserved mechanism named the “Venus flytrap mechanism,” according to Mao et al. (1982). In this mechanism, the ligand-free protein adopts an open conformation, with the substrate binding pocket exposed to the solvent. Substrate can subsequently bind, allowing for the substrate binding protein to move to a closed conformation with a tightly bound ligand that is shielded from solvent. As the substrate binding protein docks onto the transmembrane permease protein, conformational changes resulting from the ATPase activity of the ABC transporter are thought to lead to movement of the transmembrane region, which is thought to pull apart the substrate binding domain, releasing the substrate into the translocation pathway of the permease (Williams et al., 2004). Originally, this hypothesis proposed that the “open” or non-ligand-bound state of the binding protein adopted a conformation in which the two lobes of the binding protein were 20° further apart than in the bound state (Mao et al., 1982).

Interestingly, there are few binding protein structures that have been solved in both the ligand-unbound and ligand-bound conformations. The first example was the maltose binding protein, which revealed a 35° rotation about the hinge upon ligand binding (Sharff et al., 1992). Another comparison has been made for the vitamin B<sub>12</sub> binding protein BtuF; in this case, there is relatively little structural change upon ligand binding, although substrate binding was shown to cause a decrease in mobility within the protein (Karpowich et al., 2003).

More recently however, there have been a number of structures presented that illustrated the binding protein interactions with the transporter; these studies have helped to understand the mechanics involved in the binding protein-transporter interaction. The structure of BtuF in complex with BtuCD, the only binding protein-ABC transport complex without a ligand present, corroborates with the Venus flytrap

hypothesis. The binding protein in this structure is seen in an open conformation, with the two lobes spread apart. At the interface, loops from the BtuC permease insert into the B<sub>12</sub> binding site, resulting in the open conformation for BtuF (Hvorup et al., 2007). This notion is further supported by the structure of the maltose binding protein in complex with the maltose transporter. In this structure, the substrate maltose is present, but within the permease translocation pathway, not the binding protein. Interestingly, the maltose binding protein is an open state as well, and a loop from the MalG permease inserts into the binding site. It has been hypothesized that this loop acts as a scoop, as it is responsible for dislodging the sugar and forcing it to transfer into the translocation pathway (Oldham et al., 2007). The third structure of an intact transporter-binding protein complex, ModABC, possesses a ligand within the binding protein, suggesting that this conformation is pre-transport. This interaction however, supports the notion that docking is mediated by attractions between oppositely charged amino acid side chains on both the permease and binding protein (Hollenstein et al., 2007).

Amino acid binding proteins exhibit a preference for ligands with similar structures and properties; certain proteins in this family can bind a group of similar amino acids, such as the leucine/isoleucine/valine binding protein. The selectivity for these amino acids is determined by the binding pocket. Hydrophobic residues line the active site for the leucine/isoleucine/valine binding protein, while the histidine binding protein presents polar hydrogen bonding sites as well as a  $\pi$ -stacking interaction via an active site tyrosine. Similarly, the lysine/arginine/ornithine binding protein has a binding site lined with acidic amino acids to form salt bridges with the substrate. Di- and tri-peptide binding proteins are also within the category of amino acid binding proteins, and exhibit similar properties. The amino acid binding proteins share certain

structural features as well: both domains participate in the ligand binding, water molecules are frequently present in the ligand binding site, and a hinge-bending motion is thought to be responsible for the difference between the open (apo) and closed (ligand-bound) states of these binding proteins (Quicho et al., 1996).

### 3.2 Methionine Binding Proteins

The structure of a methionine binding protein from the MUT family from *Treponema pallidum*, the organism responsible for the disease syphilis, has been solved previously to 1.85 Å resolution (Deka et al., 2004). The structure of this protein (PDB ID: 1XS5), called tp32, resembles other periplasmic ligand-binding proteins and is thought to be a lipoprotein in physiologic conditions (Figure 3.1). As is common for these binding proteins, tp32 possesses two  $\alpha/\beta$  domains that are linked by two crossovers. The binding pocket is located between these two domains, and an L-methionine residue was present in the electron density map. Each domain consists of a central core, comprised of a five stranded  $\beta$ -sheet with  $\alpha$ -helices on either side. In each  $\beta$ -sheet, there is one anti-parallel strand. While one of the regions connecting the two domains possesses no secondary structure, the other features a short  $3_{10}$  helix that is proximal to the methionine binding site. The binding pocket was identified to contain a non-covalently bound molecule of L-methionine, identified by shape and through an anomalous difference Fourier analysis of protein from a selenomethionine-containing sample. The binding of the L-methionine was unexpected, as no exogenous methionine was added to the medium, or to any of the purification steps; the methionine must be bound tightly enough to survive through multiple purification steps after the initial growth, and the protein must be selective enough to avoid binding any of the other small molecules (amino acids and numerous other small metabolites) in the growth

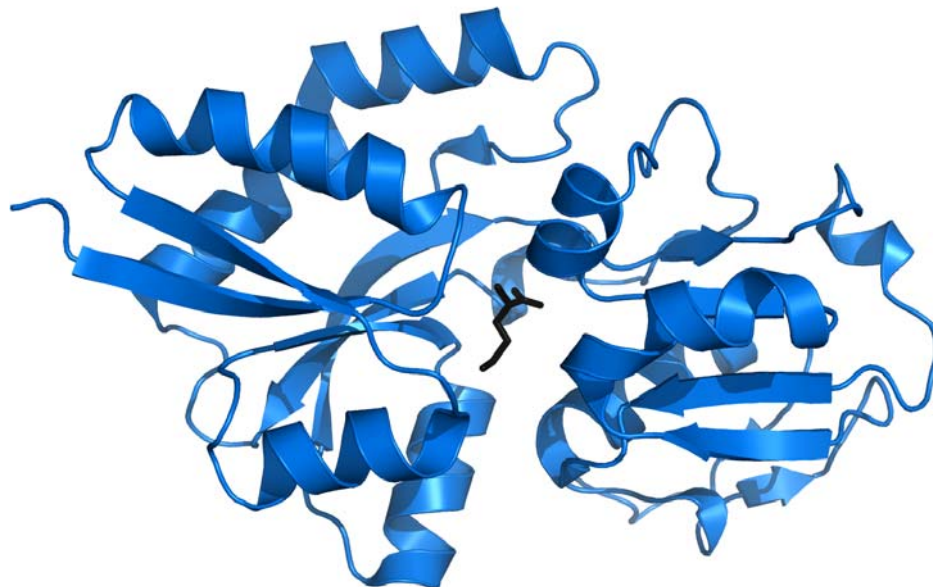


**Figure 3.1.** Above is the structure of the methionine binding protein tp32 from *Treponema pallidum*. The bound ligand, methionine, is shown in black.

medium. The binding pocket has polar and charged residues around the amino and carboxyl groups of methionine, which are expected to be charged at physiological pH. These charges are neutralized by Glu87 and Arg119. To stabilize the hydrophobic side chain of the methionine residues, Phe61 and Tyr44 participate in van der Waals contacts with the S-methyl group. Other hydrophobic residues stabilize the side chain, while a polar residue (Asn116) hydrogen bonds to the sulfur atom of the methionine residue. Deka et al. (2004) describe the active site as being particularly well suited to binding methionine, between the van der Waals contacts, the stabilization of the main chain atoms and their charges, and the hydrogen bonding of the sulfur atom. Interestingly, they found it difficult to remove methionine from the binding site and efforts to crystallize an apo form proved impossible. Approximately 20% of the protein denatured with guanidine hydrochloride and later renatured was found to have L-methionine still bound.

In addition to the structure described above, the structure of a glycylmethionine

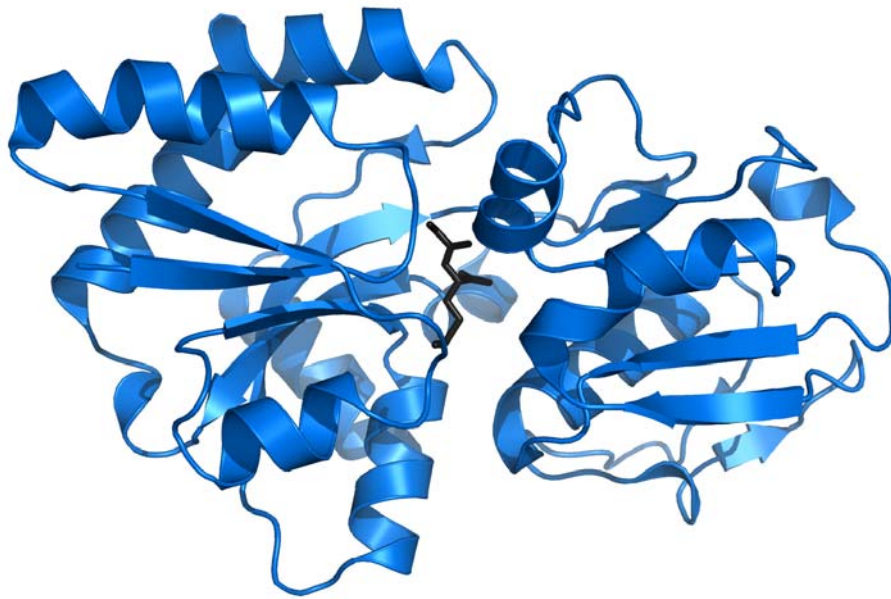


**Figure 3.2.** Above is a cartoon of the glyclmethionine dipeptide binding protein from *S. aureus*. This structure was solved with the glyclmethionine dipeptide bound, shown in black.

dipeptide binding protein from the MUT family of *Staphylococcus aureus* has been solved to 1.7 Å resolution in complex with its substrate (Williams et al., 2004). The structure of this protein, pg110 (PDB ID: 1P99), is quite similar to that of tp32, and demonstrated to be a lipoprotein by Williams et al. (2004). The structure of pg110 is made up of two domains in a similar fashion to tp32 (Figure 3.2). The ligand bound in this structure clearly showed a glycine-methionine dipeptide, suggesting a high specificity for this ligand, as other dipeptide binding proteins frequently are crystallized with a heterogeneous mix of peptides present in the binding site. To stabilize the methionine side chain, a hydrophobic pocket is formed by Phe82, His79, Phe77, and Tyr60. Asn192, Asn223, and Arg136 form hydrogen bonds with the carboxylate group from the methionine, while Arg144 appears to form a salt bridge to neutralize the carboxylate charge. Ser32 forms a hydrogen bond with the N-terminus of the peptide, which also forms a water-mediated hydrogen bond to Asp34 and Glu261. The glycl-carbonyl group is stabilized with hydrogen bonding from Gly194 and Tyr60. Analysis by Williams et al. (2004) suggests that glycine is the only other residue besides

methionine that can be accommodated by this active site, suggesting a high specificity for the Gly-Met dipeptide. Overall, the peptide is completely inaccessible to solvent, and fourteen different residues help to stabilize ligand binding.

### 3.3 Structural Analysis of MetQ

The structure of the cognate binding protein to the MetNI system, MetQ, was solved to 1.8 Å resolution using molecular replacement with a modified version of the protein pg110 (PDB ID: 1P99) (Figure 3.3). An L-methionine was discovered in the ligand binding pocket, presumably carried over from the expression process, a phenomenon seen with other binding proteins due to the high binding affinity. The ability of this protein to bind D-methionine was not elucidated in these studies, although this methionine transporter will import D-methionine (Kadner, 1974).

The structure itself displays a similar organization to other periplasmic ligand binding proteins, and shows the ligand binding domain to be at the interface of the two domains characteristic of this family of proteins. Similar to other methionine or glycine-methionine dipeptide binding proteins, the two domains of MetQ are connected by a linker region that plays a significant role in methionine binding. Unlike tp32, however, both linker regions are loops, as MetQ does not possess the  $3_{10}$  helix thought to play a role in methionine binding in tp32. The topology of MetQ is similar to both the methionine-binding tp32 and the glycyilmethionine-binding pg110, as expected from the sequence identity of 39% and 35% to pg110 and Tp32, respectively, and as reflected in the overall r.m.s.d.s between these proteins of 1.3 to 1.5 Å (Figure 3.4). Domain I of the protein is slightly smaller and consists of a 5-stranded  $\beta$ -sheet with strand order 9-5-8-6-7, with strand 5 anti-parallel to the others, surrounded by 2  $\alpha$ -helices and 3  $3_{10}$  helices. Domain II, however, is larger and consists of a longer 5-

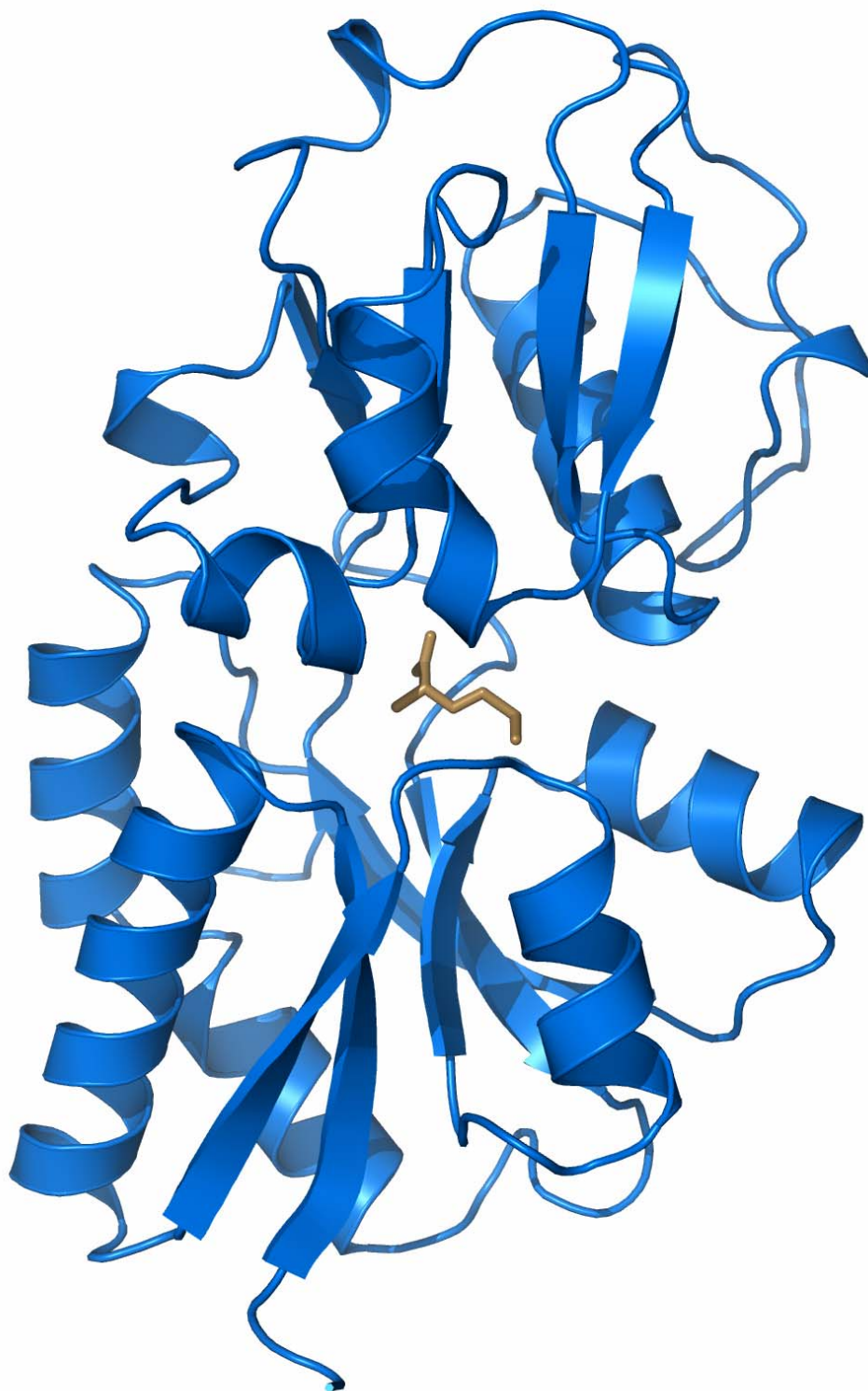


**Figure 3.3.** An overall view of the structure of the MetQ methionine binding protein (blue) illustrates the two lobes present in this structure, on either side of the bound methionine (gold).

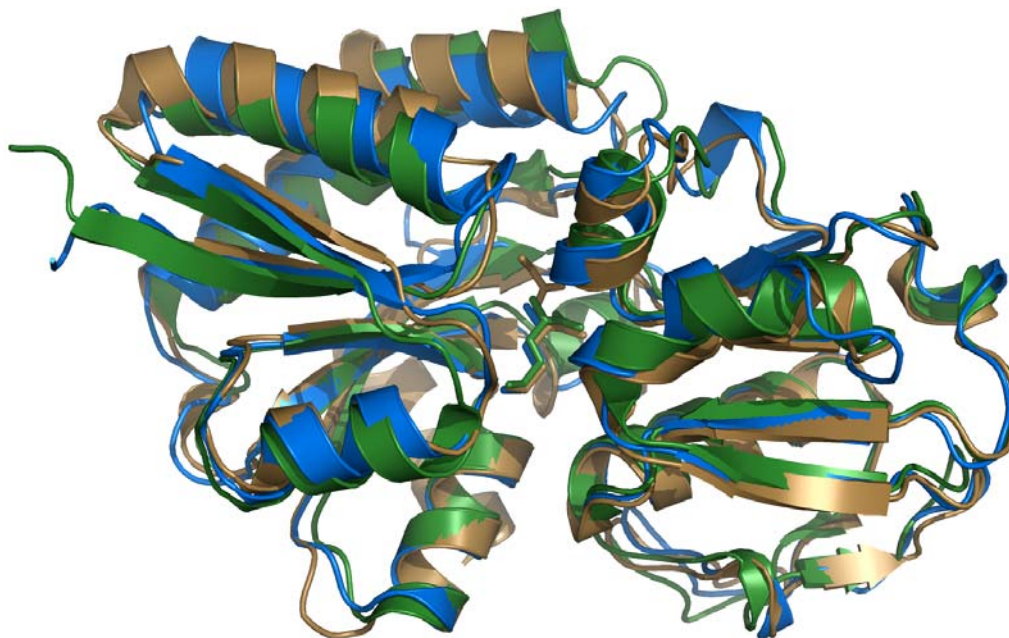


**Figure 3.4.** Above is an overlay of the three methionine binding proteins: MetQ (blue), tp32 (brown), and pg110 (green). The ligands (in the respective colors) for each are shown in the ligand binding site. Overall, there is high similarity in the folds of these proteins, as well as a high degree of similarity within the active site.

stranded  $\beta$ -sheet with strand order 2-1-3-10-4, with strand 10 anti-parallel to the others, surrounded by 4  $\alpha$ -helices on one side and 2  $\alpha$ -helices on the other. The first domain possesses all of the  $3_{10}$  helices, and interestingly has many more loops than the second domain, which has larger helices and a considerably longer  $\beta$ -sheet.

The binding pocket appears to be well suited for L-methionine binding, and possesses active site features found in pg10 and tp32 (Figure 3.5). The C-terminal negative charges of the L-methionine ligand hydrogen bond with Asn229 and a water molecule on the first oxygen, while Arg144, Asn202, and another water molecule form salt bridges and hydrogen bonds with the second oxygen. The N-terminal positive charge is balanced by a salt bridge with Glu42, and hydrogen bonding to Thr204, Asn229, and another water molecule. The most hydrophobic portion of the side chain, the  $\beta$  and  $\gamma$  carbons, are in van der Waals contacts with Tyr69 and His88. The

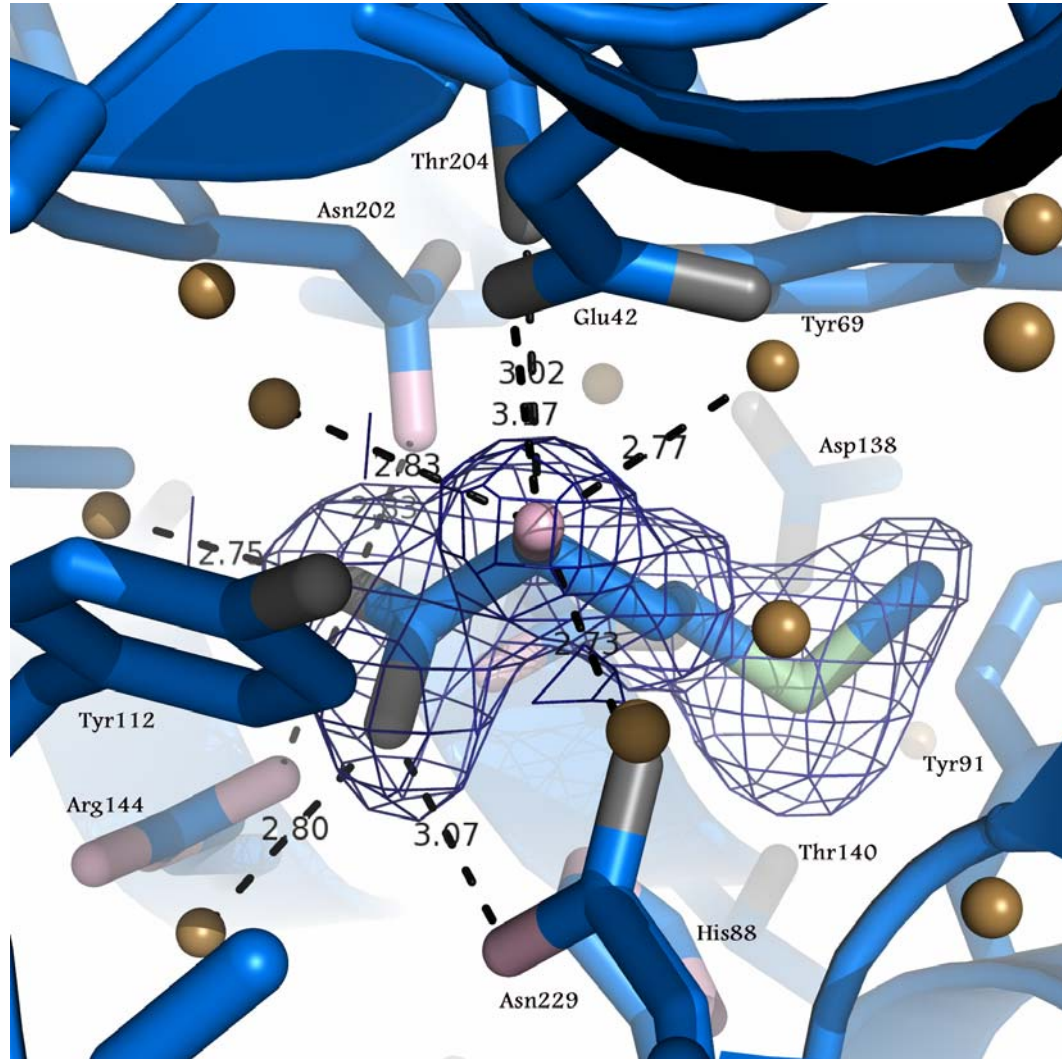


**Figure 3.5.** A close-up view of the ligand binding site presents the residues important for ligand binding as well as numerous binding site waters (gold) that are important for stabilizing the ligand. Residues and waters participating in hydrogen bonding are marked with dashed black lines.

hydrophobic methyl group of the ligand is proximate to Tyr69, Tyr91, and Phe86, and the methionine S $\delta$  forms a hydrogen bond with Gln87 and possibly Asn 141, resulting in a tight fit for the ligand.

Many of the residues within the ligand binding site of MetQ have equivalent counterparts in tp32 and pg110 (Figure 3.5). Residues Arg144, Asn202, and Asn229, important in the negative charge neutralization for MetQ, have equivalents in tp32 as

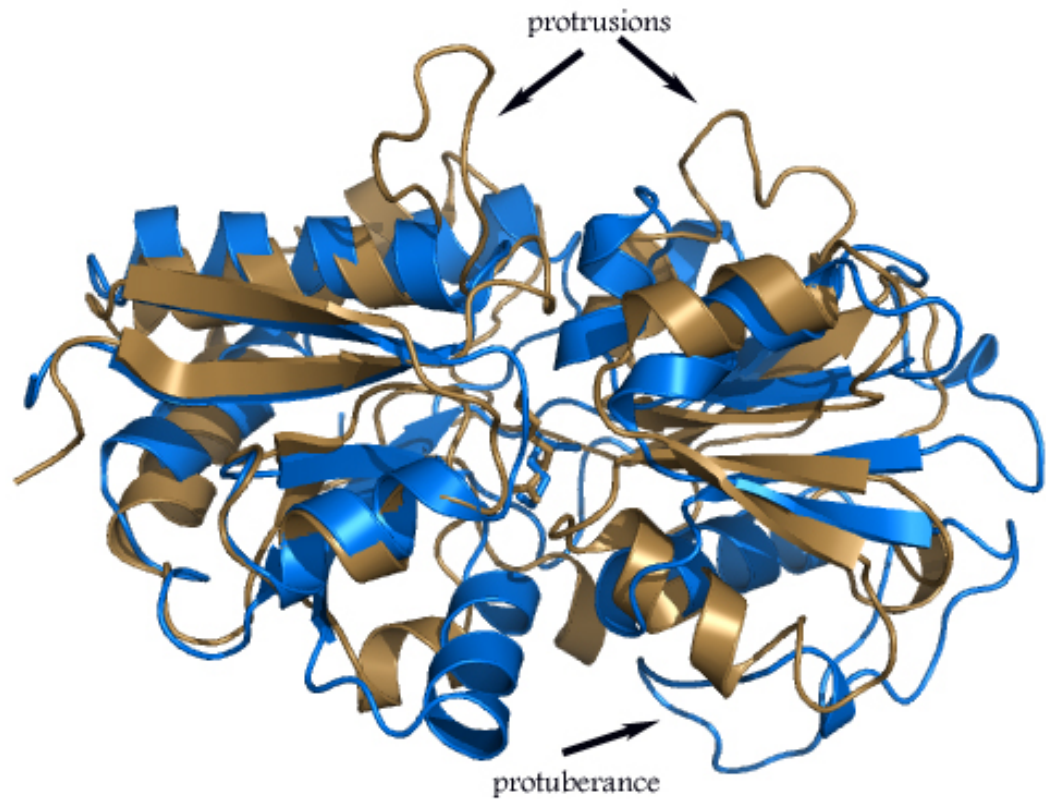


**Figure 3.6.** An overlay of the lysine/arginine/ornithine binding protein (brown) and MetQ is shown above. The LAOBP possesses two protrusions on one end of the structure, while the MetQ protein has a protuberance on the opposite face. The residues important for docking of the binding protein onto the transporter remain unclear.

Arg119, Asn175, and Asn202; and Arg151, Asn207, and Asn238 in pg110. Similarly, the van der Waals contacts of Tyr69 in MetQ are played by Tyr44 in tp32 and Tyr75 in pg110. Another important residue, Phe86, has counterparts in Phe61 and Phe92 of tp32 and pg110, respectively. Also stabilizing the S $\delta$  in all three proteins is a histidine residue: His88 in MetQ, His63 in tp32, and His94 in pg110. The residues stabilizing the positively charged N-terminus also vary slightly. There is a counterpart for Asn229 in tp32 and pg110 (Asn202 and Asn238, respectively), but the similarities end there. The protein pg110 only has one residue to stabilize this nitrogen, as instead of a free amino group, the nitrogen participates in a peptide linkage with glycine. MetQ and

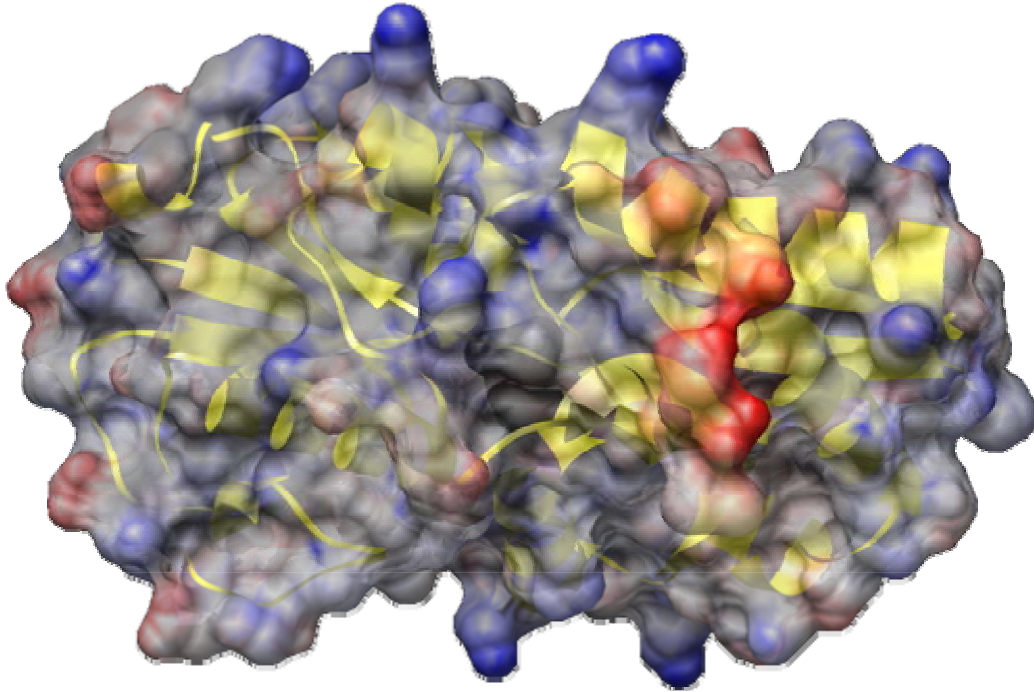


**Figure 3.7.** The surface electrostatics of the MetQ binding protein is shown above. A cartoon is shown beneath the surface in yellow. Gray spots indicate neutral charge, while red spots indicate negatively charged residues and blue spots indicate positively charged residues.

tp32 both possess a water molecule and a glutamate (Glu42 in MetQ and Glu87 in tp32) to further accommodate the positive charge of the amino group. Perhaps the biggest difference between these three ligand binding sites, besides the slight difference in ligand (L-methionine versus the glycine-methionine dipeptide), is in the residue that participates in stabilizing the S-methyl group of the methionine side chain. In MetQ, this function is carried out by Tyr91, but in tp32 this is fulfilled by His66, and in pg110 by Phe97. While these residues do share hydrophobic properties, it is interesting to see a range of residues in this location. As previously mentioned, the greatest difference between pg110 and the other L-methionine binding proteins is that pg110 binds a glycyl-methionine ligand, and its active site is therefore somewhat more spacious.

The overall fold of these methionine binding proteins is similar to the histidine

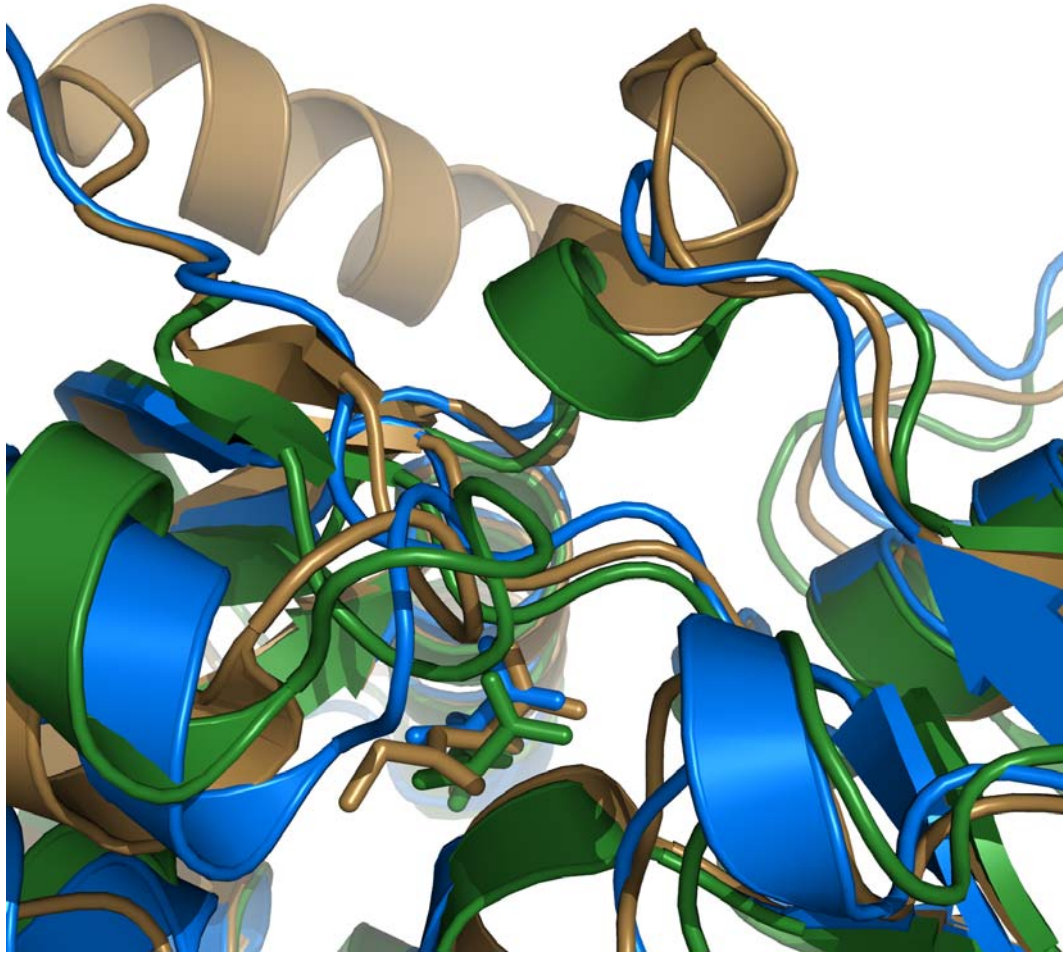


**Figure 3.8.** A comparison of the connector helices in the three methionine binding proteins is above. The connector helices are near the center of this cartoon in green (pg110) and brown (tp32), yet the blue cartoon (MetQ) has no helix in this region.

binding protein (PDB ID: 1hpb), the lysine/arginine/ornithine binding protein (PDB ID: 11st), and the glutamine binding protein (PDB ID: 1wdn). Superimposition of the analogous C $\alpha$  atoms of MetQ results in r.m.s. deviations of about 3.2 Å with the histidine binding protein HisJ, 3.4 Å with the lysine/arginine/ornithine binding protein LAOBP, and 3.1 Å with the glutamine binding protein QBP. An overlay of MetQ with the LAOBP is shown in Figure 3.6. Outside of the central domain, there are some differences between these structures. Two protrusions identified in the glutamine binding protein are not present in MetQ; these protrusions are hypothesized to form an interaction with the transmembrane domain of the ABC transporter. However, the

methionine binding proteins have a slightly different protuberance that is different than those in the histidine binding protein, and it was hypothesized by Deka et al. (2004) that this protuberance plays a role in docking on to the transmembrane domain of an ABC transporter. In MetQ, the protuberance is proximal to a slightly negatively charged patch of the protein, further encouraging the notion that this region plays a role in forming a salt bridge with the ABC transporter during the docking process (Figure 3.7). The precise interaction of MetQ with MetNI is currently unknown, although purified MetQ forms a complex with MetNI in dodecyl maltoside and co-elute on a size exclusion column. There have been hypotheses posed regarding the nature of this interaction, but further studies are necessary before this can be fully understood.

Another significant difference between the published methionine binding proteins and these other amino acid binding proteins is present in the secondary structure of the connector regions between the two domains. In other group II binding proteins, such as the histidine binding protein, the lysine/arginine/ornithine binding protein and the glutamine binding protein, the connector regions have no secondary structure. In the LAOBP, this region corresponds to residues 190-195. The two published methionine binding proteins however, contain a  $3_{10}$ -helix in the connector region, which has thus far only been found in methionine binding proteins (Figure 3.8). It has been hypothesized that this small helix may act as a restraint in movement between the apo and ligand-bound forms of the protein, thus moving less than the other, less constrained amino acid binding proteins. MetQ is more similar to the other amino acid binding proteins, as it differs from the other methionine binding proteins and does not possess this short helix in the ligand binding domain. The ligand binding domain also differs between these two groups of structures. Interestingly, the orientation of the methionine in the methionine binding protein is rotated  $\sim 90^\circ$  relative

to the amino acids bound in the other amino acid binding proteins (Deka et al., 2004). In conclusion, the MetQ structure shares certain features with other methionine binding proteins, but possesses key differences relative to ligand specificity from other amino acid binding proteins within the periplasmic binding protein-like superfamily.

## Appendix Two. Methods and Data Relevant to Chapter Three.

### A2.1. Materials and Methods

#### Cloning and Expression

The *E. coli* methionine ABC transporter operon was identified from the NCBI website and purified genomic DNA was obtained for *E. coli* K-12 strain from ATCC (American Type Culture Collection). The *E. coli metQ* (periplasmic binding protein) gene was isolated by PCR using two oligonucleotides which inserted NdeI and XhoI sites while removing the STOP codon. The PCR fragment was ligated into a pET21b(+) vector (Novagen/EMD) using the NdeI and XhoI sites to introduce a C-terminal 6xhistidine tag. The cloned plasmid was transformed into BL21-gold ( $\lambda$ DE3) cells (Novagen/EMD). The cloning was performed by Allen Lee.

Protein expression was carried out at 37°C in Terrific Broth with 0.2 mg/mL ampicillin and 1% glucose instead of glycerol in an 80 L New Brunswick fermentor containing 60 liters of medium. The cells were induced at OD 600=4.0 with 2 mM IPTG for 2 hours before harvesting and storing at -80°C.

#### Purification and Crystallization

In the purification of MetQ, the resulting cell paste was subjected to osmotic shock to obtain the periplasmic extract. Approximately 20 g of cells were re-suspended into 20 mL of an osmotic shock solution containing 40% sucrose, 1 mM EDTA, and 10 mM Tris pH 7.5 for 1 hour. The osmotic shock solution was then transferred into 1 liter of dH<sub>2</sub>O and stirred for 10 minutes before buffer components were added for the final solution to contain 250 mM NaCl, 25 mM Tris 7.5, and 17 mM Imidazole. The resulting periplasmic extract was centrifuged at 37500 x g for 30 minutes, loaded on to a 10g Ni-Sephrose column (Amersham), equilibrated with a buffer of 250 mM NaCl,

25 mM Tris pH 7.5, and 17 mM Imidazole, and finally eluted with a 150 mM imidazole buffer. The resulting protein solution was dialyzed into 250 mM NaCl and 25 mM Tris 7.5 overnight before it was concentrated to approximately 25 mg/mL using an Amicon 10 kD MWCO concentrator (Millipore). Protein purity was estimated to be greater than 90% using SDS gel electrophoresis.

Crystallization experiments were carried out with the hanging drop method at 20°C, using 2 µL protein plus 2 µL precipitant solution. Thin needle-plate crystals were obtained in 30% PEG 4000, 0.1 M sodium citrate pH 5.6, 0.2 M ammonium acetate. These crystals were used to micro-seed a 28% PEG 4000, 0.1 M sodium citrate pH 5.86, 0.2 M ammonium acetate, and 4% PEG 400 solution using 2 mg/mL protein, in order to obtain larger, single crystals. Crystals grew to 0.6 x 0.2 x 0.1 mm<sup>3</sup> in less than a week, and were frozen in liquid nitrogen prior to data collection.

#### Data Collection and Structure Determination.

A 1.8 Å resolution native dataset was collected at the Stanford Synchrotron Radiation Laboratory (SSRL) beam line 9-2, and processed using MOSFLM and SCALA (Leslie, 1992). Protein phases were determined using molecular replacement (MOLREP) (Vagin and Teplyakov, 1997) using pg110 (PDB ID: 1P99), a Gly-Met binding protein with 39% sequence identity. For molecular replacement, loops were deleted and non-identical residues were mutated to serines. The structure was primarily built using Arp/wArp (Cohen et al., 2008), with manual rebuilding using COOT (Emsley and Cowtan, 2004). Crystallographic refinement was carried out using CNS (v. 1.1) (Brunger, 1998) followed by REFMAC, resulting in a final model with an  $R_{\text{factor}}$  of ~19% and an  $R_{\text{free}}$  of ~24% at 1.8 Å.



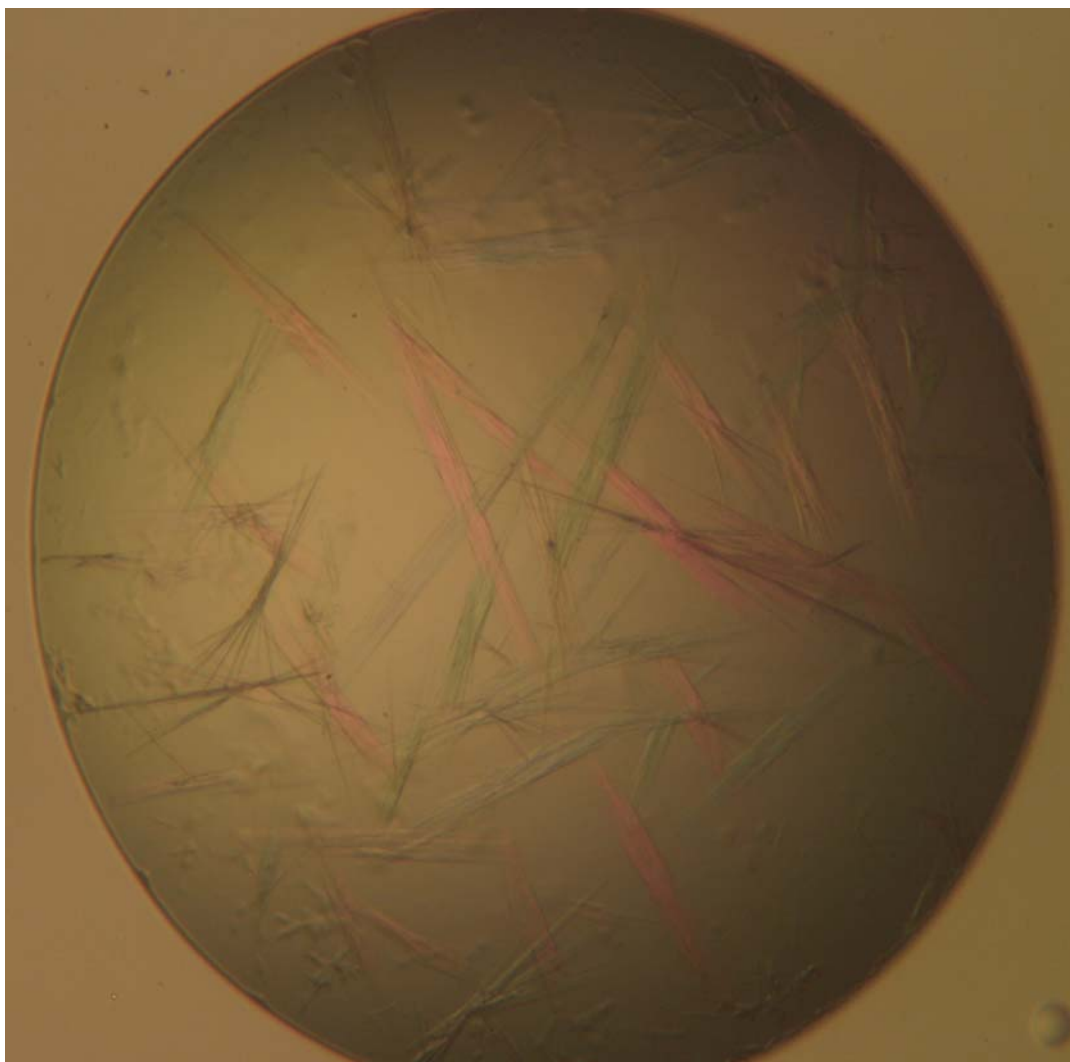


**Figure A2.2.** Above is a picture of the crystals obtained from MetQ crystallization trials. These long, rod-shaped crystals required seeding before the thickness was adequate for data collection.

**Table A2.1:** Summary of Secondary Structure for MetQ

Secondary Structure	Residue Range
$\beta$ 1	32-38
$\beta$ 2	60-66
$\beta$ 3	83-87
$\beta$ 4	103-110
$\beta$ 5	115-117
$\beta$ 6	132-136
$\beta$ 7	178-182
$\beta$ 8	198-201
$\beta$ 9	218-220
$\beta$ 10	229-234
$\alpha$ 1	41-57
$\alpha$ 2	70-78
$\alpha$ 3	89-99
$\alpha$ 4	139-152
$\alpha$ 5	184-192
$\alpha$ 6	203-209
$\alpha$ 7	241-250
$\alpha$ 8	253-263
$3_{10}$ 1	124-126
$3_{10}$ 2	167-169
$3_{10}$ 3	213-216

**Table A2.2:** Data Processing, Phasing and Refinement Statistics from MetQ

<b>Data processing</b>	
Dataset	<b>Native</b>
Spacegroup	C 2 2 2 <sub>1</sub>
Unit Cell dimensions (Å)	a= 59.89 b= 87.76 c= 113.10
Wavelength (Å)	1
Resolution (Å)	56.52-1.8
Unique reflections	25217
redundancy	5.0 (1.4)
<sup>a</sup> Completeness	90.0 (49.0)
<sup>b</sup> R <sub>merge</sub>	.11 (0.49)
<b>Refinement</b>	
Resolution (Å)	30-1.8
Reflections used	23948
Test reflections	1216
<sup>c</sup> R <sub>work</sub> (%)	19.0
<sup>c</sup> R <sub>free</sub> (%)	24.8
Average B factor (Å <sup>2</sup> )	19.93
Rmsd bond length (Å)	0.011
Rmsd bond angle (°)	1.3
<b>Ramachandran (%)</b>	
Most favored	91.6
Allowed	8.4
Disallowed	0

<sup>a</sup>Numbers in parentheses refer to the highest resolution shell only.

<sup>b</sup>R<sub>merge</sub>= $\sum |I_h - \langle I \rangle_h| / \sum I_h$ , where  $\langle I \rangle_h$  is average intensity over symmetry equivalents.

<sup>c</sup>R-factor= $\sum |F_{obs} - F_{calc}| / \sum F_{obs}$ .

## Chapter Four. Conclusions.

Members of the methionine uptake transporter (MUT) system are of considerable biological interest for their role in nutrient import by bacteria. As exogenous methionine is required for growth in certain bacterial pathogens, methionine transporters may be important for pharmaceutical development (Zhang, 2003). The regulatory functionality identified in the MetNI system provides an unexpected insight into the mechanism of these transporters and suggests additional possibilities for further studies. Opportunities for further investigation of this ABC transporter system are numerous. A higher-resolution crystal structure and a crystal structure of the MetNI transporter in complex with the MetQ binding protein would be quite interesting. Additionally, further studies characterizing the regulatory domain of this transporter, as well as studies of this transporter in other conformations (with nucleotides) would provide a better understanding of the methionine uptake transporter system of *E. coli*.

The field of research on ABC transporters is clearly growing. The papers published in the last 2 years have provided greater insight into the structure and function of this fascinating family of proteins. Specifically, the structures of intact complexes, such as the maltose, molybdate, and vitamin B<sub>12</sub> systems, as well as the higher resolution HI1470/71 importer have led to a clearer understanding of the mechanism of transport and ATP hydrolysis, and have led to the creation of a more established framework to explain the process of ATP binding, binding-protein enabled substrate delivery, substrate binding locations within the translocation pathway, and now, with the structure of this methionine uptake transporter, an understanding of one possible mechanism of regulation.

Despite these advances, there are many questions about ABC transporters that remain unanswered. Attempts to study issues concerning the binding sites within the translocation pathway and the affinity of these sites for a given substrate are underway. Similarly, a better picture of how ATP hydrolysis and substrate delivery interact and the sequence of events that lead up to the release of the substrate into the translocation pathway needs to be further clarified. Regulatory mechanisms are poorly understood, and it would be interesting to further characterize multiple additional domains to understand how they are involved in regulation. From a structural standpoint, structures of the same ABC transporter in distinct stages of the transport process, with nucleotides and substrates bound, are needed to understand the state of each transporter relative to the others within that transport process. It is hoped that this field will be advanced through a combination of structural and biochemical analyses and this information can be applied to the study of medically relevant ABC transporters. This medical need stems from the actions of certain ABC exporters (either human or bacterial) that lead to various disease states, and it will be exciting to see this field contribute to therapeutics related to these conditions. The field of research concerning ABC transporters has exploded with novel structures and mechanistic insights in the past few years, and faces an exciting future in both the scientific and medical fields.

## References.

- Alberts, B. (2002). Molecular biology of the cell. New York, Garland Science.
- Alshawi, M. K., I. L. Urbatsch and A. E. Senior (1994). "Covalent inhibitors of P-glycoprotein ATPase activity." Journal of Biological Chemistry **269**(12): 8986-8992.
- Ames, G. F., C. S. Mimura and V. Shyamala (1990). "Bacterial periplasmic permeases belong to a family of transport proteins operating from *Escherichia coli* to human: Traffic ATPases." FEMS Microbiol Rev **6**(4): 429-46.
- Aravind, L. and E. V. Koonin (1999). "Gleaning non-trivial structure, functional and evolutionary information about proteins by iterative database searches." J. Mol. Biol. **287**: 1023-1040.
- Barash, H. and Y. S. Halpern (1971). "Glutamate-binding protein and its relation to glutamate transport in *Escherichia coli* K-12." Biochemical and Biophysical Research Communications **45**(3): 681-685.
- Bass, R. B., K. P. Locher, E. Borths, Y. Poon, P. Strop, A. Lee and D. C. Rees (2003). "The structures of BtuCD and MscS and their implications for transporter and channel function." FEBS Lett **555**(1): 111-5.
- Berman, H. M., J. Westbrook, Z. Feng, G. Gilliland, T. N. Bhat, H. Weissig, I. N. Shindyalov and P. E. Bourne (2000). "The Protein Data Bank." Nuc. Acids Res. **28**: 235-42.

Biemans-Oldehinkel, E., M. K. Deoven and B. Poolman (2006). "ABC transporter architecture and regulatory roles of accessory domains." FEBS Lett. **580**: 1023-1035.

Boos, W., H. D. Price, R. E. Hall and A. S. Gordon (1972). "Transport properties of galactose-binding protein of *Escherichia coli* - substrate-induced conformational change." Journal of Biological Chemistry **247**(3): 917-923.

Borths, E. L., K. P. Locher, A. T. Lee and D. C. Rees (2002). "The structure of *Escherichia coli* BtuF and binding to its cognate ATP binding cassette transporter." Proceedings of the National Academy of Sciences of the United States of America **99**(26): 16642-16647.

Bricogne, G., C. Vonrhein, C. Flensburg, M. Schiltz and W. Paciorek (2003). "Generation, representation and flow of phase information in structure determination: recent developments in and around SHARP 2.0. ." Acta crystallogr. **D59**: 2023-2030.

Brunger, A. T. (2007). "Version 1.2 of the crystallography and NMR system." Nature Protocols **2**: 2728-2733.

Chanyangam, M., A. L. Smith, S. L. Moseley, M. Kuehn and P. Jenny (1991). "Contribution of a 28-kilodalton membrane-protein to the virulence of *Haemophilus influenzae*." Infection and Immunity **59**(2): 600-608.

Chen, J., G. Lu, J. Lin, A. L. Davidson and F. A. Quioco (2003). "A tweezers-like motion of the ATP-binding cassette dimer in an ABC transport cycle." Mol Cell **12**(3): 651-61.

Chen, J., S. Sharma, F. A. Quioco and A. L. Davidson (2001). "Trapping the transition state of an ATP-binding cassette transporter: evidence for a concerted mechanism of maltose transport." Proc Natl Acad Sci U S A **98**(4): 1525-30.

Chipman, D. M. and B. Shaanan (2001). "The ACT domain family." Curr. Opin. Struct. Biol. **11**: 694-700.

Cohen, S. X., M. Ben Jelloul, F. Long, A. Vagin, P. Knipscheer, J. Lebbink, T. K. Sixma, V. S. Lamzin, G. N. Murshudov and A. Ferrakis (2008). "ARP/wARP and molecular replacement: the next generation." Acta Crystallographica Section D-Biological Crystallography **64**: 49-60.

Collaborative Computational Project, N. (1994). "The CCP4 suite: programs for protein crystallography." Acta crystallogr. **D50**: 760-763.

Cowtan, K. (1994). "dm': An automated procedure for phase improvement by density modification." Joint CCP4 and ESF-EACBM Newsletter on Protein Crystallography **31**: 34-38.

Dassa, E., M. Hofnung, I. T. Paulsen and M. H. Saier, Jr. (1999). "The *Escherichia coli* ABC transporters: an update." Mol Microbiol **32**(4): 887-9.

Davidson, A. L. and J. Chen (2004). "ATP-binding cassette transporters in bacteria."

Annu Rev Biochem **73**: 241-68.

Davis, F. and M. Solowey (1950). "The utilization of some organic compounds by one strain each of *Salmonella anatum*, *Salmonella oranienburg*, and *Samonella pullorum*."

Journal of Bacteriology **59**(3): 361-366.

Dawson, R. J. P. and K. P. Locher (2006). "Structure of a bacterial multidrug ABC transporter." Nature **443**: 180-185.

Dawson, R. J. P. and K. P. Locher (2007). "Structure of the multidrug ABC transporter Sav1866 from *Staphylococcus aureus* in complex with AMP-PNP." Febs Letters **581**(5): 935-938.

Deka, R. K., L. Neil, K. E. Hagman, M. Machius, D. R. Tomchick, C. A. Brautigam and M. V. Norgard (2004). "Structural evidence that the 32-kilodalton lipoprotein (Tp32) of *Treponema pallidum* is an L-methionine-binding protein." Journal of Biological Chemistry **279**(53): 55644-55650.

DeLano, W. L. (2002). The PyMOL Molecular Graphics System. San Carlos, CA, DeLano Scientific.

Ehrmann, M., R. Ehrle, E. Hofmann, W. Boos and A. Schlosser (1998). "The ABC maltose transporter." Mol Microbiol **29**(3): 685-94.

Emsley, P. and K. Cowtan (2004). "Coot: Model-building tools for molecular graphics." Acta crystallogr. **D60**: 2126-2132.

Gál, J., A. Szvetnik, R. Schnell and M. Kálmán (2002). "The *metD* D-methionine transporter locus of *Escherichia coli* is an ABC transporter gene cluster." J. Bact. **184**: 4930-4932.

Grant, G. A. (2006). "The ACT domain: A small molecule binding domain and its role as a common regulatory element." Journal of Biological Chemistry **281**(45): 33825-33829.

Grant, G. A., D. J. Schuller and L. J. Banaszak (1996). "A model for the regulation of D-3-phosphoglycerate dehydrogenase, a  $V_{max}$ -type allosteric enzyme." Protein Sci. **5**: 34-41.

Greene, E. A. and G. B. Spiegelman (1996). "The SpoOA protein of *Bacillus subtilis* inhibits transcription of the *abrB* gene without preventing binding of the polymerase to the promoter." Journal of Biological Chemistry **271**(19): 11455-11461.

Grundy, C. E. and P. D. Ayling (1992). "Fine-structure mapping and complementation studies of the MetD methionine transport system in *Salmonella typhimurium*." Genetical Research **60**(1): 1-6.

Hendricks, J. K. and H. L. T. Mobley (1997). "*Helicobacter pylori* ABC transporter: Effect of allelic exchange mutagenesis on urease activity." Journal of Bacteriology **179**(18): 5892-5902.

Higgins, C. F. (1992). "ABC transporters: from microorganisms to man." Annu Rev Cell Biol **8**: 67-113.

Higgins, C. F. (1995). "The ABC of channel regulation." Cell **82**(5): 693-6.

Higgins, C. F. (2001). "ABC transporters: physiology, structure and mechanism--an overview." Res Microbiol **152**(3-4): 205-10.

Higgins, C. F. and K. J. Linton (2001). "Structural biology. The xyz of ABC transporters." Science **293**(5536): 1782-4.

Higgins, C. F. and K. J. Linton (2004). "The ATP switch model for ABC transporters." Nat Struct Mol Biol **11**(10): 918-26.

Holland, I. B. and M. A. Blight (1999). "ABC-ATPases, adaptable energy generators fuelling transmembrane movement of a variety of molecules in organisms from bacteria to humans." J Mol Biol **293**(2): 381-99.

Holland, I. B., S. P. C. Cole, K. Kuchler and C. F. Higgins (2003). ABC proteins: From Bacteria to Man. London, Academic.

Hollenstein, K., R. J. P. Dawson and K. P. Locher (2007). "Structure and mechanism of ABC transporter proteins." Curr. Opin. Struct. Biol. **17**: 412-418.

Hollenstein, K., D. C. Frei and K. P. Locher (2007). "Structure of an ABC transporter in complex with its binding protein." Nature **446**: 213-216.

Holm, L. and C. Sander (1998). "Touring protein fold space with Dali/FSSP." Nucl. Acids Res. **26**: 316-319.

Hopfner, K. P., A. Karcher, D. S. Shin, L. Craig, L. M. Arthur, J. P. Carney and J. A. Tainer (2000). "Structural biology of Rad50 ATPase: ATP-driven conformational control in DNA double-strand break repair and the ABC-ATPase superfamily." Cell **101**(7): 789-800.

Humphrey, W., A. Dalke and K. Schulten (1996). "VMD - Visual Molecular Dynamics." J. Mol. Graphics **14**: 33-38.

Hung, L. W., I. X. Wang, K. Nikaido, P. Q. Liu, G. F. Ames and S. H. Kim (1998). "Crystal structure of the ATP-binding subunit of an ABC transporter." Nature **396**(6712): 703-7.

Hvorup, R. N., B. A. Goetz, M. Niederer, K. Hollenstein, E. Perozo and K. P. Locher (2007). "Asymmetry in the structure of the ABC transporter binding protein complex BtuCD-BtuF." Science **317**: 1387-1390.

Jardetzky, O. (1966). "Simple Allosteric Model for Membrane Pumps." Nature **211**(5052): 969-972.

Jones, P. M. and A. M. George (1999). "Subunit interactions in ABC transporters: towards a functional architecture." FEMS Microbiol. Lett. **179**(2): 187-202.

Jones, P. M. and A. M. George (2004). "The ABC transporter structure and mechanism: perspectives on recent research." Cell Mol Life Sci **61**(6): 682-99.

Kaback, H. R. (1970). "Transport." Annual Review of Biochemistry **39**: 561-565.

Kabsch, W. (1976). "A solution for the best rotation to relate two sets of vectors." Acta crystallogr. **A32**: 922-923.

Kadner, R. J. (1974). "Transport systems for L-methionine in *Escherichia coli*." J. Bact. **117**: 232-241.

Kadner, R. J. (1975). "Regulation of methionine transport activity in *Escherichia coli*." J. Bact. **122**: 110-119.

Kadner, R. J. (1977). "Transport and utilization of D-methionine and other methionine sources in *Escherichia coli*." J. Bact. **129**: 207-216.

Kadner, R. J. and W. J. Watson (1974). "Methionine transport in *Escherichia coli*: Physiological and genetic evidence for two uptake systems." J. Bact. **119**: 401-409.

Kadner, R. J. and H. H. Winkler (1975). "Energy coupling for methionine transport in *Escherichia coli*." Journal of Bacteriology **123**(3): 985-991.

Karpowich, N., O. Martsinkevich, L. Millen, Y. R. Yuan, P. L. Dai, K. MacVey, P. J.

Thomas and J. F. Hunt (2001). "Crystal structures of the MJ1267 ATP binding cassette reveal an induced-fit effect at the ATPase active site of an ABC transporter." Structure **9**(7): 571-86.

Karpowich, N. K., H. H. Huang, P. C. Smith and J. F. Hunt (2003). "Crystal structures of the BtuF periplasmic-binding protein for vitamin B<sub>12</sub> suggest a functionally important reduction in protein mobility upon ligand binding." Journal of Biological Chemistry **278**(10): 8429-8434.

Konagurthu, A. S., J. C. Whisstock, P. J. Stuckey and A. M. Lesk (2006). "MUSTANG: A multiple structural alignment algorithm." Proteins Struct., Funct., Gen. **64**: 559-574.

Köster, W. (2001). "ABC transporter-mediated uptake of iron, siderophores, heme and vitamin B<sub>12</sub>." Res. Microbiol. **152**: 291-301.

Lee, Y. H., M. R. Dorwart, K. R. O. Hazlett, R. K. Deka, M. V. Norgard, J. D. Radolf and C. A. Hasemann (2002). "The crystal structure of Zn(II)-free *Treponema pallidum* TroA, a periplasmic metal-binding protein, reveals a closed conformation." Journal of Bacteriology **184**(8): 2300-2304.

Leslie, A. G. W. (1992). "Recent changes to the MOSFLM package for processing film and image plate data." Joint CCP4 and ESF-EACBM Newsletter on Protein Crystallography.

Liberles, J. S., M. Thorolfson and A. Martinez (2005). "Allosteric mechanisms in ACT domain containing enzymes involved in amino acid metabolism." Amino Acids **28**(1): 1-12.

Linton, K. J. and C. F. Higgins (1998). "The *Escherichia coli* ATP-binding cassette (ABC) proteins." Mol Microbiol **28**(1): 5-13.

Little, R. V. and R. R. Brubaker (1972). "Characterization of deoxyribonucleic acid from *Yersinia pestis* by ethidium bromide-caesium chloride density gradient centrifugation." Infection and Immunity **5**(4): 630-7.

Liu, R. X., T. W. Blackwell and D. J. States (2001). "Conformational model for binding site recognition by the E.coli MetJ transcription factor." Bioinformatics **17**(7): 622-633.

Locher, K. P. (2004). "Structure and mechanism of ABC transporters." Curr Opin Struct Biol **14**(4): 426-31.

Locher, K. P., A. T. Lee and D. C. Rees (2002). "The *E. coli* BtuCD structure: a framework for ABC transporter architecture and mechanism." Science **296**(5570): 1091-8.

Lombardi, F. J. and H. R. Kaback (1972). "Mechanisms of active-transport in isolated bacterial membrane vesicles .8. Transport of amino acids by membranes prepared from *Escherichia coli*." Journal of Biological Chemistry **247**(24): 7844-7857.

Loo, T. W. and D. M. Clarke (1995). "Covalent modification of human P-glycoprotein mutants containing a single cysteine in either nucleotide-binding fold abolishes drug-stimulated ATPase Activity." Journal of Biological Chemistry **270**(39): 22957-22961.

Lu, G., J. M. Westbrook, A. L. Davidson and J. Chen (2005). "ATP hydrolysis is required to reset the ATP-binding cassette dimer into the resting-state conformation." Proc. Natl. Acad. Sci. USA **102**(50): 17969-74.

Mao, B., M. R. Pear, J. A. McCammon and F. A. Quioco (1982). "Hinge-bending in L-arabinose-binding protein - the Venus-flytrap model." Journal of Biological Chemistry **257**(3): 1131-1133.

Merlin, C., G. Gardiner, S. Durand and M. Masters (2002). "The *Escherichia coli* metD locus encodes an ABC transporter which includes Abc (MetN), YaeE (MetI), and YaeC (MetQ)." J. Bact. **184**: 5513-5517.

Miller, D. M., J. S. Olson, J. W. Pflugrath and F. A. Quioco (1983). "Rates of ligand-binding to periplasmic proteins involved in bacterial transport and chemotaxis." Journal of Biological Chemistry **258**(22): 3665-3672.

Mimmack, M. L., M. P. Gallagher, S. R. Pearce, S. C. Hyde, I. R. Booth and C. F. Higgins (1989). "Energy coupling to periplasmic binding protein-dependent transport systems: stoichiometry of ATP hydrolysis during transport in vivo." Proc Natl Acad Sci U S A **86**(21): 8257-61.

Mimura, C. S., A. Admon, K. A. Hurt and G. F. Ames (1990). "The nucleotide-binding site of HisP, a membrane protein of the histidine permease. Identification of amino acid residues photoaffinity labeled by 8-azido-ATP." J Biol Chem **265**(32): 19535-42.

Mimura, C. S., S. R. Holbrook and G. F. Ames (1991). "Structural model of the nucleotide-binding conserved component of periplasmic permeases." Proc Natl Acad Sci U S A **88**(1): 84-8.

Mourez, M., N. Hofnung and E. Dassa (1997). "Subunit interactions in ABC transporters: A conserved sequence in hydrophobic membrane proteins of periplasmic permeases defines an important site of interaction with the ATPase subunits." EMBO J **16**: 3066-3077.

Murata, K., K. Mitsuoka, T. Hirai, T. Walz, P. Agre, J. B. Heymann, A. Engel and Y. Fujiyoshi (2000). "Structural determinants of water permeation through aquaporin-1." Nature **407**: 599-605.

Murschudov, G. N., A. A. Vagin and E. J. Dodson (1996). "Refinement of macromolecular structures by the maximum-likelihood method." Acta crystallogr. **D53**: 240-255.

Murschudov, G. N., A. A. Vagin, A. Lebedev, K. S. Wilson and E. J. Dodson (1999).

"Efficient anisotropic refinement of macromolecular structures using FFT." Acta crystallogr. **D55**: 247-255.

Neijssel, O. M., M. J. Teixeira de Mattos and D. W. Tempest (1996). Growth yield and energy distribution. Escherichia coli and Salmonella: cellular and molecular biology. F. C. Neidhardt. Washington, D.C., ASM Press.

Neu, H. C. and L. A. Heppel (1965). "Release of enzymes and nucleotides from *E. Coli* by osmotic shock." Federation Proceedings **24**(2P1): 349-354.

Nikaido, H. (1994). "Maltose transport system of *Escherichia coli*: an ABC-type transporter." FEBS Lett **346**(1): 55-8.

Nikaido, H. (2002). "How are the ABC transporters energized?" Proc Natl Acad Sci U S A **99**(15): 9609-10.

Oldham, M. L., D. Khare, F. A. Quioco, A. L. Davidson and J. Chen (2007). "Crystal structure of a catalytic intermediate of the maltose transporter." Nature **450**: 515-522.

Pattery, T., J. P. Hernalsteens and H. De Greve (1999). "Identification and molecular characterization of a novel *Salmonella enteritidis* pathogenicity islet encoding an ABC transporter." Molecular Microbiology **33**(4): 791-805.

Patzlaff, J. S., T. van der Heide and B. Poolman (2003). "The ATP/Substrate stoichiometry of the ATP-binding cassette (ABC) transporter OpuA." Journal of Biological Chemistry **278**(32): 29546-29551.

Ferrakis, A., R. Morris and V. S. Lamzin (1999). "Automated protein model building combined with iterative structure refinement." Nature Str. Mol. Biol. **6**: 458-463.

Pinkett, H. W., A. T. Lee, P. Lum, K. P. Locher and D. C. Rees (2007). "An inward-facing conformation of a putative metal-chelate type ABC transporter." Science **315**: 373-377.

Piperno, J. R. and D. L. Oxender (1968). "Amino acid transport systems in *Escherichia coli* K12." Journal of Biological Chemistry **243**(22): 5914-5919.

Pornillos, O. and G. Chang (2006). "Inverted repeat domains in membrane proteins." FEBS Lett. **580**: 358-362.

Quioco, F. A. and P. Ledvina (1996). "Atomic structure and specificity of bacterial periplasmic receptors for active transport and chemotaxis: variation of common themes." Mol. Microbiol. **20**: 17-25.

Saintgiron, I., N. Duchange, G. N. Cohen and M. M. Zakin (1984). "Structure and auto-regulation of the MetJ regulatory gene in *Escherichia coli*." Journal of Biological Chemistry **259**(22): 4282-4285.

Saraste, M., P. R. Sibbald and A. Wittinghofer (1990). "The P-loop--a common motif in ATP- and GTP-binding proteins." Trends Biochem Sci **15**(11): 430-4.

Saurin, W., W. Koster and E. Dassa (1994). "Bacterial binding protein-dependent permeases - characterization of distinctive signatures for functionally related integral cytoplasmic membrane proteins." Mol. Micro. **12**: 993-1004.

Schmitt, L. (2002). "The first view of an ABC transporter: the X-ray crystal structure of MsbA from *E. coli*." Chembiochem **3**(2-3): 161-5.

Schmitt, L., H. Benabdelhak, M. A. Blight, I. B. Holland and M. T. Stubbs (2003). "Crystal structure of the nucleotide-binding domain of the ABC-transporter haemolysin B: identification of a variable region within ABC helical domains." J. Mol. Biol. **330**: 333-342.

Schneider, T. R. and G. M. Sheldrick (2002). "Substructure solution with SHELXD." Acta crystallogr. **D58**: 1772-1779.

Schuller, D., G. A. Grant and L. Banaszak (1995). "Crystal structure reveals the allosteric ligand site in the  $V_{max}$ -type cooperative enzyme; D-3-phosphoglycerate dehydrogenase." Nature Struct. Biol. **2**: 69-76.

Sekowska, A., H. F. Kung and A. Danchin (2000). "Sulfur metabolism in *Escherichia coli* and related bacteria: Facts and fiction." Journal of Molecular Microbiology and Biotechnology **2**(2): 145-177.

Sharff, A. J., L. E. Rodseth, J. C. Spurlino and F. A. Quiocho (1992). "Crystallographic evidence of a large ligand-induced hinge-twist motion between the 2 domains of the maltodextrin binding-protein involved in active-transport and chemotaxis."

Biochemistry **31**(44): 10657-10663.

Smith, P. C., N. Karpowich, L. Millen, J. E. Moody, J. Rosen, P. J. Thomas and J. F. Hunt (2002). "ATP binding to the motor domain from an ABC transporter drives formation of a nucleotide sandwich dimer." Mol. Cell **10**: 139-149.

Spreng, S., I. Gentschev, W. Goebel, H.-J. Mollenkopf, M. Eck, H. K. Müller-Hermelink and B. Schmausser (2006). "Identification of immunogenic antigens of *Helicobacter pylori* via the *Escherichia coli* hemolysin secretion system." FEMS Microbiol. Lett. **186**: 251-256.

Story, R. M., I. T. Weber and T. A. Steitz "The structure of the *E. coli* recA protein monomer and polymer."

Stouthamer, A. H. (1979). "The search for correlation between theoretical and experimental growth yields." Int. Rev. Biochem. **21**: 1-47.

Strong, M., M. R. Sawaya, S. Wang, M. Phillips, D. Cascio and D. Eisenberg (2006). "Toward the structural genomics of complexes: Crystal structure of a PE/PPE protein complex from *Mycobacterium tuberculosis*." Proc. Natl. Acad. Sci. USA **103**: 8060-8065.

Tam, R. and M. H. Saier (1993). "Structural, functional, and evolutionary relationships among extracellular solute-binding receptors of bacteria." Microbiological Reviews **57**(2): 320-346.

Toyoshima, C., M. Nakasako, H. Nomura and H. Ogawa (2000). "Crystal structure of the calcium pump of sarcoplasmic reticulum at 2.6Å resolution." Nature **405**: 647-655.

Turk, D. (2001). Towards automatic macromolecular crystal structure determination. Methods in Macromolecular Crystallography, NATO Science Series I. **325**: 148-155.

Vagin, A. and A. Teplyakov (1997). "MOLREP: an automated program for molecular replacement." Journal of Applied Crystallography **30**: 1022-1025.

van der Heide, T. and B. Poolman (2002). "ABC transporters: one, two or four extracytoplasmic substrate-binding sites?" EMBO Rep **3**(10): 938-43.

Walker, J. E., M. Saraste, M. J. Runswick and N. J. Gay (1982). "Distantly related sequences in the alpha- and beta-subunits of ATP synthase, myosin, kinases and other ATP-requiring enzymes and a common nucleotide binding fold." Embo J **1**(8): 945-51.

Wang, C. Y., N. Karpowich, J. F. Hunt, M. Rance and A. G. Palmer (2004). "Dynamics of ATP-binding cassette contribute to allosteric control, nucleotide binding and energy transduction in ABC transporters." Journal of Molecular Biology **342**(2): 525-537.

Ward, A., C. L. Reyes, J. Yu, C. B. Roth and G. Chang (2007). "Flexibility in the ABC transporter MsbA: Alternating access with a twist." Proc. Natl. Acad. Sci. USA **104**: 19005-19010.

Webb, M. R. (1992). "A continuous spectrophotometric assay for inorganic phosphate and for measuring phosphate release kinetics in biological systems." Proc. Natl. Acad. Sci. USA **89**: 4884-4887.

Weiss, M. S. (2001). "Global indicators of X-ray data quality." J. Appl. Cryst. **34**: 130-135.

Weissbach, H. and N. Brot (1991). "Regulation of Methionine Synthesis in Escherichia-Coli." Molecular Microbiology **5**(7): 1593-1597.

Widdas, W. F. (1952). "Inability of diffusion to account for placental glucose transfer in the sheep and consideration of the kinetics of a possible carrier transfer." J. Physiology **118**: 23-39.

Williams, W. A., R. G. Zhang, M. Zhou, G. Joachimiak, P. Gornicki, D. Missiakas and A. Joachimiak (2004). "The membrane-associated lipoprotein-9 GmpC from *Staphylococcus aureus* binds the dipeptide GlyMet via side chain interactions." Biochemistry **43**(51): 16193-16202.

Xu, J., Y. Liu, Y. Yang, S. Bates and J. T. Zhang (2004). "Characterization of oligomeric human half-ABC transporter ATP-binding cassette G2." J Biol Chem **279**(19): 19781-9.

Yuan, Y. R., S. Blecker, O. Martsinkevich, L. Millen, P. J. Thomas and J. F. Hunt (2001). "The crystal structure of the MJ0796 ATP-binding cassette. Implications for the structural consequences of ATP hydrolysis in the active site of an ABC transporter." J Biol Chem **276**(34): 32313-21.

Zaitseva, J., C. Oswald, T. Jumpertz, S. Jenewein, A. Wiedenmann, I. B. Holland and L. Schmitt (2006). "A structural analysis of asymmetry required for catalytic activity of an ABC-ATPase domain dimer." EMBO J. **25**: 3432-3443.

Zhang, Z., J. N. Feige, A. B. Chang, I. J. Anderson, V. M. Brodianski, A. G. Vitreschak, M. S. Gelfand and M. H. J. Saier (2003). "A transporter of *Escherichia coli* specific for L- and D-methionine is the prototype for a new family within the ABC superfamily." Arch. Microbiol. **180**: 88-100.

## **About the Author.**

The author was born in 1981 in Bridgeport, Connecticut. She grew up in various cities in Southern California and graduated from San Clemente High School in 1998. She attended the Massachusetts Institute of Technology and received an S.B. in Chemistry along with a minor in Brain and Cognitive Sciences in 2002. While an undergraduate, she worked in the laboratory of Dr. Ann Graybiel on neurochemical and behavioral modifications induced by dopaminergic agents. After graduation, she joined the lab of Professor John Essigmann in order to pursue a project focused on developing novel therapeutics for tuberculosis in a master's program at MIT. As part of her master's project, she accompanied MIT faculty to Bangkok, Thailand, to teach a summer course on Biotechnology and Engineering at the Chulabhorn Research Institute. She received her master's degree in Molecular and Systems Toxicology in the Department of Bioengineering from MIT in June 2003. After receiving her PhD in Chemistry from the California Institute of Technology in June 2008, Neena plans to pursue a job in the private sector.

## Index.

- $\alpha$ -helices, 6, 40, 44, 64, 67, 70
- ABC signature sequence, 3
- ABC transporters, 1, 3, 6, 16, 20, 36, 39, 47, 85
- ACT, 4, 20, 21, 23, 30, 34, 43, 44, 45
- ATP, 4, 9, 1, 2, 3, 6, 10, 11, 12, 15, 16, 18, 20, 24, 26, 29, 37, 38, 39, 42, 43, 44, 45, 46, 48, 51, 85
- ATPase, 5, 8, 13, 16, 24, 27, 30, 35, 38, 39, 40, 41, 42, 43, 44, 48, 65
- ATP-binding, 4, 3, 15
- binding protein, 4, 1, 6, 10, 11, 13, 24, 27, 48, 62, 63, 65, 66, 67, 69, 70, 76, 77, 80, 85
- $\beta$ -sheet, 6, 22, 40, 43, 64, 67, 70, 72
- $\beta$ -strands, 6, 40BtuCD, 6, 8, 13, 15, 36, 42, 65
- conformation, 3, 4, 5, 8, 9, 11, 16, 17, 18, 20, 30, 42, 44, 45, 65, 85
- coupling helices, 15, 38
- cytoplasm, 6, 7, 35, 36, 43
- helices, 4, 3, 6, 8, 11, 13, 15, 20, 22, 27, 30, 34, 35, 37, 40, 42, 43, 48, 70
- HI1470/1, 8, 20, 36, 43, 85
- hydrolysis, 4, 1, 3, 10, 11, 13, 16, 20, 38, 85
- hydrophobic, 1, 3, 6, 68, 69, 72, 75
- importers, 1, 6, 14, 15, 18, 41, 48
- MalF, 13, 36, 37
- MalG, 13, 34, 36, 37, 66
- MalK, 3, 13, 17, 20, 21, 41
- MetD, 24, 26, 27, 28
- methionine, 4, 24, 25, 26, 27, 28, 29, 40, 46, 47, 49, 51, 67, 68, 69, 70, 72, 75, 77, 79, 85
- MetI, 9, 24, 27, 30, 34, 36, 37, 59
- MetN, 9, 24, 27, 30, 38, 39, 40, 41, 43, 44, 45, 46, 58
- MetQ, 4, 9, 24, 27, 62, 70, 73, 75, 76, 77, 79, 83, 84, 85
- ModB, 11, 34, 36, 37
- motifs, 3, 6, 15, 16, 18, 20, 27, 41, 42
- NBD, 9, 3, 15, 16, 18, 20, 38
- NBDs, 2, 16, 20
- nucleotide binding domain, 2, 3, 8, 9, 11, 15
- P-loop, 3, 18, 20, 42
- Q-loop, 6, 16
- regulation, 4, 20, 22, 23, 26, 48, 85
- SAV1866, 15, 20
- substrate, 1, 3, 8, 10, 11, 15, 20, 26, 37, 42, 47, 62, 63, 65, 66, 69, 85
- subunits, 5, 8, 30, 34, 36, 41, 48
- TMD, 9, 2, 15, 18, 38
- TMDs, 2, 17
- translocation, 2, 6, 8, 10, 11, 12, 13, 20, 30, 35, 37, 38, 47, 48, 65, 66, 85
- transmembrane domain, 6, 8, 11, 15, 24, 27, 30, 34, 38, 42, 47, 48, 62, 76
- transport, 1, 4, 5, 8, 11, 14, 15, 16, 20, 24, 25, 26, 29, 38, 42, 46, 47, 48, 62, 65, 85
- Walker A, 3, 16, 41